Oxygen-independent Coproporphyrinogen III Oxidase: Characterization of *Escherichia coli* HemN and Investigation of Proposed Functional Analogs

Vom Fachbereich für Biowissenschaften und Psychologie
der Technischen Universität Carolo-Wilhelmina
zu Braunschweig
zur Erlangung des Grades einer
Doktorin der Naturwissenschaften
(Dr. rer. nat.)
genehmigte
D i s s e r t a t i o n

von Katrin Grage
aus Schleswig

1. Referent: Prof. Dr. Dieter Jahn
2. Referent: Prof. Dr. Dirk W. Heinz
eingereicht am: 04. August 2005
mündliche Prüfung (Disputation) am: 30. September 2005
Druckjahr: 2005

Vorveröffentlichungen der Dissertation

Teilergebnisse aus dieser Arbeit wurden mit Genehmigung des Fachbereiches für Biowissenschaften und Psychologie, vertreten durch den Mentor der Arbeit, in folgenden Beiträgen vorab veröffentlicht:

Publikationen

*Layer, G., Grage, K., Teschner, T., Schünemann, V., Breckau, D., Masoumi, A., Jahn, M., Heathcote, P., Trautwein, A. X. & Jahn, D. (2005) Radical SAM enzyme coproporphyrinogen III oxidase HemN: functional features of the [4Fe-4S] cluster and the two bound *S*-adenosyl-L-methionines. *J. Biol. Chem.* **280**, 29038-29046.
*G. Layer und K. Grage trugen gleichermaßen zu dieser Publikation bei.

*Layer, G., Grage, K., Pierik, A. J., Trost, M., Jänsch, L., Leech, H. K., Warren, M. J., Astner, I., Breckau, D., Heinz, D. W. & Jahn, D. (2005) The substrate radical of *Escherichia coli* oxygen-independent coproporphyrinogen III oxidase HemN. Manuskript eingereicht bei *J. Biol. Chem.*
*G. Layer und K. Grage trugen gleichermaßen zu dieser Publikation bei.

Tagungsbeiträge

Grage, K., Layer, G., Schubert, W.-D., Heinz, D.W. and Jahn, D. (2004) The Radical SAM enzyme coproporphyrinogen III oxidase: crystal structure, enzyme mechanism and mutational analysis. Posterpräsentation. *Gordon Research Conference on the Chemistry and Biology of Tetrapyrroles.* Newport, Rhode Island, USA.

TABLE OF CONTENTS

ABBREVIATIONS

A	Ampere
A_λ	absorption at wavelength λ in nm
Å	Ångström
ALA	5-aminolevulinic acid
amp	ampicillin
anRNR-ae	anaerobic ribonucleotide reductase activating enzyme
APS	ammonium peroxodisulfate
ATP	adenosine triphosphate
bp	base pair
BioB	biotin synthase
C	Celsius (° C)
[^{14}C]-methionine	L-[*methyl*-^{14}C]methionine
[^{14}C]-SAM	*S*-adenosyl-L-[*methyl*-^{14}C]methionine
CD	circular dichroism
Ci	Curie
CPO	coproporphyrinogen III oxidase
Da	Dalton
DNA	deoxyribonucleic acid
(d)dNTP	(di)deoxyribonucleotide triphosphate
DSMZ	Deutsche Sammlung von Mikroorganismen und Zellkulturen
DT	sodium dithionite
DTT	1,4-dithio-D,L-threitol
EDTA	ethylenediamine tetraacetic acid
e.g.	*exempli gratia* (for instance)
et al.	*et alteri* (and others)
F	farad
Fnr	fumarate and nitrate reduction regulator
FRT sites	FLP recognition target sites
fwd	forward
g	→ *centrifugation*: earth gravity
	→ *weight*: gram

GBq	giga Becquerel
GluTR	glutamyl-tRNA reductase
GSA	glutamate-1-semialdehyde
GSAM	glutamate-1-semialdehyde-2,1-aminomutase
GST	glutathione S-transferase
h	hour
HEPES	4-(2-hydroxyethyl)-piperazine-1-ethane sulfonic acid
HemF	oxygen-dependent coproporphyrinogen III oxidase
HemN	oxygen-independent coproporphyrinogen III oxidase
HemY	protoporphyrinogen IX oxidase
HemZ	proposed oxygen-independent coproporphyrinogen III oxidase
HPLC	high performance liquid chromatography
i.e.	*id est* (that is to say)
IPTG	isopropyl-β-D-thiogalactopyranoside
IRP	iron regulatory protein
k	kilo
kan	kanamycin
l	liter
λ	wavelength
LAM	lysine-2,3-aminomutase
LB	Luria Bertani
m	milli
M	molar (mol/l)
µ	micro
min	minute
MoaA	enzyme catalyzing precursor Z synthesis during molybdenum cofactor biosynthesis
MiaB	tRNA-methylthiotransferase
n	nano
n.d.	not detectable
n.t.	not tested
NAD(P)H	nicotinamide adenine dinucleotide (phosphate), reduced form
Ω	Ohm
OD_λ	optical density at wavelength λ in nm

Pa	Pascal
p.a.	*pro analysi*
PBG	porphobilinogen
PBGD	porphobilinogen deaminase
PBGS	porphobilinogen synthase
PBS	phosphate-buffered saline
PCA	perchloric acid
PCR	polymerase chain reaction
PFL-ae	pyruvate formate lyase activating enzyme
PM	N-methylphenazonium methyl sulfate
PPO	protoporphyrinogen IX oxidase
p.s.i.	pounds per square inch
rev	reverse
rpm	rotations per minute
SAM	*S*-adenoyl-L-methionine
SAM1	SAM molecule coordinating one of the iron atoms of the [4Fe-4S] cluster of HemN
SAM2	SAM molecule not involved in HemN [4Fe-4S] cluster coordination
SDS	sodium dodecyl sulfate
SDS-PAGE	sodium dodecyl sulfate polyacrylamide gel electrophoresis
SMEB	sucrose magnesium electroporation buffer
SMM	Spizizen minimal medium
SPP lyase	spore photoproduct lyase
TAE	Tris-acetate/EDTA
TB	terrific broth
TE	Tris-EDTA
TEMED	tetramethylen diamine
tet	tetracycline
TIM	triose phosphate isomerase
Tris	tris-(hydroxymethyl)-aminomethane
(t)RNA	(transfer) ribonucleic acid
U	unit
UV	ultraviolet
V	volt

vol.	volume
vs.	versus
v/v	volume per volume
w/v	weight per volume

1. INTRODUCTION

1.1 Tetrapyrroles

1.1.1 Structure and Function of Naturally Occurring Tetrapyrroles

Due to their participation in fundamental biological processes, tetrapyrroles are indispensable components of the metabolism of practically all organisms on earth. They play a central role in electron transfer - dependent energy generating processes such as photosynthesis and respiration and function as prosthetic groups for a variety of enzymes. A tetrapyrrole consists of four pyrrole rings, in general attached to each other in a cyclic or linear form via methine bridges. One exception are the corrinoids which lack one brigde carbon (see below). The basic structure of a cyclic tetrapyrrole is the porphyrin macrocycle shown in Figure 1.

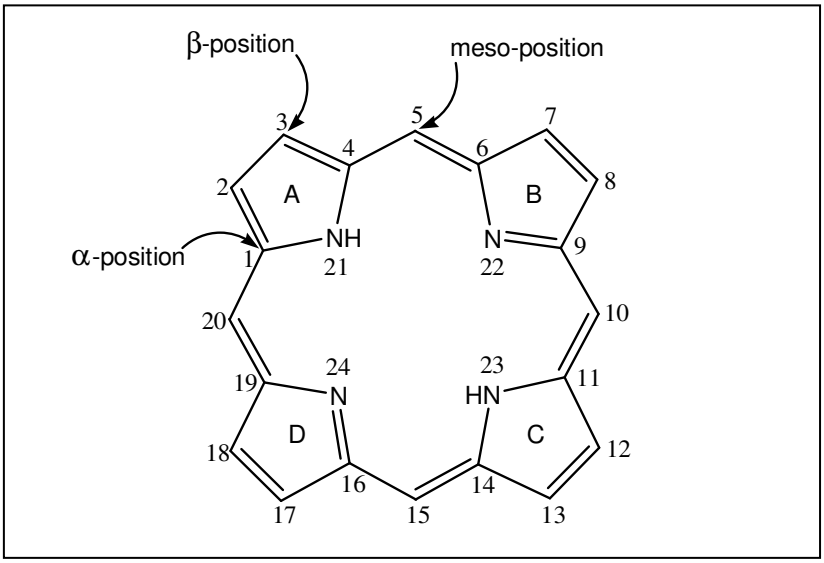

Figure 1: Basic structure of cyclic tetrapyrroles, the porphyrin ring. The pyrrole rings are labelled A - D, the carbon and nitrogen atoms are numbered 1 - 20 and 21 - 24, respectively. The α-carbons refer to carbon atoms adjacent to nitrogen atoms, the remaining pyrrole ring carbons are designated β-carbons and the methine bridge carbons are in meso-position.

The pyrrole rings of the macrocycle are denoted A - D in a clockwise orientation. Numbering of the carbon and nitrogen atoms is also clockwise and illustrated in Figure 1. Within each pyrrole ring, the carbon atoms adjacent to the nitrogen atoms are termed α-carbons (e.g. C1 and C4 in ring A), while those carbon atoms without a direct bond to a nitrogen atom are

termed β-carbons (e.g. C2 and C3 in ring A). The carbon atoms that constitute the methine bridges are in meso-position (e.g. C5 between ring A and B).

Due to the size and complexity of the different tetrapyrroles, most of the structural information about these molecules only became available during the past 100 years (reviewed in Battersby, 2000). The first structures - those of heme and chlorophyll - were determined in the first half of the 20th century.

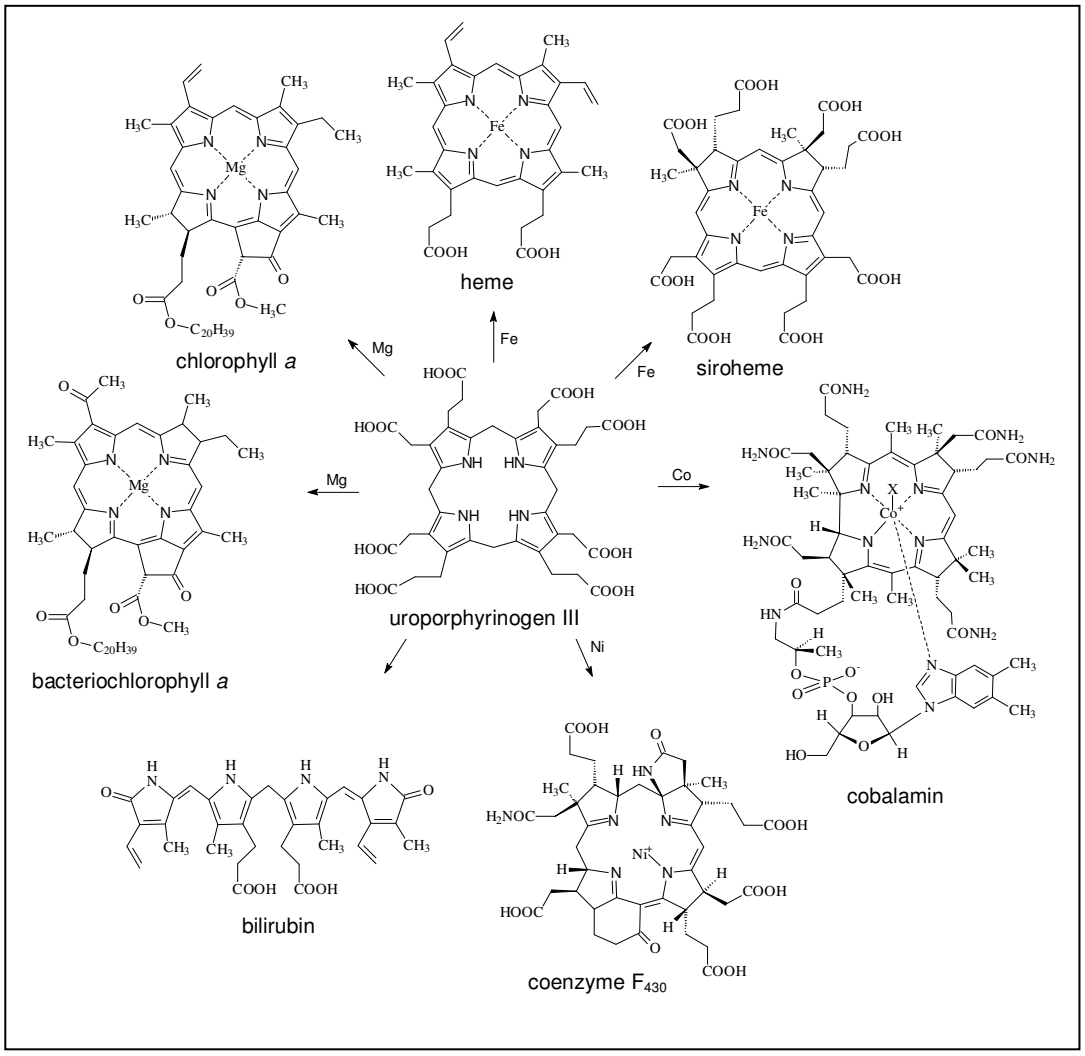

Figure 2: Important representatives of naturally occurring tetrapyrroles and their common precursor molecule uroporphyrinogen III.

Today, seven different groups of cyclic tetrapyrroles are known. The individual functional properties of each group are mainly determined by the nature of the metal ion which is chelated by the nitrogen atoms in the center of the ring system, by the oxidation state of the macrocycle and by the nature of the substituents at the β-positions of the pyrrole rings. Figure 2 shows the structures of representatives of different groups of tetrapyrroles discussed

in this section.

Heme, the prosthetic group of e.g. hemoglobin and myoglobin, but also of cytochromes, catalases and peroxidases, is a true porphyrin. This iron-chelating tetrapyrrole contains a complete aromatic ring system which is responsible for its red colour and characteristic spectroscopic properties. Tetrapyrroles with variations of the basic porphyrin structure are known as porphinoids. This group includes more reduced cyclic tetrapyrroles such as chlorophylls (chlorins), bacteriochlorophylls (chlorins or bacteriochlorins), siroheme (an isobacteriochlorin), coenzyme F_{430} and heme d_1. Magnesium-containing chlorophylls and bacteriochlorophylls function as photoreceptors during photosynthesis (Beale and Weinstein, 1990, 1991). Siroheme and heme d_1 are the cofactors of assimilatory sulfite and nitrite reductase and of dissimilatory nitrite reductase, respectively (Chang, 1994; Warren *et al.*, 1994). Both contain iron as central atom. Cofactor F_{430} - the tetrapyrrole discovered most recently - chelates nickel and serves as prosthetic group of methyl coenzyme M reductase, an enzyme involved in archaeal methanogenesis (Friedmann *et al.*, 1991; Thauer and Bonacker, 1994). Finally, tetrapyrroles like coenzyme B_{12} belong to the class of corrinoids characterized by a missing methine bridge (C20) between pyrrole rings A and D (Scott and Santander, 1991; Martens *et al.*, 2002). Members of the cobalt-containing corrinoids are e.g. cofactors in methyl transfer reactions. Linear tetrapyrroles are derived from cyclic tetrapyrroles by oxidative cleavage. The cleavage product of heme, biliverdin, then serves as a precursor for the biosynthesis of phycobilins (e.g. chromophores of cyanobacterial phycobiliproteins) and phytochrome chromophores (Beale, 1993; Beale and Yeh, 1999).

1.1.2 Biosynthesis of Tetrapyrroles

In accordance with their common structural core all currently known tetrapyrroles are derived from a single precursor molecule, 5-aminolevulinic acid (ALA). Consequently, the initial steps of the biosynthetic pathway from ALA are conserved throughout the different biosynthetic routes. Only after the formation of the first cyclic intermediate, uroporphyrinogen III, the pathways diverge. Representing a major branching point in tetrapyrrole biosynthesis, uroporphyrinogen III is converted either into protoporphyrin IX or into precorrin 2 (dehydrosirohydrochlorin). Protoporphyrin IX is the precursor for the synthesis of hemes, chlorophylls and bacteriochlorophylls, while precorrin 2 is used to synthesize the remaining classes of cyclic tetrapyrroles, including siroheme, heme d_1, corrinoids and coenzyme F_{430}. An overview of the divergent biosynthetic pathways is provided in Figure 3. Only prokaryotes are capable of synthesizing all classes of tetrapyrroles. In eukaryotes

tetrapyrrole biosynthesis is limited to the formation of hemes, chlorophylls and siroheme. Tetrapyrroles and their biosynthesis have been reviewed in numerous publications, some of which focus solely on heme biosynthesis (e.g. Lascelles, 1964; Dailey, 1990a; Jordan, 1991a; Jahn, 1996; Jahn *et al.*, 1996; Shoolingin-Jordan and Cheung, 1999; O'Brian and Thöny-Meyer, 2002; Frankenberg *et al.*, 2003).

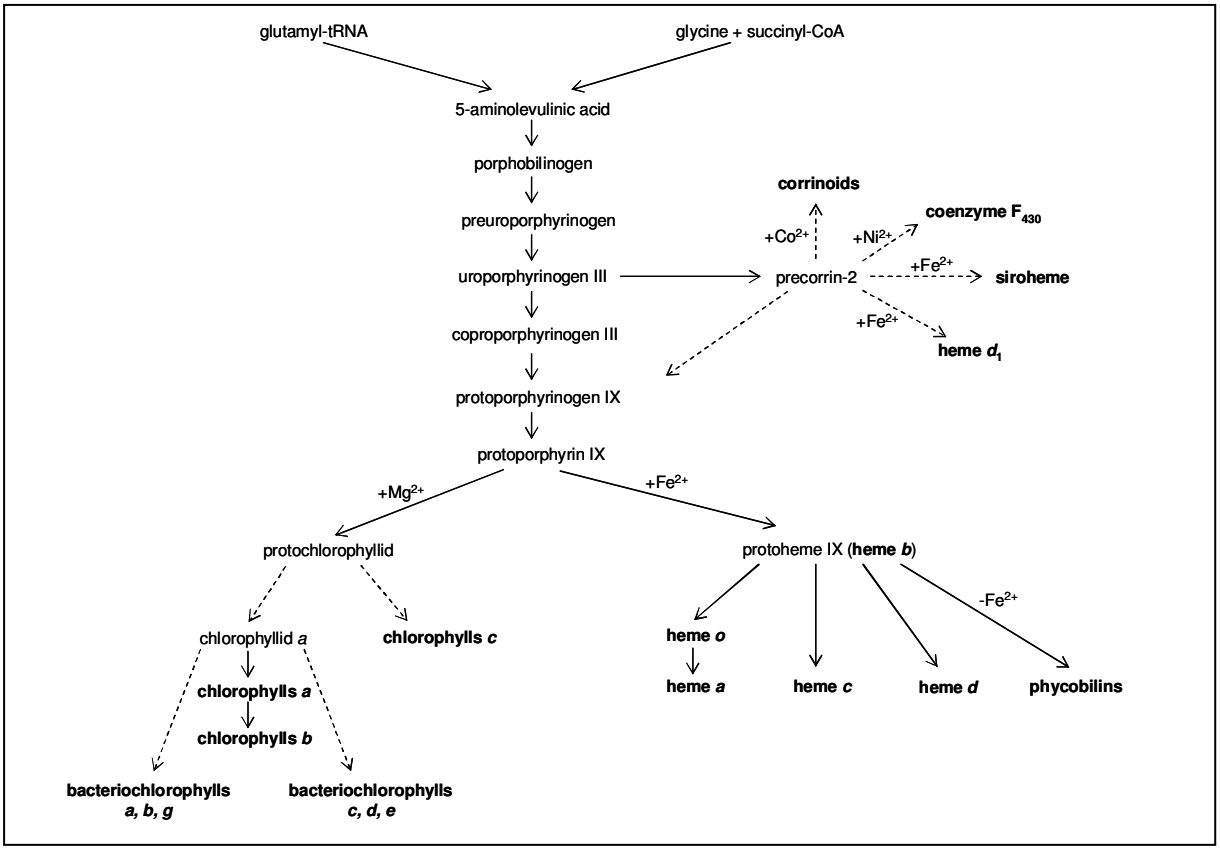

Figure 3: Overview of biosynthetic pathways of biologically relevant tetrapyrroles. Dotted arrows indicate pathways which are not shown completely or have not yet been entirely understood (modified from Jahn *et al.*, 1996).

1.1.3 Heme Biosynthesis with Emphasis on the Terminal Steps

The heme biosynthesis pathway (Figure 4) can be divided into three main stages: (1) formation of the ubiquitous precursor molecule ALA; (2) transformation of eight molecules of ALA into the first cyclic tetrapyrrole precursor uroporphyrinogen III; (3) conversion of uroporphyrinogen III into heme. This last step comprises oxidation of the ring system, modification of the side chains and finally chelation of ferrous iron. The enzymes of the pathway are conserved to a large extent among prokaryotes and eukaryotes. ALA synthesis and the conversion of coproporphyrinogen III into protoporphyrinogen IX have been shown to be major targets of pathway regulation (Jahn, 1996; Rompf *et al.*, 1998;

Schobert and Jahn, 2003). Detailed information on all steps can be found in a variety of reviews on heme biosynthesis, listed in section 1.1.2.

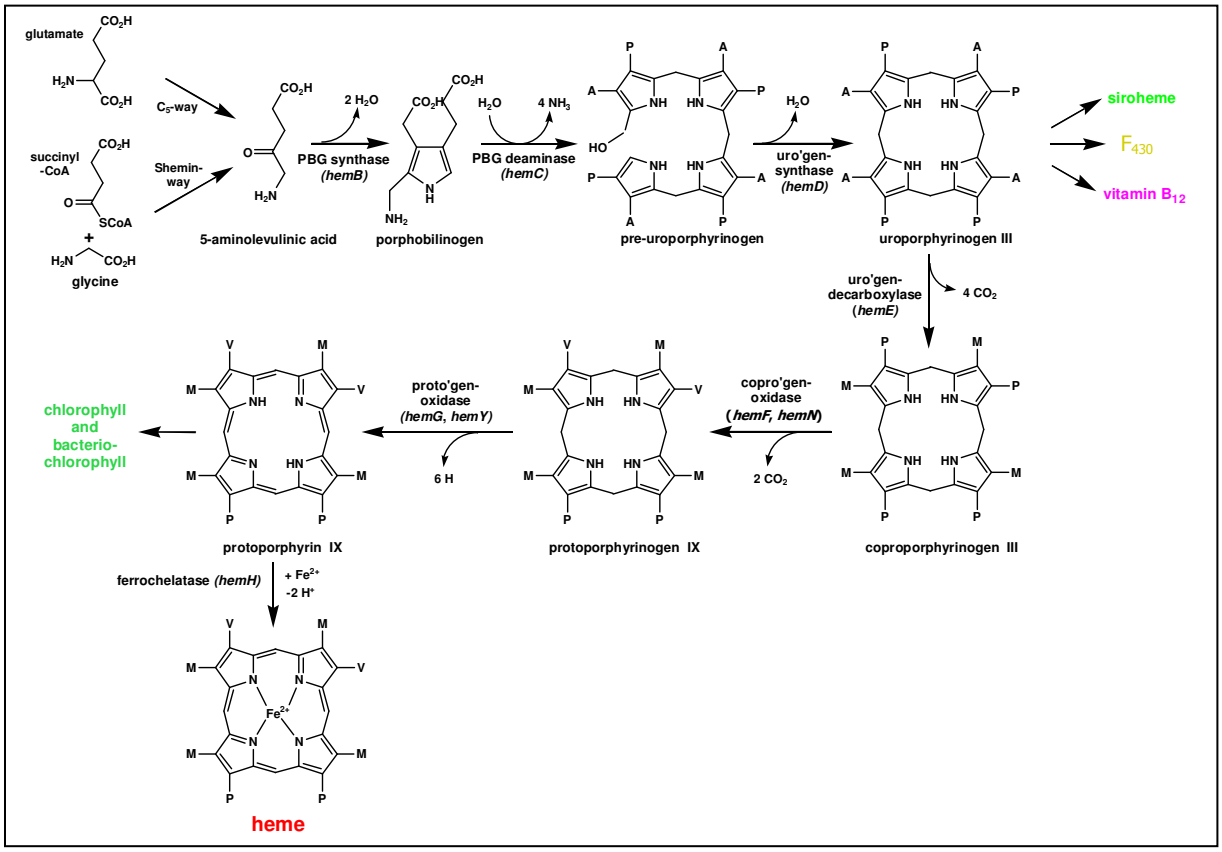

Figure 4: Biosynthesis of heme. All steps from the precursors glutamate or succinyl-CoA and glycine, respectively, via the central intermediates 5-aminolevulinic acid, uroporphyrinogen III and protoporphyrin IX are shown. The names of enzymes and respective genes are given above/below the arrows. A, acetate side chain, P, propionate side chain, M, methyl group, V, vinyl group. PBG, porphobilinogen, uro'-/copro'-/proto'gen, uro-/copro-/protoporphyrinogen.

1.1.3.1 Biosynthesis of ALA

The common precursor of all tetrapyrroles, ALA, which contains all carbon and nitrogen atoms required to build the porphyrin macrocycle, is synthesized in nature by two unrelated routes (Jordan, 1991b). The pathway discovered first was the Shemin pathway. It is employed by animals, fungi and α-proteobacteria (Shemin and Russell, 1953). In these organisms the pyridoxal 5'-phosphate dependent enzyme ALA synthase catalyzes the condensation of succinyl-CoA and glycine to ALA with the release of coenzyme A and CO_2 (Gibson *et al.*, 1958; Kikuchi *et al.*, 1958). It should be mentioned in this context that the ancestors of mitochondria are placed in the same phylogenetic group as the α-proteobacteria.

Several years later a second, unusual pathway was described (Beale and Castelfranco, 1973). The C_5-pathway, found in plants, archaea and most bacteria, starts from glutamyl-tRNA and

involves the subsequent action of two enzymes (Jahn *et al.*, 1992). First, the NADPH-dependent enzyme glutamyl-tRNA reductase (GluTR) reduces glutamyl-tRNA to glutamate-1-semialdehyde (GSA). The $tRNA^{Glu}$ is released during this reaction. GSA is subsequently converted into ALA by glutamate-1-semialdehyde-2,1-aminomutase (GSAM) in a pyridoxamine 5'-phosphate dependent transamination reaction (Moser *et al.*, 1999). Only recently, complex formation between the two enzymes GluTR and GSAM was verified experimentally (Lüer *et al.*, 2005). This had previously been proposed based on the high reactivity of the intermediate GSA and the structural complementarity of the two enzymes (Moser *et al.*, 2002).

1.1.3.2 The Central Pathway from ALA to Uroporphyrinogen III

The enzyme porphobilinogen synthase (PBGS; also ALA dehydratase) catalyzes the asymmetric condensation of two molecules of ALA to form the monopyrrole porphobilinogen (PBG). This reaction is the first step common to the biosynthesis of all tetrapyrroles. All PBGS enzymes characterized so far are metal-dependent, requiring either Mg^{2+}, Zn^{2+} or both (Erskine *et al.*, 1997; Frankenberg *et al.*, 1999; Shoolingin-Jordan *et al.*, 2002; Frère *et al.*, 2005).

Four molecules of PBG are consecutively polymerized to the unstable linear tetrapyrrole pre-uroporphyrinogen (1-hydroxymethylbilane) (Jordan, 1994). Four molecules of NH_3 are lost during this tetramerization. The enzyme catalyzing the reaction, porphobilinogen deaminase (PBGD; also hydroxymethylbilane synthase), requires the unusual cofactor dipyrromethane which consists of two molecules of PBG (Jordan and Warren, 1987). The cofactor is covalently attached to the enzyme and acts as a starting point for the tetramerization of PBG without being integrated into the final product.

Pre-uroporphyrinogen is directly passed on from PBGD to the next enzyme, uroporphyrinogen III synthase. This enzyme completes the conversion of PBG into uroporphyrinogen III by catalyzing the inversion of ring D of pre-uroporphyrinogen with subsequent cyclization of the molecule. The reaction yields the first asymmetric cyclic tetrapyrrole intermediate uroporphyrinogen III (Battersby and Leeper, 1990). The generation of an asymmetric macrocycle is a prerequisite for the recognition of the molecule by the following enzymes. For this reason solvent exposure of the intermediate pre-uroporphyrinogen has to be avoided, as this would result in spontaneous cyclization to the symmetric molecule uroporphyrinogen I which inhibits heme biosynthesis.

1.1.3.3 Conversion of Uroporphyrinogen III into Heme

As mentioned in section 1.1.2, uroporphyrinogen III represents a branching point in tetrapyrrole biosynthesis. On the branch leading to the formation of heme and (bacterio-) chlorophyll uroporphyrinogen decarboxylase catalyzes the sequential decarboxylation of the four acetate side chains of uroporphyrinogen III (located in positions C2, C7, C12 and C18; compare Figure 1) to methyl groups, yielding coproporphyrinogen III (Akhtar, 1991). The decarboxylation of the four rings was found to proceed in the order D, A, B, C (Jackson *et al.*, 1976); but even though a crystal structure of the enzyme in complex with its product is now available (Phillips *et al.*, 2003), the exact mechanism of uroporphyrinogen decarboxylase is still not understood.

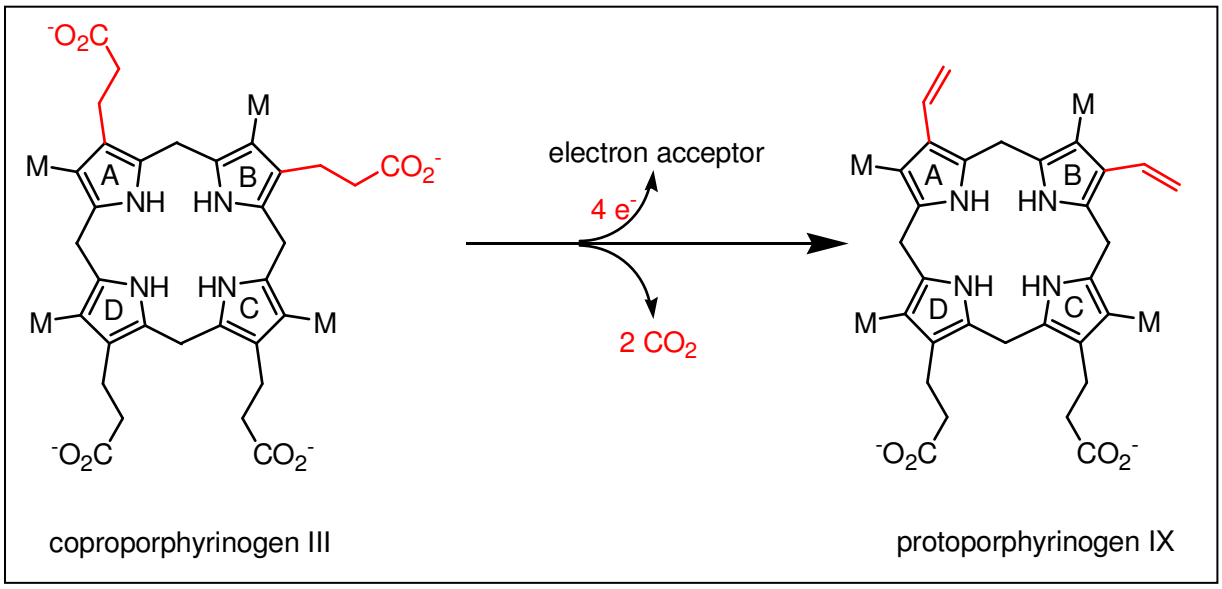

Figure 5: The oxidative decarboxylation of coproporphyrinogen III to protoporphyrinogen IX catalyzed by the enzyme coproporphyrinogen III oxidase. The two propionate side chains to be decarboxylated and the resulting vinyl groups are shown in red. M, methyl group.

In the next step, which is illustrated in Figure 5, the propionate side chains of rings A and B of coproporphyrinogen III (positions C3 and C8; compare Figure 1) are consecutively converted into the corresponding vinyl groups of the product protoporphyrinogen IX (Sano and Granick, 1961; Akhtar, 1991). During this oxidative decarboxylation reaction two molecules of CO_2 are released and a terminal electron acceptor is required. Two types of enzymes catalyzing the reaction are found in nature. One is the oxygen-dependent coproporphyrinogen oxidase (CPO) HemF, which catalyzes the reaction under aerobic conditions using molecular oxygen as electron acceptor. The other is the oxygen-independent coproporphyrinogen oxidase HemN, which functions independently of oxygen utilizing an

alternative electron acceptor. Comparison of the amino acid sequences of the O_2-dependent and the O_2-independent enzyme did not reveal any significant homology. For the aerobic reaction the isolation of harderoporphyrinogen (C3: vinyl group, C8: propionate group) as an intermediate has provided evidence that the propionate side chain of ring A is decarboxylated prior to that of ring B (Kennedy *et al.*, 1970; Jackson *et al.*, 1980).

The O_2-dependent CPO HemF is mainly a eukaryotic enzyme although it has been found in a few bacteria. In prokaryotes, however, the O_2-independent enzyme HemN is prevalent (Panek and O'Brian, 2002). HemF proteins from several - mostly eukaryotic - organisms have been investigated and quite different results have been obtained e.g. with regard to their metal content (Dailey, 2002). Human HemF did not contain any detectable cofactors or metals (Medlock and Dailey, 1996) while the mouse enzyme was reported to contain copper (Kohno *et al.*, 1996). The recently purified and characterized *E. coli* enzyme was shown to be manganese-dependent (Breckau *et al.*, 2003). Very recently the first crystal structure of an O_2-dependent CPO - the yeast enzyme - has been solved, revealing the absence of any bound metal ion (Phillips *et al.*, 2004). The O_2-independent enzyme HemN is presented in more detail in section 1.3.

The penultimate step of heme biosynthesis, the six electron oxidation of protoporphyrinogen IX to protoporphyrin IX, is catalyzed by the enzyme protoporphyrinogen IX oxidase (PPO). Protoporphyrin IX contains a system of completely conjugated double bonds. PPOs of eukaryotic origin are again the predominantly characterized enzymes (Koch *et al.*, 2004). They contain a flavin cofactor and utilize molecular oxygen as terminal electron acceptor, as does the *B. subtilis* enzyme HemY (Hansson and Hederstedt, 1992, 1994) which is highly homologous to the eukaryotic proteins. In *E. coli* and very few other bacterial genera an entirely different gene, termed *hemG*, was identified in connection with PPO activity. However, no enzyme activity could be shown for the corresponding protein, indicating that the gene might encode a subunit of a larger PPO complex (Sasarman *et al.*, 1979, 1993). In the genomes of the majority of heme-synthesizing prokaryotes no potential *hemG* or *hemY* gene has been detected (Panek and O'Brian, 2002).

The last step of heme biosynthesis is the insertion of ferrous iron into protoporphyrin IX. This reaction is catalyzed by ferrochelatase. Interestingly, human ferrochelatase was shown to be a homodimer (Wu *et al.*, 2001), while the *B. subtilis* enzyme is a monomer (Al-Karadaghi *et al.*, 1997; Lecerof *et al.*, 2000). For the eukaryotic enzymes the existence of a ternary complex or at least close interaction of the last three enzymes of the pathway (CPO, PPO and ferrochelatase) has been discussed (Ferreira *et al.*, 1988; Dailey, 1990b, 2002; Proulx *et al.*,

1993; Koch *et al.*, 2004).

1.1.3.4 Examples for Medical Applications

Porphyrias are a group of inherited or acquired disorders of heme biosynthesis. A deficiency of any of the enzymes in the biosynthetic pathway can lead to a variety of clinical symptoms (Foran and György, 2003). Depending on the defective enzyme, certain toxic intermediates accumulate, causing neurovisceral symptoms, photosensitivity or both. A prerequisite for effective treatment in these cases is a better understanding of the molecular function of the respective enzymes.

The phototoxic effect of free porphyrins is utilized in cancer therapy (Fuchs *et al.*, 2000). Application of heme precursors to tumor cells leads to the accumulation of photoexitable intermediates and facilitates the subsequent destruction of the tissue. Strategies to avoid the metabolization of these intermediates - e.g. by inhibition of certain enzymes - could improve the treatment.

1.2 Radical SAM Enzymes

1.2.1 Iron-Sulfur Cluster Containing Proteins

Although first evidence for a role of iron-sulfur (FeS) compounds in biological reactions existed earlier, it was not until the 1960s that the first FeS cluster proteins were identified. Then, however, knowledge began to increase quickly and the significance of FeS cluster proteins was soon recognized, as they are ubiquitous in all living matter and involved in three major processes required to sustain life on earth - nitrogen fixation, photosynthesis and respiration. FeS clusters, the prosthetic groups of many FeS proteins, are considered to have possibly been among the oldest cofactors on earth, assuming that sulfur and iron were abundant at the time of cellular genesis (Beinert *et al.*, 1997; Beinert, 2000).

The basic structural feature of FeS clusters is the Fe_2S_2 rhombus with tetrahedral iron coordination. This basic arrangement can be varied to a wide range of structures of increasing complexity. The most common cluster types found in nature are the [2Fe-2S] and the [4Fe-4S] cluster (Figure 6). Binding to the respective protein usually occurs via cysteine ligands. However, FeS clusters of higher nuclearity also exist (Beinert, 2000; Frazzon and Dean, 2003). Furthermore, these clusters can contain metals other than iron and use ligands other than cysteine. An example of a complex FeS cluster is provided by the FeMo-cofactor of

nitrogenase with a [7Fe-9S-Mo] core (Figure 6). FeS cluster properties are additionally influenced by the protein environment surrounding the cluster, and certain cluster cores can be mutually interconverted.

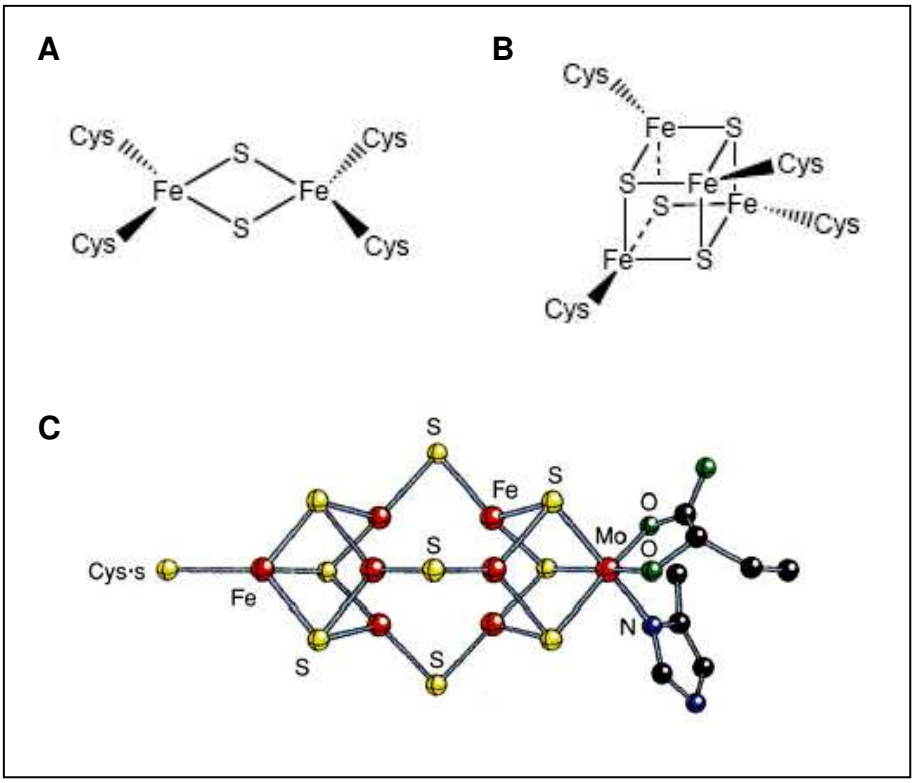

Figure 6: Different types of iron-sulfur clusters found in nature. The most common types are the [2Fe-2S] cluster (**A**) and the [4F-4S] cluster (**B**). The FeMo-cofactor from nitrogenase (**C**) represents an example of a more complex iron-sulfur cluster. (A and B, from Kiley and Beinert, 2003; C, from Beinert *et al.*, 1997)

The versatile chemical and electronic properties of FeS clusters are reflected by the functional diversity of FeS proteins (Beinert, 2000; Kiley and Beinert, 2003). Their role in electron transfer was recognized first and for a long time remained the only known function. In the meantime, however, participation of FeS proteins in other processes has been shown. One example is substrate binding and catalysis in aconitase (Werst *et al.*, 1990). Other functions include sensing and gene regulation as found for the *E. coli* transcription factors SoxR and Fnr. SoxR responds to superoxide stress and is activated for DNA binding and transcription activation only when its FeS cluster is in the oxidized $[2Fe\text{-}2S]^{2+}$ form (Ding and Demple, 1997; Demple *et al.*, 2002). Fnr acts as a global regulator under anaerobic conditions, promoting the switch from aerobic to anaerobic energy metabolism in *E. coli*. In its active form Fnr is a homodimer containing one [4Fe-4S] cluster per subunit. Upon exposure to oxygen the cluster is converted into a [2Fe-2S] cluster, causing disintegration of the oligomeric state and thereby a loss of activity (Khoroshilova *et al.*, 1997). Response to iron

availability is regulated on the translational level by the mRNA binding iron regulatory protein (IRP), the apo-form of a cytosolic aconitase (Beinert *et al.*, 1996). Furthermore, FeS clusters are involved in initiating reactions that occur by free radical mechanisms.

1.2.2 A New Family of Enzymes Generating a Radical from *S*-Adenosyl-L-Methionine: Radical SAM Enzymes

For a long time free radicals were considered to be rarely involved in enzymatic reactions. The main radical species in enzymatic catalysis which have already been known for decades are the semiquinone forms of flavins and quinone cofactors in electron transfer and the tyrosine radical in ribonucleotide reductases (Frey, 2001). In recent years radical-based enzymatic reactions have increasingly been recognized in diverse biological processes (Stubbe and van der Donk, 1998). In these systems the radical is either located on a protein or on a substrate molecule. Despite the considerable range of catalytic reactions involving a radical known today, relatively few biochemical mechanisms have been described that facilitate the initial generation of an organic radical. One established mechanism uses molecular oxygen, resulting in the formation of a stable tyrosyl radical after hydrogen atom abstraction from the tyrosine residue (Stubbe, 2003). O_2-dependent radical generation is also discussed for some heme- and copper-dependent oxidases (Rogers and Dooley, 2003).

As far as O_2-independent enzymatic reactions are concerned, two types of mechanisms have now been recognized for radical generation. Of these, adenosylcobalamin-dependent reactions were first associated with free radical biochemistry in the 1970s (Frey, 1990; Frey and Reed, 2000). Enzymes containing adenosylcobalamin cofactors induce homolytic cleavage of the weak C-Co bond in the B_{12} cofactor, generating cob(II)alamin and a 5'-deoxyadenosyl radical. This highly reactive radical can subsequently abstract hydrogen atoms from unactivated C-H bonds in the substrate, thereby forming the corresponding substrate radicals. A second class of enzymes - also generating a 5'-deoxyadenosyl radical but from *S*-adenosyl-L-methionine (SAM) - emerged more recently (Sofia *et al.*, 2001). SAM had long been known as a source of methyl groups in biological methylation reactions. It now becomes apparent that SAM actually initiates a greater diversity of radical reactions than adenosylcobalamin (Frey and Magnusson, 2003). As the S-C bond in SAM is too stable to be broken homolytically, SAM-dependent enzymes utilize a reduced FeS cluster to facilitate reductive cleavage of this bond yielding the 5'-deoxyadenosyl radical and methionine (Jarrett, 2003). The SAM cleavage reaction is illustrated in Figure 7.

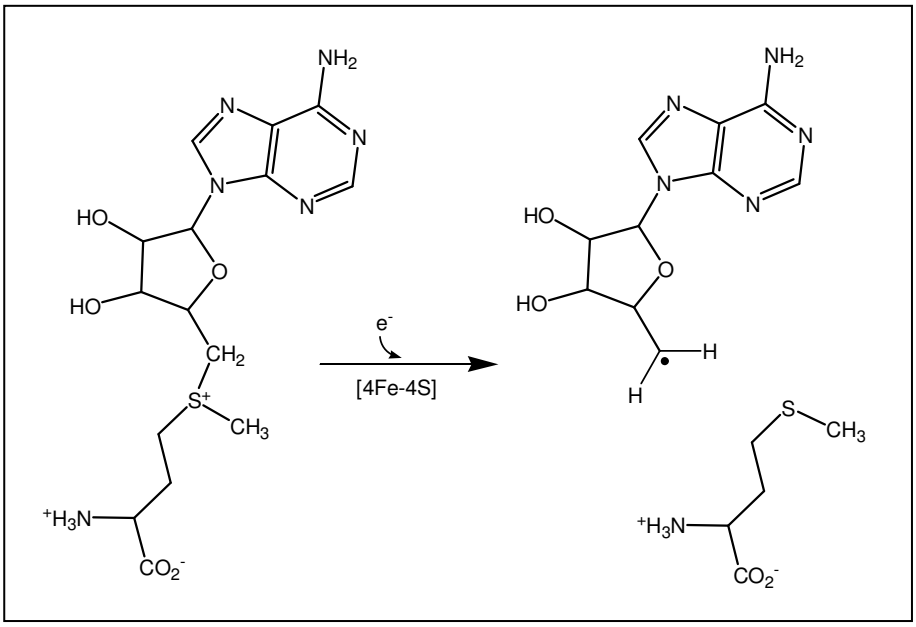

Figure 7: Cleavage of *S*-adenosyl-L-methionine into a 5'-deoxyadenosyl radical and methionine

Over the last decade, common features have been recognized for some SAM-dependent radical enzymes (Frey and Reed, 2000; Cheek and Broderick, 2001). However, it was not until 2001 that a bioinformatics study finally proposed the definition of a large new class of radical enzymes, the Radical SAM protein family (Sofia *et al.*, 2001). Putative members are found in all three domains of life and encompass enzymes involved in very diverse reactions, e.g. DNA precursor, vitamin, cofactor, antibiotic and herbicide biosynthesis and biodegradation pathways. Among the most extensively investigated representatives of the Radical SAM enzyme family are lysine-2,3-aminomutase (LAM), anaerobic ribonucleotide reductase activating enzyme (anRNR-ae), pyruvate formate lyase activating enzyme (PFL-ae) and biotin synthase (BioB).

Despite the wide range of functions Radical SAM enzymes share some common characteristics and mechanisms. In addition to requiring SAM as a cofactor for radical generation (e.g. Moss and Frey, 1987; Ollagnier de-Choudens *et al.*, 2002), all members of the group contain a unique [4Fe-4S] cluster. Three iron atoms of this cluster are coordinated by the three cysteines of the characteristic CxxxCxxC motif conserved in the amino acid sequences of all Radical SAM enzymes (e.g. Ollagnier *et al.*, 1997; Tamarit *et al.*, 2000). A conserved glycine-rich sequence motif is also found in all members of the protein family, but apart from these two motifs there is little sequence homology between the different groups of enzymes.

The mechanism leading to radical generation is identical in all Radical SAM enzymes (Figure 8). The radical is subsequently used to initiate the diverse reactions catalyzed by the

different enzymes. The first step of the common mechanism is the reduction of the iron-sulfur cluster by a cellular system like flavodoxin reductase / flavodoxin in *E. coli* (e.g. Mulliez *et al.*, 2001). The reduced FeS cluster subsequently transfers its electron to SAM which is cleaved into methionine and a 5'-deoxyadenosyl radical (see above) (Padovani *et al.*, 2001; Ollagnier de-Choudens *et al.*, 2002). This radical is too unstable to be observed, but the observation of an allylic analog of the 5'-deoxyadenosyl radical was reported for LAM when 3', 4'-anhydroadenosylmethionine was used (Magnusson *et al.*, 1999, 2001). The 5'-deoxyadenosyl radical then abstracts a hydrogen atom from an appropriately positioned carbon atom either of the enzyme, generating a glycyl radical, or of the substrate, giving rise to the corresponding substrate radical. Examples for the first case are anRNR-ae and PFL-ae (Duboc-Toia *et al.*, 2003), examples for the second case are LAM and BioB (Ballinger *et al.*, 1992a/b; Escalettes *et al.*, 1999). In most reactions the final products of SAM cleavage are methionine and 5'-deoxyadenosine. Consequently, SAM is consumed and has to be considered as a co-substrate rather than a true cofactor. Only for LAM and spore photoproduct lyase (SPP lyase) it was shown so far that SAM is regenerated and therefore acts as a true cofactor (Moss and Frey, 1990; Cheek and Broderick, 2002). Reaction steps following the generation of the protein or substrate radical vary for each individual enzyme.

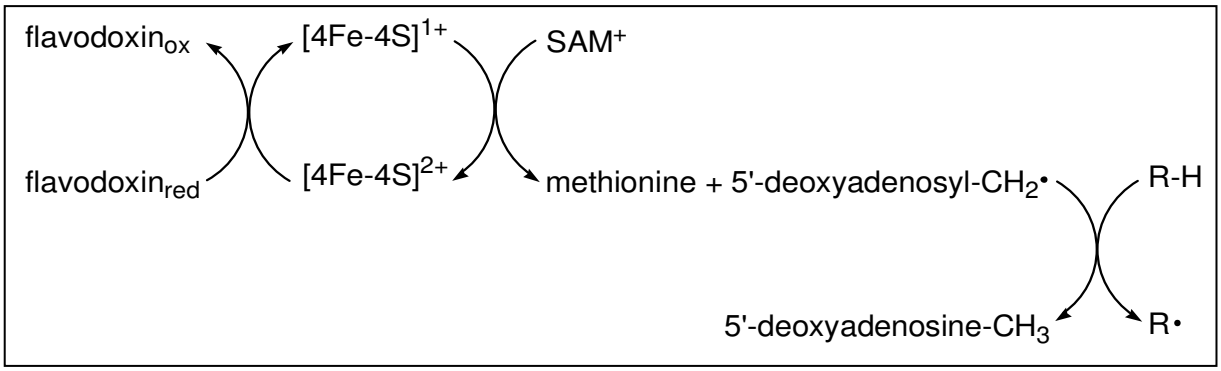

Figure 8: Initial reaction steps common to all Radical SAM enzymes. The FeS cluster is reduced and subsequently transfers its electron to SAM, causing cleavage of SAM into methionine and a 5'-deoxyadenosyl radical. The highly reactive 5'-deoxyadenosyl radical abstracts a hydrogen atom from either protein or substrate, thereby generating the corresponding protein or substrate radical. R-H, protein or substrate molecule, R•, protein or substrate radical.

Most knowledge on Radical SAM enzymes was originally obtained from spectroscopic studies. In the meantime, the crystal structures of three members of this group - HemN, BioB and MoaA - have been determined (Layer *et al.*, 2003; Berkovitch *et al.*, 2004; Hänzelmann and Schindelin, 2004; see section 1.3.1), confirming the proposed coordination of SAM to the fourth non-cysteine ligated iron atom of the [4Fe-4S] cluster (Walsby *et al.*, 2002a/b).

1.3 The Oxygen-independent Coproporphyrinogen III Oxidase

1.3.1 The O_2-independent Coproporphyrinogen III Oxidase HemN from *Escherichia coli* is a Radical SAM Enzyme

The first coproporphyrinogen III oxidase activities were shown for eukaryotic enzymes and had an absolute requirement for molecular oxygen (Sano and Granick, 1961; compare section 1.1.3.3). This finding soon raised the question how microorganisms growing under strictly anaerobic conditions but utilizing bacteriochlorophylls and cytochromes for photosynthesis and anaerobic respiration, respectively, achieve the conversion of coproporphyrinogen III into protoporphyrinogen IX. Tait was the first to report the observation of oxygen-independent CPO activity in cell-free extracts of *Rhodobacter sphaeroides* (formerly *Rhodopseudomonas spheroides*) incubated under anaerobic conditions in the presence of Mg^{2+}, ATP and L-methionine or *S*-adenosyl-L-methionine (Tait, 1969). NADH and $NADP^+$ were found to have a positive effect on the reaction, and in addition, iron appeared to be required (Tait, 1972). In the 1980s the O_2-independent conversion of coproporphyrinogen III into protoporphyrinogen IX was studied in cell-free extracts prepared from various bacteria including *R. sphaeroides* and *Rhizobium japonicum* (Keithly and Nadler, 1983; Seehra *et al.*, 1983). While the cofactor requirements described by Tait were confirmed, none of these studies resulted in identification or characterization of the protein(s) responsible for the reaction. About ten years later genetic approaches using *R. sphaeroides* and *Salmonella typhimurium* identified genetic loci related to O_2-independent coproporphyrinogen oxidase acitivtiy which were termed *hemN* (Coomber *et al.*, 1992; Xu *et al.*, 1992; Xu and Elliott, 1994). The *hemN* genes of several other bacteria including *Escherichia coli*, *Alcaligenes eutrophus* and *Pseudomonas aeruginosa* were subsequently cloned and characterized (Troup *et al.*, 1995; Lieb *et al.*, 1998; Rompf *et al.*, 1998).

E. coli hemN was cloned into vector pET-3a and a purification procedure was established for the recombinant protein (Verfürth, 1999). Subsequently, an enzyme assay was developed which demonstrated O_2-independent CPO activity for recombinant purified *E. coli* HemN in the presence of NADH, SAM and an *E. coli* cell-free extract (Layer, 2001; Layer *et al.*, 2002). Furthermore, the protein was shown to contain a [4Fe-4S] cluster and site-directed mutagenesis revealed that the first three cysteine residues of the characteristic CxxxCxxCxC motif conserved in the amino acid sequences of all HemN proteins are essential for FeS cluster coordination (Layer *et al.*, 2002). Clearly, HemN possesses several characteristics typical of Radical SAM enzymes, and the bioinformatics study defining the Radical SAM

protein family in 2001 indeed included HemN in this group (Sofia *et al.*, 2001). In 1994 Xu and Elliott had already suggested that a parallel might exist between HemN and enzymes like LAM, anRNR-ae and PFL-ae, because they all seemed to require SAM without a methylation taking place (Xu and Elliott, 1994). Further studies were carried out in our laboratory to unambiguously identify *E. coli* HemN as a Radical SAM enzyme. An adequate reaction mechanism was proposed as working hypothesis which is shown in Figure 9 (for a detailed description of the mechanism see figure legend).

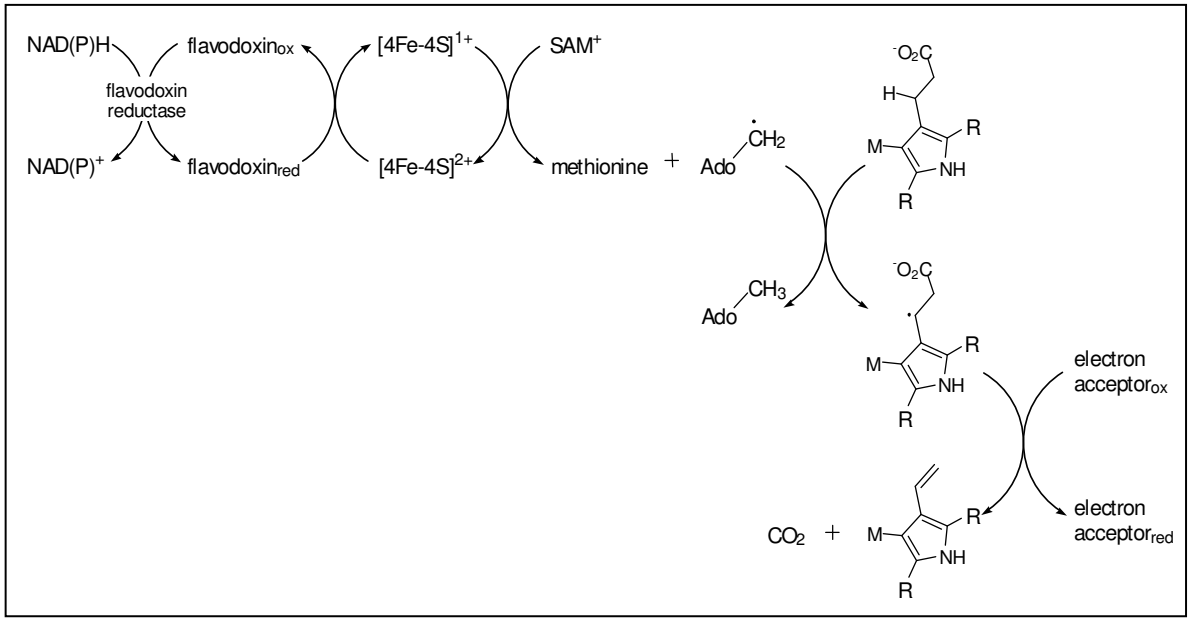

Figure 9: Proposed mechanism for the oxidative decarboxylation of coproporphyrinogen III catalyzed by HemN. The initial steps of radical generation are identical for all Radical SAM enzymes. (1) The FeS cluster is reduced by a so far unknown system (e.g. flavodoxin reductase/flavodoxin). (2) The reduced FeS cluster transfers the electron to SAM and SAM is cleaved into methionine and a 5'-deoxyadenosyl radical. (3) The 5'-deoxyadenosyl radical abstracts a hydrogen atom from the β-carbon of the substrate propionate side chain. This results in the formation of 5'-deoxyadenosine and a substrate radical. (4) In a concerted process, CO_2 is released and the vinyl group of the product is formed. This final step requires an external electron acceptor. As two propionate side chains of the substrate coproporphyrinogen III have to be decarboxylated for the formation of protoporphyrinogen IX, this scenario has to proceed twice (modified from Layer, 2004).

Cleavage of SAM into 5'-deoxyadenosine and methionine was shown to occur during the conversion of coproporphyrinogen III into protoporphyrinogen IX catalyzed by HemN (Layer *et al.*, 2005). SAM is consumed during this reaction as it is the case for the majority of Radical SAM enzymes (compare section 1.2.2). EPR experiments indicated the presence of a substrate radical in samples containing reduced HemN, SAM and coproporphyrinogen III (Layer, 2004). Additional EPR spectra recorded in the presence of different deuterium- and ^{15}N-labeled substrates revealed that the unpaired electron is at least partly localized on the β-carbon atom of the propionate side chain and partly on the carbon atom of the pyrrole ring

between the methine bridge position and the pyrrole nitrogen (C4 or C9). Using Mössbauer spectroscopy it was shown that three iron atoms of the [4Fe-4S] cluster are coordinated by cysteine residues and that the fourth iron atom is coordinated by SAM (Layer *et al.*, 2005). This had previously been demonstrated for other Radical SAM enzymes (Cosper *et al.*, 2002; Krebs *et al.*, 2002).

The Mössbauer spectroscopic data were in agreement with the crystal structure of *E. coli* HemN, which represented the first crystal structure of a member of the Radical SAM protein family (Layer *et al.*, 2003). HemN is a monomeric, two-domain protein (Figure 10). The larger N-terminal domain (residues 36-364) has a $(\beta/\alpha)_6$ core reminiscent of an incomplete $(\beta/\alpha)_8$ or TIM barrel. In comparison to a TIM barrel, the curvature of the β-sheet is less tight in the case of HemN, resulting in a large active site cavity. In the meantime, two other structures of Radical SAM enzymes have been determined, those of biotin synthase (BioB) and of an enzyme involved in molybdenum cofactor biosynthesis (MoaA) (Berkovitch *et al.*, 2004; Hänzelmann and Schindelin, 2004). Interestingly, MoaA also contains a $(\beta/\alpha)_6$ fold and BioB exhibits a complete $(\beta/\alpha)_8$ fold. In a recent bioinformatics study based on structural information, a partial or entire TIM barrel fold was predicted for all Radical SAM proteins included in the study (Nicolet and Drennan, 2004).

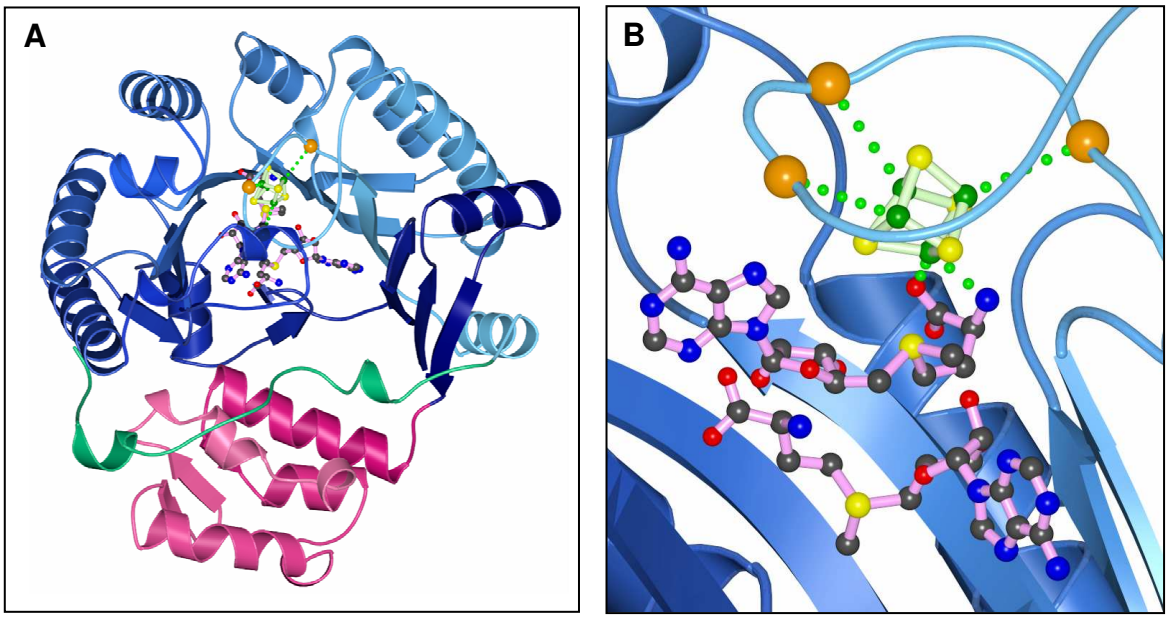

Figure 10: Crystal structure of *E. coli* HemN. A, Overall structure, showing the N-terminal catalytic domain in blue, the C-terminal domain in pink and the N-terminal 'trip-wire' in green. **B**, Enlarged section of the active site cavity of the catalytic domain showing the [4Fe-4S] cluster and the two SAM molecules. Orange spheres mark the conserved cysteines which coordinate three iron atoms (green) of the FeS cluster. The fourth iron atom is coordinated by SAM1. (A, from Layer *et al.*, 2003)

The C-terminal domain of HemN (residues 365-448) consists of a bundle of four α-helices

and a small antiparallel β-sheet. N-terminal residues 1-35 form an extended loop without pronounced secondary structure. For both the C-terminal domain and the short N-terminal 'trip-wire' a possible function in covering the active site upon substrate binding has been suggested. Three cofactors - a [4Fe-4S] cluster and two SAM molecules (SAM1 and SAM2) - are bound within the active site pocket (Figure 10). Three iron atoms of the cluster are coordinated by the three conserved cysteine residues of the Radical SAM CxxxCxxC motif (Cys^{62}, Cys^{66} and Cys^{69} in *E. coli* HemN). The fourth non-cysteine ligated iron atom is coordinated by the amino nitrogen and one carboxylate oxygen of the methionine moiety of SAM1. SAM2 is located in close proximity to SAM1. This observed binding of a second SAM molecule in the HemN crystal structure was entirely unexpected as it had not previously been shown for any of the other Radical SAM proteins. A preliminary model of substrate binding as well as potential binding sites for an electron donor like flavodoxin and a final electron acceptor have been proposed (Layer *et al.*, 2003).

1.3.2 In Several Prokaryotic Genomes Genes Encoding HemF and HemN have not been Found – Do These Organisms Possess an Alternative CPO?

In the majority of prokaryotes not all genes required for heme biosynthesis have been identified. A database search performed in 2002 considered all 69 prokaryotes of which the entire genome had been sequenced at that date (Panek and O'Brian, 2002). This approach revealed that in about two-thirds of the genomes one or several genes of the heme biosynthetic pathway were missing.

In the genomes of several heme synthesizing archaea only the genes required for uroporphyrinogen III formation have been detected. This raises the possibility of an alternative pathway for the remaining steps. In some bacteria, on the other hand, only one or two enzymes could not be identified by homology searches. In these cases it is more likely that an identical or at least very similar reaction is carried out by a structurally different and, therefore, yet unrecognized enzyme. The missing homologues are most often those of either *hemD*, *hemF*/*hemN* or *hemG*/*hemY* (encoding uroporphyrinogen III synthase, coproporphyrinogen III oxidase and protoporphyrinogen IX oxidase).

Genes encoding putative alternative O_2-independent CPOs have been described for some organisms and considerable confusion has been created due to inconsistent naming. Today, the general consent is that O_2-dependent CPOs are designated HemF and O_2-independent CPOs HemN.

However, when a putative second O_2-independent CPO was discovered in *Rhodobacter sphaeroides* 2.4.1, it was named HemZ (Zeilstra-Ryalls and Kaplan, 1995), probably to distinguish it from the first – even though this first O_2-independent enzyme had been designated HemF (renamed HemN in the meantime) (Coomber *et al.*, 1992). In 1996 a first potential CPO encoding gene was detected in *B. subtilis* (Homuth *et al.*, 1996). The gene was identified by the significant homology of its deduced amino acid sequence to *E. coli* HemN (29 % identity) and was consequently termed *hemN*.

These first discoveries and namings did not consider certain differences between the potential O_2-independent CPOs, particularly in the conserved cysteine motif. All O_2-independent CPOs for which CPO activity has been demonstrated on the enzyme level have in common a conserved motif of four cysteine residues (CxxxCxxCxC). In contrast, the newly discovered *B. subtilis* enzyme had only three conserved cysteine residues (CxxxCxxC). However, both *R. sphaeroides* CPOs possessed the entire motif. Taking into account their high sequence identity to each other (45 %) and to other HemN proteins (e.g. 34 % to *E. coli* HemN) it seems obvious that *R. sphaeroides* has two HemNs and that the first potential CPO detected in *B. subtilis* should rather be termed HemZ.

It has been established for *E. coli* HemN that only the first three cysteine residues of the CxxxCxxCxC motif are involved in iron-sulfur cluster coordination (Layer *et al.*, 2003). However, also the fourth cysteine has been shown to be essential for enzyme function (Layer *et al.*, 2002). The distinction between enzymes containing three and enzymes containing four conserved cysteines should also be made to differentiate between the group of enzymes for which O_2-independent CPO activity has been experimentally confirmed and the group of enzymes for which direct evidence is still lacking. Table 1 provides an overview of the occurrence of the alternative CPO encoding genes in a variety of bacteria. As Table 1 indicates *hemZ* is widely distributed among bacteria. Unlike *hemN*, it has also been found in some eukaryotic genomes, e.g. in humans.

Shortly after the first, a second potential O_2-independent CPO encoding gene in *B. subtilis* was described (Homuth *et al.*, 1999). The corresponding enzyme also contained only three conserved cysteines and was ‘correctly’ termed HemZ. In order to allow clearer differentiation between the different groups of CPOs, the first *B. subtilis* CPO (‘HemN’ in the original publication) will be designated HemZ in this work and the second *B. subtilis* CPO (‘HemZ’ in the original publication) will be designated HemZ2.

The most important information to be drawn from the overview in Table 1 is that for *B. subtilis* and some related organisms none of the well characterized CPOs (HemF or HemN)

have been identified. They have either one or two HemZ proteins. Initial steps to investigate their function have been undertaken for both HemZ and HemZ2 from *B. subtilis* (Homuth *et al.*, 1996, 1999; Hippler *et al.*, 1997). For both genes successful complementation of a heme-requiring *S. typhimurium hemF hemN* double mutant has been reported. However, neither a *B. subtilis hemZ* or *hemZ2* single mutant nor a *hemZ hemZ2* double mutant exhibited a distinct growth phenotype. Mutants were shown to accumulate coproporphyrin III under anaerobic, but not under aerobic conditions. In consequence, it is still unclear whether *B. subtilis hemZ* and/or *hemZ2* indeed encode proteins with CPO activity. In particular, no characterization of a HemZ protein has been published to date.

Table 1: Occurrence of genes encoding coproporphyrinogen III oxidases in different bacteria

Organism[1]	CPO encoding genes	CPO gene homologue
Gram-negative bacteria		
α-proteobacteria		
Agrobacterium tumefaciens	*hemF*, *hemN*	*hemZ*
Mesorhizobium loti	*hemF*, *hemN*	*hemZ*
Sinorhizobium meliloti	*hemF*, *hemN*	*hemZ*
γ-proteobacteria		
Buchnera sp.		*hemZ*
Escherichia coli	*hemF*, *hemN*	*hemZ*
Haemophilus influenzae		*hemZ*
Pseudomonas aeruginosa	*hemF*, *hemN*	*hemZ*
Salmonella typhimurium	*hemF*, *hemN*	*hemZ*
Vibrio cholerae	*hemF*, *hemN*	*hemZ*
Yersinia pestis	*hemF*, *hemN*	*hemZ*
other groups of *proteobacteria*		
Helicobacter pylori	*hemN*	*hemZ*
Neisseria meningitidis	*hemN*	*hemZ*
Ralstonia solanacearum	*hemF*, *hemN*	*hemZ*
Gram-positive bacteria		
Bacillus halodurans		*hemZ* (2 x)
Bacillus subtilis		*hemZ* (2 x)
Clostridium acetobutylicum		*hemZ* (2 x)
Clostridium perfringens		*hemZ* (2 x)

Table 1 (cont.): Occurrence of genes encoding coproporphyrinogen III oxidases in different bacteria

Organism[1]	CPO encoding genes	CPO gene homologue
Gram-positive bacteria		
Lactococcus lactis		*hemZ*
Listeria monocytogenes		*hemZ*
Mycobacterium tuberculosis		*hemZ*
Staphylococcus aureus		*hemZ*
Streptococcus pneumoniae		*hemZ*
Streptococcus pyogenes		*hemZ*
Cyanobacteria		
Nostoc sp.	*hemF*, *hemN*	*hemZ*
Synechocystic sp.	*hemF*, *hemN*	*hemZ*

[1] Of all organisms included in this table, the complete genome sequence has been determined. The list does not encompass all prokaryotes which have been sequenced. Many genes have been identified by BLAST alignments. (modified from Panek and O'Brian, 2002)

1.4 Objectives of the Work

Two major aims were pursued within the scope of this work. One was the further characterization of *E. coli* HemN, particularly with regard to the proposed reaction mechanism. As the information provided by the crystal structure was available, the focus of this work was placed on a structure-based mutagenesis approach. Suitable HemN mutant proteins were to be generated by site-directed mutagenesis to investigate the functional role of SAM2 and the proposed substrate binding site. In addition, an approach was to be undertaken to quantitatively assess the stoichiometry between protoporphyrinogen IX formation and cleavage of *S*-adenosyl-L-methionine during HemN catalysis.

The second objective of this work was to investigate whether HemZ, the proposed second oxygen-independent coproporphyrinogen III oxidase, does indeed catalyze the oxidative decarboxylation of coproporphyrinogen III to protoporphyrinogen IX. The *hemZ* gene from a suitable organism was to be cloned, the protein produced and a purification procedure established. The purified HemZ protein was then to be tested for CPO activity. In case that this biochemical approach should not provide satisfactory evidence, functional complementation of a CPO-deficient mutant strain was to be carried out.

2. MATERIALS AND METHODS

2.1 Instruments and Chemicals

2.1.1 Instruments

Agarose Gel Electrophoresis	Agagel Mini	Biometra
Agarose Gel Documentation	GelDoc	Bio-Rad
	Flu-O-blu	Biozym
Anaerobic Chamber		Coy Laboratories
Autoclave	LVSA 50/70	Zirbus
CD Spectropolarimeter	Jasco J810	Jasco
Centrifuges	5403	Eppendorf
	5804	Eppendorf
	miniSpin	Eppendorf
	RC 5B Plus	Sorvall
	L7-65 Ultracentrifuge	Beckman
	Speed Vac SPD 110B with Refrigerated Vapor Trap RVT400	Savant
DNA Sequencing	ABI PRISM™ 310 Genetic Analyzer	Applied Bioystems
Electroporation	Gene Pulser® II with Pulse Controller Plus	Bio-Rad
Fluorescence Spectrometer	PE LS50B	PerkinElmer
FPLC	ÄKTAprime™	Amersham Biosciences
French Press	French® Pressure Cell Press	Thermo Electron
HPLC	Jasco 1500	Jasco
pH Determination	pH meter C 6840 B	Schott
Protein Concentrating Device	Stirred Ultrafiltration Cell	Millipore
Scales	BL 1500	Sartorius
	BP 61S	Sartorius
	SBA 52	Scaltec
Scintillation Analyzer	Tri-Carb 2900 TR	PerkinElmer
SDS-PAGE	Mini Protean II	Bio-Rad

Thermocycler	Tpersonal	Biometra
	Tgradient	Biometra
Thermomixer	Thermomixer compact	Eppendorf
Ultrasonic Bath		Merck eurolab
UV/Visible Spectrophotometer	Ultrospec 2000	Amersham Biosciences
	Lambda 2	PerkinElmer
Water Purification	Synthesis A10	Millipore

2.1.2 Chemicals and Kits

Bio-Rad Protein Assay	Bio-Rad
Blue Sepharose	Amersham Biosciences
Enzymes for molecular biological applications	MBI Fermentas, New England Biolabs, Amersham Biosciences, Promega
GelStar® Nucleic Acid Gel Stain	Cambrex
Glutathion Sepharose	Amersham Biosciences
Mini Dialysis Units (Slide-A-Lyzer)	Pierce
OptiPhase HiSafe 2 (scintillation cocktail)	PerkinElmer
PD-10 columns	Amersham Biosciences
PreScission™ Protease	Amersham Biosciences
QIAquick Gel Extraction Kit	Qiagen
QIAquick PCR Purification Kit	Qiagen
QuikChange® Site-Directed Mutagenesis Kit	Stratagene
S-adenosyl-L-[*methyl*-^{14}C]methionine	Amersham Biosciences
Size standards for agarose gels:	
GeneRuler™ DNA Ladder Mix	MBI Fermentas
MassRuler™ DNA Ladder Mix	MBI Fermentas
Size standards for SDS-PAGE:	
Dalton Mark VII-L	Sigma
Protein Molecular Weight Marker	MBI Fermentas

Chemicals and reagents not specifically listed here were purchased from the following manufacturers: Amersham Biosciences, Fluka, Gerbu, Merck, Paesel+Lorei, Roth, Sigma.

2.2 Bacterial Strains and Plasmids

All bacterial strains and plasmids used for this work are listed in Table 2 and Table 3.

Table 2: Bacterial strains used in this work

Strain	Description	Reference
Escherichia coli strain		
DH5α	F⁻ Φ80d*lac*ZΔM15(*lac*ZYA-*arg*F) U169 *rec*A1 *end*A1 *hsd*R17(r_k^-, m_k^+) *pho*A *sup*E44 λ⁻ *thi*-1 *gyr*A96 *rel*A1	Invitrogen
DH10b	F⁻ *mcrA* Δ(*mrr-hsd*RMS-*mcr*BC) Φ80*lac*ZΔM15 Δ*lac*X74 *rec*A1 *end*A1 *ara*Δ139 Δ(*ara*, *leu*)7697 *gal*U *gal*K λ- *rps*L (Str^R) *nup*G	Invitrogen
XL1-Blue	*rec*A1 *end*A1 *gyr*A96 *thi-1 hsd*R17 *sup*E44 *rel*A1 *lac* [F´*pro*AB $lacI^q$ZΔM15 Tn*10* (Tet^r)]	Stratagene
BL21(DE3)	F⁻ *dcm omp*T *hsd*S(r_B^- m_B^-) *gal* λ(DE3)	Stratagene
BL21CodonPlus(DE3)-RIL	F⁻ *omp*T *hsd*S(r_B^- m_B^-) dcm^+ Tet^r *gal* λ(DE3) *end*A Hte[*arg*U *ile*Y *leu*W Cam^r]	Stratagene
MC4100	F⁻ Δ(*arg*F-*lac*) *ara*D139 U169 *rps*L150 (Str^r) *rel*A1 *flb*B5301 *deo*C1 *pts*F25 *rbs*R	Casadaban, 1976
MC4100 Δ*hemN*	derivative of strain MC4100, carrying chomosomal *hemN* deletion	this work
Salmonella typhimurium strain		
TE3006	*env-53 hemN704*::Mud-J(b) *hemF707*::Tn*10d*-Tet	Xu *et al.*, 1992
Bacillus subtilis strain		
DSM 168	*trp*C2	DSMZ

Table 3: Plasmids used in this work

Plasmid	Description	Reference
pET-21b	Expression vector carrying C-terminal His-Tag® sequence, T7 promoter, amp^r	Novagen
pET-22b	Expression vector carrying C-terminal His-Tag® sequence, T7 promoter, amp^r	Novagen
pGEX-6P-1	Expression vector carrying N-terminal sequence for GST from *Schistosoma japonicum* and recognition sequence for PreScission™ Protease, *tac* promoter, amp^r	Amersham Biosciences
pBlueskript SK^+	Cloning vector, *lac* promoter, amp^r	Stratagene

Table 3 (cont.): Plasmids used in this work

Plasmid	Description	Reference
pKD13	Gene disruption system, carries Kan^r flanked by FRT (FLP recognition target) sites, amp^r	Datsenko and Wanner, 2000
pKD46	Gene disruption system, carries genes for λ Red recombinase system (α, β, *exo*) under control of P_{araB} promoter, temperature sensitive replicon, amp^r	Datsenko and Wanner, 2000
pET-3a-*hemN*	pET-3a derivative encoding *E. coli* HemN	Verfürth, 1999
pET-3a-*hemN*R22A	Exchange of triplet CGA (nucleotides 64-66) for GCA, protein carries Ala instead of Arg in position 22	this work
pET-3a-*hemN*Y56A	Exchange of triplet TAC (nucleotides 166-168) for GCC, protein carries Ala instead of Tyr in position 56	this work
pET-3a-*hemN*Y56L	Exchange of triplet TAC (nucleotides 166-168) for TTG, protein carries Leu instead of Tyr in position 56	this work
pET-3a-*hemN*E145A	Exchange of triplet GAA (nucleotides 433-435) for GCA, protein carries Ala instead of Glu in position 145	this work
pET-3a-*hemN*E145I	Exchange of triplet GAA (nucleotides 433-435) for ATA, protein carries Ile instead of Glu in position 145	this work
pET-3a-*hemN*R308A	Exchange of triplet CGT (nucleotides 922-924) for GCT, protein carries Ala instead of Arg in position 308	this work
pET-3a-*hemN*R308K	Exchange of triplet CGT (nucleotides 922-924) for AAA, protein carries Lys instead of Arg in position 308	this work
pET-3a-*hemN*F310A	Exchange of triplet TTC (nucleotides 928-930) for GCC, protein carries Ala instead of Phe in position 310	this work
pET-3a-*hemN*F310L	Exchange of triplet TTC (nucleotides 928-930) for TTG, protein carries Leu instead of Phe in position 310	this work
pET-3a-*hemN*Q311A	Exchange of triplet CAG (nucleotides 931-933) for GCG, protein carries Ala instead of Gln in position 311	this work
pET-3a-*hemN*I329A	Exchange of triplet ATC (nucleotides 985-987) for GCC, protein carries Ala instead of Ile in position 329	this work

Table 3 (cont.): Plasmids used in this work

Plasmid	Description	Reference
pET-3a-*hemN*Q338A	Exchange of triplet CAG (nucleotides 1012-1014) for GCG, protein carries Ala instead of Gln in position 338	this work
pET-3a-*hemN*Q338N	Exchange of triplet CAG (nucleotides 1012-1014) for AAC, protein carries Asn instead of Gln in position 338	this work
pET-3a-*hemN*R359K	Exchange of triplet CGT (nucleotides 1075-1077) for AAA, protein carries Lys instead of Arg in position 359	this work
pET-3a-*hemN*R434A	Exchange of triplet CGC (nucleotides 1300-1302) for GCC, protein carries Ala instead of Arg in position 434	this work
pET-3a-*hemN*R434K	Exchange of triplet CGC (nucleotides 1300-1302) for AAA, protein carries Lys instead of Arg in position 434	this work
pBlue13	pBlueskript SK^+ derivative, carries 6.5 kbp fragment containing *E. coli hemF*	Troup, 1995
pBlueN7	pBlueskript SK^+ derivative, carries 2.6 kbp fragment containing *E. coli hemN*	Troup, 1995
pBlue-$hemZ_{B.s.}$	pBlueskript SK^+ derivative, carries 1.3 kbp fragment with *B. subtilis hemZ* including region 130 bp upstream of start codon	this work
pBlue-$hemZ2_{B.s.}$	pBlueskript SK^+ derivative, carries 1.8 kbp fragment with *B. subtilis hemZ2* including region 200 bp upstream of start codon	this work
pGEX-*hemZ*	pGEX-6P-1 derivative, encodes N-terminal fusion of GST with HemZ from *E. coli*	this work
pGEX-*hemZ*F25C	Exchange of triplet TTC (nucleotides 73-75) for TGC, protein carries Cys instead of Phe in position 25	this work
pGEX-$hemZ_{B.s.}$	pGEX-6P-1 derivative, encodes N-terminal fusion of GST with HemZ from *B. subtilis*	this work
pET-21b-*hemZ*	pET-21b derivative, encodes C-terminal fusion of His-Tag with HemZ from *E. coli*	this work
pET-22b-$hemZ2_{B.s.}$	pET-22b derivative, encodes C-terminal fusion of His-Tag with HemZ2 from *B. subtilis*	this work
pET-22b-$hemZ2_{B.s.}$L502Stop	Insertion of stop codon in its original position in front of sequence coding for His-Tag, production of HemZ2 without tag	this work

2.3 Growth Media and Media Additives

2.3.1 Media

As a standard medium for growth of all bacterial strains Luria Bertani (LB) medium was used unless indicated otherwise (Sambrook *et al.*, 1989). For the production of recombinant *E. coli* HemN wild type and mutant proteins, *E. coli* BL21(DE3) carrying the respective plasmids was grown in Spizizen minimal medium (SMM). TB medium (modified) was used to grow *S. typhimurium* TE3006 prior to the generation of electrocompetent cells and also to anaerobically grow *E. coli* for the generation of cell-free extract. SOC medium was used to incubate *S. typhimurium* TE3006 and *E. coli* MC4100 cells after electroporation. For solid media 1.5 % (w/v) agar-agar was added before sterilization.

LB medium	tryptone	10.0	g
	yeast extract	5.0	g
	NaCl	5.0	g
	$H_2O_{dest.}$	ad 1.0	l
TB medium	tryptone	12.0	g
	yeast extract	24.0	g
	glycerol	4.0	ml
	casamino acids	1.0	g
	$H_2O_{dest.}$	ad 880.0	ml
after autoclaving addition of:	KH_2PO_4/K_2HPO_4		
	(0.17 M/0.72 M)	100.0	ml
	glucose monohydrate (1 M)	20.0	ml
	thiamin chloride		
	hydrochloride (50 µg/ml)	1.0	ml
SOC medium	tryptone	20.0	g
	yeast extract	5.0	g
	NaCl	500.0	mg
	KCl	186.0	mg
	casamino acids	1.0	g
	$H_2O_{dest.}$	ad 970.0	ml

after autoclaving addition of:	$MgCl_2$ (2 M)	5.0	ml
	$MgSO_4$ (2 M)	5.0	ml
	glucose monohydrate (1 M)	20.0	ml
SMM medium	$(NH_4)_2SO_4$	2.0	g
	K_2HPO_4	14.0	g
	KH_2PO_4	6.0	g
	Na_3 citrate x 2 H_2O	1.0	g
	$MgSO_4$ x 7 H_2O	200.0	mg
	$H_2O_{dest.}$	ad 890.0	ml
after autoclaving addition of:	SMM mix	100.0	ml
	Trace elements	10.0	ml
SMM mix	thiamin chloride hydrochloride	5.0	mg
	glucose monohydrate	100.0	g
	Na pyruvate	55.0	g
	casamino acids	1.0	g
	$H_2O_{dest.}$	ad 1.0	l
Trace elements	$CaCl_2$ x 2 H_2O	400.0	mg
	$FeCl_2$ x 4 H_2O	575.0	mg
	$MnCl_2$ x 4 H_2O	50.0	mg
	$ZnCl_2$	85.0	mg
	$CuCl_2$ x 2 H_2O	20.0	mg
	$CoCl_2$ x 6 H_2O	30.0	mg
	Na_2MoO_4 x 2 H_2O	30.0	mg
	$H_2O_{dest.}$	ad 500.0	ml

2.3.2 Additives

Antibiotics and other additives were prepared as concentrated stock solutions, sterilized by filtration and added to the medium after autoclaving. Solutes and concentrations are summarized in Table 4. The hemin stock solution was prepared as described by McConville

and Charles (1979). Following this protocol, 200 mg of hemin (Sigma) were mixed with 5 ml Tween 80 and slowly diluted to 50 ml with H_2O; a few drops of 5M NaOH were added to support solubilization.

Table 4: Media additives

Substance	Solute	Concentration of stock solution	Final concentration
ampicillin	H_2O	100 mg/ml	50 or 100 µg/ml
kanamycin	H_2O	50 mg/ml	25 or 50 µg/ml
chloramphenicol	ethanol (70 % (v/v))	34 mg/ml	34 µg/ml
tetracycline	ethanol (70 % (v/v))	5 mg/ml	5 µg/ml
IPTG	H_2O	100 mM and 1M	50 µM – 1 mM
hemin	Tween 80 (10 % (v/v)), NaOH	4 mg/ml	40 µg/ml
$NaNO_3$	H_2O	1 M	10 mM
$(NH_4)_2Fe(SO_4)_2$ x 6 H_2O	nitrilotriacetic acid (0.6 M)	25 mg/ml	25 µg/ml

2.4 Microbiological Techniques

2.4.1 Sterilization

All media were vapour sterilized at 121 °C and 1 bar positive pressure for 20 min. Other substances and solutions were either vapour sterilized or - if temperature sensitive - sterilized by filtration (pore width 0.2 µm).

2.4.2 Growth of Bacteria

Cells for recombinant protein production were grown under anaerobic conditions. Anaerobic pre-cultures (volume 100 ml) were grown overnight at 37 °C and 100 rpm. 1 l cultures were also grown at 37 °C until induction of protein production. After induction cultures were incubated at 25 °C, either for 5 h or overnight. For the generation of cell-free extract *E. coli* cells were grown anaerobically at 37 °C for 24 h.

For the investigation of the growth phenotype of an *E. coli hemN* knock-out mutant and for functional complementation experiments using this mutant, 140 ml cultures of the respective strains were incubated under anaerobic conditions for 24-30 h. These cultures were inoculated with 1 % (v/v) of an aerobic overnight culture.

Aerobic cultures were incubated at 37 °C and 180 rpm. 5 ml tubes were used for aerobic cell

growth unless described otherwise.

Agar plates were utilized for plating 50-100 µl of a bacterial cell suspension with a Drygalski spatula, for streaking cells from another plate with an inoculating loop or a single colony from another plate with a sterile toothpick or pipette tip. They were normally incubated aerobically at 37 °C overnight.

2.4.3 Determination of Cell Density

The cell density of liquid cultures was determined by measuring the optical density (OD) at a wavelength of 578 nm. For cell densities with an $OD_{578} \geq 0.6$ dilutions were prepared before the measurement. An OD_{578} of 1 corresponds to approximately 1 x 10^9 cells/ml.

2.4.4 Storage of Bacterial Strains

Strains were kept on agar plates at 4 °C for up to four weeks. For long-term storage glycerol stocks were prepared. This was done by growing a culture for 6 to 8 h, cooling it on ice for 30 min and mixing 500 µl of the culture with 500 µl of sterile glycerol (80 % (v/v)). Stocks were immediately frozen and kept at -80 °C.

2.5 Molecular Biology Techniques

2.5.1 General Considerations when Working with DNA

To avoid contaminations with nucleases, all solutions and other equipment which was used in direct contact with DNA were sterilized either by autoclaving or filtration (compare section 2.4.1).

2.5.2 Preparation of DNA

2.5.2.1 Preparation of Genomic DNA from *Escherichia coli*

A 5 ml overnight culture of *E. coli* DH5α was harvested by centrifugation (5 min, 7000 g) and after washing the pellet once in TE buffer it was resuspended in 1 ml TE buffer. 200 µl of a 1 M NaCl solution were added and the sample was incubated on ice for 30 min. After addition of 100 µl SDS solution (10 % (w/v)) the sample was incubated at 37 °C for 1 h. 100 µl proteinase K solution (0.2 % (w/v)) were then added and incubation at 37 °C was

continued for another 30-60 min. This suspension was mixed with one volume of phenol-chloroform (1:1). After centrifugation (10 min, 7000 g) the upper (hydrous) phase was transferred into a fresh tube, and the phenol-chloroform extraction was repeated. To remove traces of phenol the extraction was then repeated once with pure chloroform. The upper (hydrous) phase of this step was again transferred into a fresh tube and DNA precipitation initiated by addition of 0.7 vol. isopropanol and 0.3 vol. of a 7.5 M ammonium acetate solution. Precipitation took place overnight at -20 °C. The sample was centrifuged at 4 °C for 30 min (7000 g) and the DNA pellet washed once with 70 % (v/v) ethanol p.a.. After all traces of ethanol had evaporated, the DNA was solubilized in 50 µl TE buffer.

TE buffer	Tris-HCl, pH 8.0	50.0 mM
	EDTA	10.0 mM

2.5.2.2 Preparation of Genomic DNA from *Bacillus subtilis*

A 25 ml overnight culture of *B. subtilis* DSM 168 was harvested by centrifugation (20 min, 3000 g). After resuspending the cell pellet in 4 ml lysis buffer, 1 point of a spatula of lysozyme was added and the suspension incubated at 37 °C for 40 min. 300 µl of a 20 % (w/v) N-lauroylsarcosine solution were added, the sample mixed carefully by inverting the tube 2-3 times and incubation at 37 °C continued for another 5 min. After addition of 4 ml phenol and 30 min of careful mixing at room temperature the sample was centrifuged at 4 °C for 15 min (8000 g). The upper (hydrous) phase was transferred into a fresh tube, 2 ml phenol were added, the sample was mixed, 2 ml chloroform-isoamyl alcohol (24:1) were added, the sample was mixed again and centrifuged at 4 °C for 15 min (3000 g). The upper phase was again transferred into a fresh tube and the chloroform-isoamyl alcohol extraction repeated, this time adding 4 ml. After another centrifugation step (15 min at 3000 g and 4 °C) the upper phase was once more transferred into a fresh tube and DNA precipitation initiated by adding 400 µl of a 3 M Na acetate solution (pH 4.8) and 10 ml ice-cold ethanol p.a. (100 % (v/v)). The solution was agitated carefully until the DNA became visible as a white precipitate. This was collected with a sterile pipette tip and transferred into a new tube. The DNA was washed twice with 70 % (v/v) ethanol p.a., including incubation at 50 °C for 30 min and air dried after a last centrifugation step (10 min, 8000 g). Solubilization of the DNA pellet in 100-200 µl of TE buffer was also supported by incubating the tube at 50 °C.

Lysis buffer	NaCl	100.0 mM
	EDTA	50.0 mM

TE buffer see above (2.5.2.1)

2.5.2.3 Preparation of Plasmid DNA (Mini Prep)

4.5 ml of an overnight culture were harvested by centrifugation (5 min, 7000 g) and the pellet resuspended in 300 µl of buffer P1. 300 µl of buffer P2 were added, the sample carefully mixed by inverting the tube and incubated at room temperature for 5 min. 300 µl of buffer P3 were then added, the sample again carefully mixed and incubated at room temperature for another 5 min. After centrifugation (15 min at 15000 g and 4 °C) 800 µl of the supernatant were added to 560 µl isopropanol in a fresh tube. Precipitation of plasmid DNA was allowed to proceed during a 10 min incubation step at 4 °C, followed by a 30 min centrifugation step also at 4 °C (15000 g). The DNA pellet was washed once with 70 % (v/v) ethanol p.a.. After all traces of ethanol had evaporated, the DNA was solubilized in 50-100 µl H_2O or TE buffer.

P1 buffer	Tris-HCl, pH 8.0	50.0	mM
	EDTA	10.0	mM
	RNase	200.0	µg/ml
P2 buffer	NaOH	200.0	mM
	SDS	1.0	% (w/v)
P3 buffer	potassium acetate, pH 5.5	3.0	M

TE buffer see above (2.5.2.1)

2.5.3 Determination of DNA Concentration

The concentration of a DNA solution was determined by measuring the absorbance at 260 nm and additionally at 280 nm to account for protein impurities. For a pure DNA solution an A_{260} of one corresponds to a dsDNA concentration of 50 µg/ml. The puritiy of the DNA solution can be deduced from the ratio of A_{260} to A_{280}. With A_{260}/A_{280} = 1.8 - 2.0 the DNA can be considered as pure.

2.5.4 Transformation of Bacteria

2.5.4.1 Generation of Electrocompetent Cells

Cells (different *E. coli* strains and *S. typhimurium* TE3006) were grown aerobically in 500 ml LB medium containing the required additives (*E. coli*) or in TB medium containing 40 µg/ml hemin, 50 µg/ml kanamycin and 5 µg/ml tetracycline (*S. typhimurium* TE3006). When the culture reached an OD_{578} of 0.6 (*E. coli*) or 0.8 (*S. typhimurium*), respectively, it was cooled on ice for 30 min and cells were then harvested by centrifugation (10 min at 6000 g and 4 °C). The *E. coli* cell sediment was resuspended in sterile ice-cold H_2O, transferred into a 50 ml tube and centrifuged again (10 min at 3000 g and 4 °C). This washing step was repeated once with H_2O and once with sterile ice-cold 10 % (v/v) glycerol. After the last centrifugation step the cells were resuspended in 1 vol. (refering to the volume of the pellet) of 10 % (v/v) glycerol and divided into 40 µl aliquots. These were either immediately used for electroporation or stored at -80 °C. The *S. typhimurium* cells were treated accordingly, however, ice-cold SMEB buffer was used instead of H_2O for the first two washing steps.

SMEB buffer	HEPES, pH 7.0	1.0 mM
	Sucrose	300.0 mM
	$MgCl_2$	1.0 mM

2.5.4.2 Transformation by Electroporation

Electroporation was applied as standard transformation method, both for plasmids and linear DNA. 40 µl of electrocompetent cells were combined with 1-2 µl DNA solution (0.1-1.0 µg/µl) and transferred into an electroporation cuvette. In a Gene Pulser (Bio-Rad) cells were subjected to a short electric pulse and thereby temporarily rendered permeable for DNA. Conditions were as follows: voltage 2.2 kV, capacity 25 µF, resistance 200 Ω, duration of pulse 10-40 ms. Immediately after the transformation 1 ml of preheated LB medium or SOC medium was added and cells were incubated at 37 °C for 1 h. Depending on the expected colony density, different volumes were then streaked on agar plates containing the appropriate antibiotics and plates incubated overnight at 37 °C. In cases where volumes or incubation temperatures were modified, this is indicated in the respective sections.

2.5.4.3 Transformation by the $CaCl_2$ Method

This alternative transformation method was only used after site-directed mutagenesis (section

2.5.6). Supercompetent *Epicurian coli* XL1-Blue cells were supplied with the Site-Directed Mutagenesis Kit (Stratagene) and transformation was performed according to the manufacturer's instructions.

2.5.5 Electrophoretic Separation of DNA

For the analytical separation of DNA fragments agarose gels consisting of 1 % (w/v) agarose in TAE buffer were prepared. For exceptionally small DNA fragments (below 1000 bp) the agarose concentration was increased to 1.2 % (w/v). Depending on the size of the gel, a voltage of 80-100 V was applied. The DNA fragments migrate towards the anode with a velocity that is proportional to the negative logarithm of their length. Prior to loading, the DNA samples were mixed with loading dye to facilitate loading and to indicate the progress of the samples in the gel. GeneRuler™ DNA Ladder Mix or MassRuler™ DNA Ladder Mix (MBI Fermentas) were used as size standard according to the manufacturer's instructions.
After electrophoresis, gels were incubated in an ethidium bromide solution for 10-30 min, briefly rinsed with H_2O and the DNA was detected via its fluorescence under UV light (λ = 312 nm). In cases where DNA fragments were to be extracted from the gel, GelStar® Nucleic Acid Gel Stain and a blue light detector (Flu-O-blu) were used instead of ethidium bromide to avoid DNA damage by UV irradiation. Extraction was carried out using the QIAquick Gel Extraction Kit (Qiagen) according to the manufacturer's instructions.

TAE buffer	Tris-acetate, pH 8.0	40.0	mM
	EDTA	1.0	mM
DNA loading dye	bromophenol blue	350.0	µM
	xylene cyanol FF	450.0	µM
	orange G	0.25	% (w/v)
	sucrose	115.0	mM
Ethidium bromide solution	ethidium bromide in H_2O	0.1	% (w/v)

2.5.6 Site-Directed Mutagenesis of DNA

Single amino acids in a protein of interest can be exchanged by inserting site-specific

mutations into the DNA sequence of the corresponding gene. The QuikChange Site-Directed Mutagenesis Kit (Stratagene) was employed in this work for mutational analysis of *E. coli* HemN as well as for modification of *E. coli* HemZ and *B. subtilis* HemZ2. The method - which is illustrated in Figure 11 - utilizes a dsDNA plasmid carrying the gene of interest and two synthetic oligonucleotide primers which contain the desired mutation and are complementary to opposite strands of the vector. During PCR (polymerase chain reaction) with *PfuTurbo* DNA polymerase a mutated plasmid is generated. The PCR product is treated with *Dpn*I, an endonuclease specifically digesting (partially) methylated DNA, in this case the parental template DNA. This allows isolation of the newly synthesized unmethylated DNA of the mutated plasmid, which is subsequently transformed into a suitable *E. coli* strain. In the *E. coli* cells DNA ligase closes the nicked DNA circles.

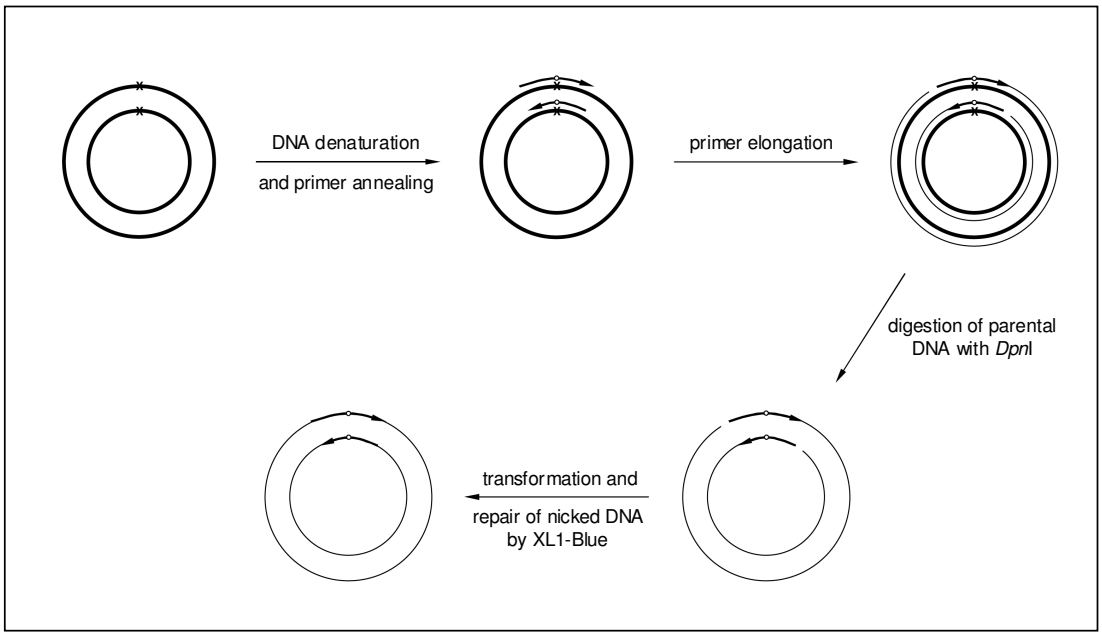

Figure 11: Overview of the QuikChange Site-Directed Mutagenesis method (modified from Stratagene Instruction Manual, 1998). ▬ parental DNA, — mutated DNA, **x** position of the desired mutation, —o→ mutagenic primer. A detailed description is given in the text (section 2.5.6).

PCR reactions with the QuikChange Site-Directed Mutagenesis Kit were carried out exactly as described in the instruction manual. Mutated plasmids were either transformed into the supercompetent *E. coli* XL1-Blue cells supplied with the kit or into electrocompetent *E. coli* DH10b cells (2.5.4).

Oligonucleotide primers were designed following the guidelines provided in the instruction manual and ordered from MWG Biotech AG. They are listed in Table 5. Nucleotides exchanged in comparison with the wild type sequence are underlined. All mutated genes were subjected to complete DNA sequence determination (2.5.9).

Table 5: Oligonucleotide primers used for site-directed mutagenesis

Mutant designation	Sequence of oligonucleotide primer (forward)[1]
E. coli HemN	
R22A	CTATTCCGGGCCAGCATACACCTCGTACCCGACCGC
Y56A	CCTGAGCGTCCATTATCTCTCGCCGTACATATCCCG
Y56L	CCTGAGCGTCCATTATCTCTCTTGGTACATATCCCG
E145A	GCGGAGATTTCGATCGCAGTCGATCCGC
E145I	GCGGAGATTTCGATCATAGTCGATCCGCGGG
R308A	CGTGAAGGCGTGCTGCATGCTAACTTCCAGGGC
R308K	GCGTGAAGGCGTGCTGCATAAAAACTTCCAGGGCTACACC
F310A	GCGTGCTGCATCGTAACGCCCAGGGCTACACC
F310L	GTGCTGCATCGTAACTTGCAGGGCTACACC
Q311A	GCATCGTAACTTCGCGGGCTACACCACTCAGGGC
I329A	GGCGTTTCCGCCGCCAGCATGATTGGCGACTGC
Q338A	GGCGACTGCTACGCGGCGAACCAGAAAGAGTTGAAGC
Q338N	GGCGACTGCTACGCGAACAACCAGAAAGAGTTGAAGC
R359K	CAAGGCAATGCGCTGTGGAAAGGTATTGCGCTAACGCGTG
R434A	CGAAAGGTCGCTTGCTGATCGCCAACATTTGCATGTGC
R434K	GTGACGGCGAAAGGTCGCTTGCTGATCAAAAACATTTGCATGTGC
E. coli HemZ	
F25C	GCCCGTACTGCGATTGCAACTCTCACGCG
B. subtilis HemZ2	
L502Stop	CGACAAAGCAGCACTGAGAGCACCACCACCACCACC

[1] Only oligonucleotide primers in forward orientation are listed. The second oligonucleotide (reverse) always corresponds to the reverse complementary sequence.

2.5.7 Amplification of DNA Fragments by Polymerase Chain Reaction (PCR)

2.5.7.1 Design and Synthesis of Oligonucleotide Primers

Oligonucleotide primers for the amplification of the genes *hemZ* from *E. coli* and *hemZ* and *hemZ2* from *B. subtilis* with the aim of susequent cloning into different vectors were designed. Recognition sequences for restriction endonucleases were inserted via these primers

at both ends of the genes. For the disruption of the *hemN* gene on the *E. coli* chromosome (2.5.10), primers for the amplification of the kanamycin resistance (kan^r) gene from plasmid pKD13 were designed including extensions homologous to the regions up- and downstream of *E. coli hemN*. All oligonucleotide primers are listed in Table 6. Recognition sequences of restriction endonucleases or the extensions homologous to the *E. coli* genome are underlined. Primers were purchased from MWG Biotech AG or biomers.net GmbH.

Table 6: Oligonucleotide primers used for PCR amplification of DNA fragments

Primer designation	Primer sequence (5' → 3')[3]	Additional information
$hemZ_{E.c.}$pGEX-fwd[1]	ACGGGATCCGTAATGGTTAAATTACCTC	*Bam*HI restriction site
$hemZ_{E.c.}$pGEX-rev[2]	CGCCTCGAGCAATACAAGTTTACTCAGC	*Xho*I restriction site
$hemZ_{E.c.}$pET-fwd	TGGACGCTTTACCATATGGTTAAATTACC	*Nde*I restriction site
$hemZ_{E.c.}$pET-rev	AATCTCGAGGTACTCAGCCAGAAAAAG	*Xho*I restriction site
$hemZ_{B.s.}$pBlue-fwd	TAGTCTAGAAGGTCGGCTCAGTTGAAGT	*Xba*I restriction site
$hemZ_{B.s.}$pBlue-rev	GCTGGATCCGAGTGCTAATTCTATAACA	*Bam*HI restriction site
$hemZ2_{B.s.}$pBlue-fwd	CGTCTAGAGCAAGGTGTCGCTTATATGA	*Xba*I restriction site
$hemZ2_{B.s.}$pBlue-rev	TAGGATCCGCTTGCTGAACAAGGTATTT	*Bam*HI restriction site
$hemZ_{B.s.}$pGEX-fwd	AAGGTGGAATTCTTGAAATCAG	*Eco*RI restriction site
$hemZ_{B.s.}$pGEX-rev	AAAACTCGAGTGCCTAATAATTTC	*Xho*I restriction site
$hemZ2_{B.s.}$pET-fwd	AGGTGAGCCATATGCAAATTAAAATAGAAG	*Nde*I restriction site
$hemZ2_{B.s.}$pET-rev	AATTACTCGAGGTGCTGCTTTGTC	*Xho*I restriction site
pKD13hemN-fwd	ACGCCGTAGCCGCCAGAGACGCCATCGGAAGGA GTGAGCGTGTAGGCTGGAGCTGCTTC	for *hemN* disruption: amplification of kan^r from pKD13 with extensions homologous to *E. coli* genome
pKD13hemN-rev	TGGCGCTTTCGTTTTCTACTTTGTAAACGAAGCG CCATTCACTATATTCCGGGGATCCGTCGACC	
kt	CGGCCACAGTCGATGAATCC	first primer pair for PCR verification of *hemN* disruption
controlhemN-rev	GGTATCGAGTGGCGCAGTTG	
k2	CGGTGCCCTGAATGAACTGC	second primer pair for PCR verification of *hemN* disruption
controlhemN-fwd	TGGAAACGGATGAGCGTCTG	

[1] fwd, forward
[2] rev, reverse
[3] Recognition sequences of restriction endonucleases or extensions homologous to the *E. coli* genome are underlined.

For subsequent cloning into the vector pGEX-6P-1 *E. coli hemZ* (1134 bp) was amplified

using primers $hemZ_{E.c.}$pGEX-fwd and $hemZ_{E.c.}$pGEX-rev. For cloning into vector pET-21b primers $hemZ_{E.c.}$pET-fwd and $hemZ_{E.c.}$pET-rev were used. *B. subtilis hemZ* (1098 bp) was amplified with primers $hemZ_{B.s.}$pBlue-fwd and $hemZ_{B.s.}$pBlue-rev for cloning into pBlueskript SK^+ and with primers $hemZ_{B.s.}$pGEX-fwd and $hemZ_{B.s.}$pGEX-rev for cloning into pGEX-6P-1. *B. subtilis hemZ2* (1503 bp) was amplified with primers $hemZ2_{B.s.}$pBlue-fwd and $hemZ2_{B.s.}$pBlue-rev for cloning into pBlueskript SK^+ and with primers $hemZ2_{B.s.}$pET-fwd and $hemZ2_{B.s.}$pET-rev for cloning into pET-22b.

2.5.7.2 PCR Conditions

Taq DNA polymerase (Amersham Biosciences) was used for all reactions except for the amplification of *E. coli hemZ* for cloning into vectors pGEX-6P-1 and pET-21b and for the amplification of *B. subtilis hemZ2* for cloning into vector pET-22b. In these cases amplification was only achieved with $Vent_R$ DNA polymerase (New England BioLabs). A standard reaction was composed as listed below.

Standard PCR composition	10 x *Taq* or Vent PCR buffer	5.0	µl
	dNTP mix (2 mM each)	5.0	µl
	forward primer	20.0	pmol
	reverse primer	20.0	pmol
	template DNA	20 – 100.0	ng
	DNA polymerase	1 - 2.5	U
	$H_2O_{deion.}$	ad 50.0	µl

After an initial DNA denaturation step, a cycle consisting of the three steps denaturation, primer annealing and primer elongation was completed 30 times and the reaction terminated by a final elongation step. The denaturation temperature of 95 °C and the elongation temperature of 72 °C remained unchanged; the annealing temperature depends on oligonucleotide length and G+C content and is furthermore influenced by the insertion of mismatches. It can be calculated as follows:

$$T_m\ [°C] = 69.3 + 0.41\ (\%\ G+C) - 650/n$$

% G+C represents the G+C content of the primer in % and *n* represents the number of nucleotides.

The duration of the elongation step is chosen according to the length of the DNA fragment to be amplified. The enzyme *Taq* polymerase inserts approximately 1000 nucleotides per minute, $Vent_R$ polymerase is slower due to its proofreading activity (1000 nucleotides in 2 minutes).

Standard thermocycler program	95 °C	5	min	
	95 °C	1	min	
	50 - 60 °C	30	s	30 x
	72 °C	1 - 4	min	
	72 °C	5 - 10	min	
	4 °C	∞		

2.5.7.3 Purification of PCR Products

After a PCR, an aliquot of the reaction mixture was analyzed by agarose gel electrophoresis (section 2.5.5). If only one PCR product was detected in the gel, the entire sample was subjected to purification with the QIAquick PCR Purification Kit (Qiagen). If more than one PCR product was visible in the gel, the entire reaction mixture was separated gel electrophoretically. The DNA fragment of interest was then excised from the gel and purified using the QIAquick Gel Extraction Kit (Qiagen). All kits were used according to the manufacturer's instructions.

2.5.8 Enzymatic Modification of DNA

2.5.8.1 Cutting DNA with Restriction Endonucleases

Restriction of DNA (vectors and PCR products) was carried out using restriction endonucleases purchased from New England BioLabs or MBI Fermentas. Reaction buffers, concentrations of enzymes and DNA as well as incubation temperatures were chosen according to the manufacturer's instructions. The digestion was allowed to proceed for 2-3 h and was, if possible, followed by heat inactivation of the restriction endonucleases (20 min at 65 °C or 80 °C, depending on the enzyme).

2.5.8.2 Ligation

In order to avoid re-circularization of digested vector DNA, the 5'-phosphate groups of linearized vectors were removed prior to the ligation reaction. This was achieved by adding

shrimp alkaline phosphatase (Promega) to the sample immediately after restriction (1 U / µg DNA) and incubating at 37 °C for 30 min, followed by heat inactivation (15 min at 65 °C). Ligation of DNA was carried out using T4 DNA ligase (MBI Fermentas) in a reaction buffer supplied by the manufacturer. 25-50 ng of vector DNA were used in one reaction and insert DNA was added in excess (insert to vector ratio with regard to molar concentrations ≈ 5:1). 1-2 U of T4 DNA ligase were added.

2.5.9 DNA Sequencing

In all cases the successful modification of DNA - amplification followed by cloning as well as site-directed mutagenesis - was confirmed by sequence determination of the respective DNA region. With the exception of the construct pGEX-*hemZ*$_{B.s.}$ all sequencing reactions were conducted by MWG Biotech AG. The correct sequence of *B. subtilis hemZ* and its correct insertion into the vector pGEX-6P-1 were controlled in our laboratory with an ABI PRISM 310 Genetic Analyzer (Applied Biosystems). The required preparatory PCR with fluorescence-labelled ddNTPs and purification of the PCR product were carried out as described by the manufacturer.

2.5.10 Generation of a Chromosomal *hemN* Knock-out Mutant in *Escherichia coli* MC4100

The method developed by Datsenko and Wanner (2000) to disrupt chromosomal genes in *E. coli* includes replacement of the gene of interest by a kanamycin resistance (kan^r) gene (Figure 12). The kan^r gene is transformed into the strain as a linear DNA fragment and recombination is achieved by the phage λ Red recombinase system. Plasmid pKD13 (Figure 12A) carries a kan^r gene flanked by FRT sites (FLP recognition target sites) which allow elimination of the kan^r gene after successful mutagenesis. This kan^r gene was amplified using primers pKD13hemN-fwd and pKD13hemN-rev (compare section 2.5.7.1) which are complementary to the priming sites P1 and P4 of the plasmid and in addition carry extensions of 39 and 45 nucleotides that are homologous to the chromosomal regions adjacent to the gene to be inactivated (Figure 12B). Therefore, a PCR product was generated which consisted of the kan^r gene flanked by sequences homologous to the regions adjacent to *hemN* on the *E. coli* chromosome. The PCR product was treated with *Dpn*I to digest the template DNA (compare section 2.5.6) and purified as described in section 2.5.7.3.

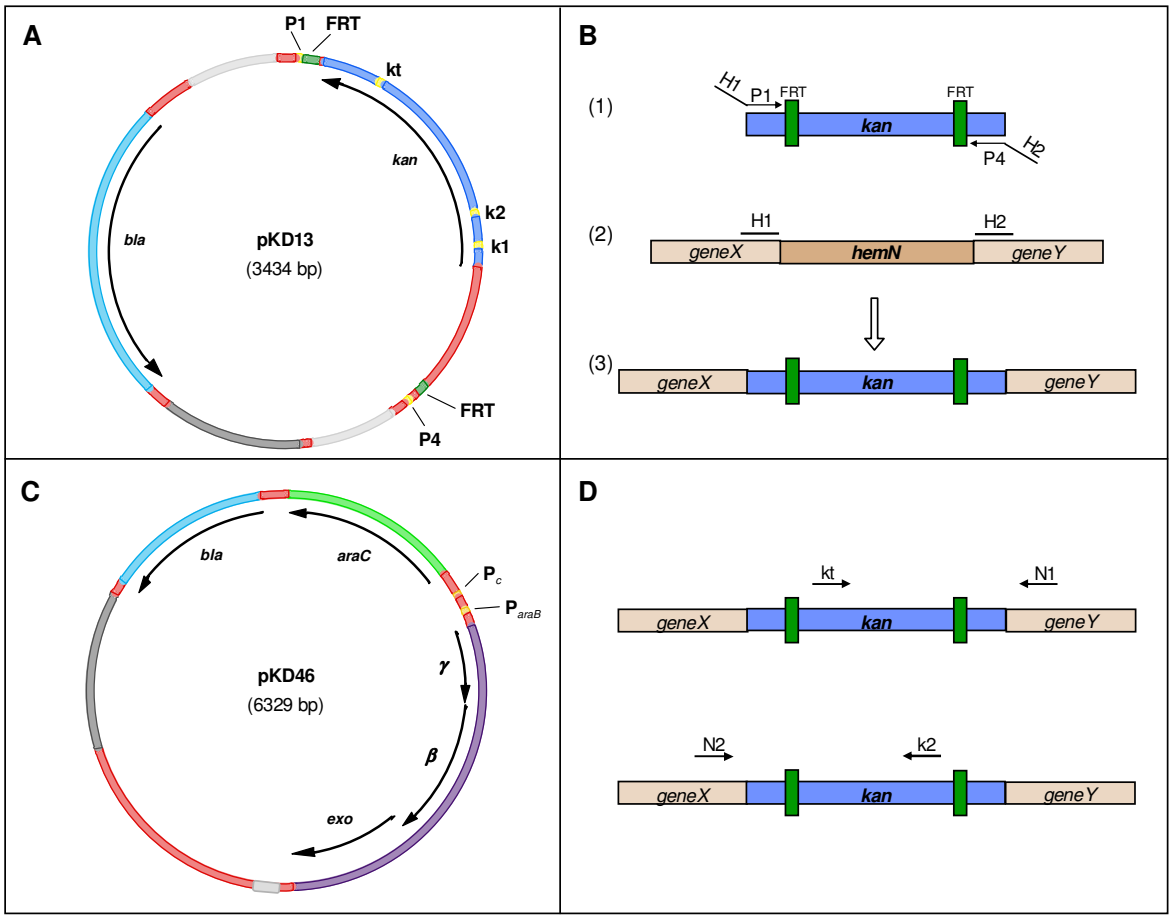

Figure 12: Method for the generation of a chromosomal gene disruption in *E. coli* (Datsenko and Wanner, 2000). **A**, Vector map of pKD13. The kanamycin resistance gene (*kan*) is shown in blue, the FLP recognition target (FRT) sites are shown in green and the priming sites 1 (P1) and 4 (P4) as well as the binding sites for test primers k1, k2 and kt are shown in yellow. Other components: light blue, ampicillin resistance gene (*bla*), dark grey, *ori*, light grey, terminator. **B**, Kanamycin resistance gene (*kan*, blue) and oligonucleotide primers (black) used for its amplification (1). Primers contain regions complementary to priming sites 1 (P1) and 4 (P4) on pKD13 and extensions homologous to the chromosomal regions adjacent to *hemN* (H1 and H2) (2). H1 and H2 enable Red-mediated recombination, resulting in the replacement of *hemN* by *kan* (3). **C**, Vector map of pKD46. The λ Red recombinase genes (*γ*, *β*, *exo*) are shown in purple, promoters (P_{araB} and P_C) are shown in yellow and the regulatory gene *araC* is shown in light green. Other components: light blue, ampicillin resistance gene (*bla*), dark grey, *ori*, light grey, terminator. **D**, Primer pairs used for PCR verification of the *hemN* disruption. N1, controlhemN-rev, N2, controlhemN-fwd.

Plasmid pKD46 (Figure 12C) sustains the expression of the genes (*α*, *β*, *exo*) encoding the λ Red recombinase system under control of an arabinose-inducible P_{araB} promoter. As pKD46 is also a temperature-sensitive replicon, it can be eliminated by raising the incubation temperature to 37 °C. Stable propagation of the plasmid is ensured by growing the cells at 30 °C. *E. coli* MC4100 was transformed with pKD46. Plasmid-bearing cells were selected by their ampicillin resistance and electrocompetent cells were again generated. In this case, however, 1 mM arabinose was added to the growth medium to induce expression of the λ Red recombinase genes. After transformation with the purified PCR product, kanamycin resistant cells were selected and after a temperature shift to 37 °C they were tested for ampicillin

sensitivity to ensure loss of the helper plasmid pKD46.

A successful recombination event should lead to the replacement of the chromosomal *hemN* gene with the kan^r gene (Figure 12B). This event was confirmed by PCR amplification of both new junction fragments (Figure 12D). Forward primer kt is complementary to the kan^r gene while reverse primer controlhemN-rev to the chromosomal region downstream of *hemN*. Accordingly, primers controlhemN-fwd and k2 bind upstream of *hemN* and within the kan^r gene.

2.5.11 Functional Complementation of a *Salmonella typhimurium hemF hemN* Mutant and an *Escherichia coli hemN* Mutant

2.5.11.1 Functional Complementation of *Salmonella typhimurium* TE 3006

In *S. typhimurium* TE 3006 both the chromosomal *hemF* and the *hemN* gene have been disrupted (Table 2). Consequently, this strain carries no functional coproporphyrinogen III oxidase and is therefore unable to grow unless hemin is added to the medium. This heme auxotrophic phenotype was confirmed by streaking single colonies in parallel on plates with and without hemin (LB/hemin/kan/tet vs. LB/kan/tet). For the subsequent complementation studies only those colonies were chosen which grew on the hemin containing plates but not on the plates without hemin. Electrocompetent cells were prepared as described in section 2.5.4.1 and were transformed with plasmids carrying *E. coli hemF* and *E. coli hemN*, *E. coli hemZ*, *B. subtilis hemZ* and *B. subtilis hemZ2* as well as plasmids carrying no inserts. Cells were plated on LB agar-plates containing hemin, ampicillin and tetracycline. When transformants grew, they were subsequently streaked in parallel on plates with and without hemin again (LB/hemin/amp/kan vs. LB/amp/kan) to test which plasmids restored the ability to grow without hemin supplementation. 40 µg/ml hemin, 50 µg/ml ampicillin, 50 µg/ml kanamycin and 5 µg/ml tetracycline were used in the indicated combinations.

2.5.11.2 Functional Complementation of *Escherichia coli* MC4100 Δ*hemN*

An *E. coli* mutant strain carrying a disruption of the chromosomal *hemN* gene was constructed as described in section 2.5.10. As this strain lacks only the O_2-independent coproporphyrinogen III oxidase, but still retains the O_2-dependent coproporphyrinogen III oxidase HemF, it should exhibit normal growth under aerobic conditions. However, growth under anaerobic conditions should be affected compared to the wild type strain *E. coli* MC4100. These growth phenotypes were confirmed by monitoring growth of wild type and

mutant strain under aerobic and anaerobic conditions. No antibiotics were added to the medium. Subsequently, electrocompetent cells were generated of both strains and were transformed with plasmids carrying *E. coli hemN*, *E. coli hemZ*, *B. subtilis hemZ* and *B. subtilis hemZ2* as well as plasmids carrying no inserts. Wild type cells were plated on LB agar-plates containing 100 µg/ml ampicillin, mutant cells on plates containing 100 µg/ml ampicillin and 25 µg/ml kanamycin. The transformants were again subjected to comparative growth experiments. Starting from aerobic overnight cultures, anaerobic cultures were inoculated. All cultures contained 100 µg/ml ampicillin. The inoculation volume for each culture was calculated according to the OD_{578} of the pre-culture. Growth was monitored over a time period of 24-30 h.

2.6 Protein Biochemical Methods

2.6.1 Recombinant Production and Purification of *Escherichia coli* HemN Wild Type and Mutant Proteins

2.6.1.1 Cell Growth for Protein Production

2 x 1 l of vapour sterilized SMM medium containing 10 mM $NaNO_3$, 25 µg/ml $(NH_4)_2Fe(SO_4)_2$ x 6 H_2O and 100 µg/ml ampicillin in 1 l anaerobic flasks were each inoculated with 10 ml of an anaerobic overnight culture of *E. coli* BL21(DE3) carrying wild type or mutant pET-3a-*hemN*. Cultures were grown at 37 °C and 100 rpm to an OD_{578} of 0.35 and expression of *hemN* was induced by addition of IPTG to a final concentration of 50 µM. Incubation was continued overnight at 25 °C and 100 rpm. Cells were subsequently harvested by centrifugation (15 min at 4000 g and 4°C).

Cell growth and centrifugation as well as all subsequent steps were carried out under strictly anaerobic conditions. To ensure anaerobic conditions, most work was done in an anaerobic chamber and all buffers and solutions were subjected to repeated cycles of evacuation and saturation with N_2 prior to use.

2.6.1.2 Cell Disruption

The cell sediment obtained by centrifugation was resuspended in 8 ml buffer A (section 2.6.1.3). Cells were disrupted by a single anaerobic passage through a French Press at 1500 p.s.i.. Cell debris and the insoluble protein fraction were removed by centrifugation for 60 min at 50000 rpm and 4 °C (Beckman ultracentrifuge, Ti 70.1). The resulting supernatant

was loaded onto a Blue Sepharose column.

2.6.1.3 Affinity Chromatography Using Blue Sepharose

The purification protocol for *E. coli* HemN under anaerobic conditions was established by Verfürth (1999). A 40 ml Blue Sepharose XK26 column (Amersham Biosciences) was equilibrated with seven column volumes of buffer A. After loading the supernatant (flow rate 0.5 ml/min), the column was washed with 250 ml of buffer A to remove unbound proteins (flow rate 1 ml/min). Bound proteins were eluted using a 150 ml linear gradient of 0-1 M NaCl in buffer A (i.e. 0-50 % buffer B) at a flow rate of 1 ml/min. The eluate was collected in 4 ml fractions. Fractions containing HemN were identified by SDS-PAGE (2.6.9), pooled and concentrated by ultrafiltration (2.6.4). The chromatography was performed in an anaerobic chamber.

Buffer A	Tris-HCl, pH 8.0	50.0	mM
	Triton X-100	0.1	% (v/v)
	dithiothreitol (DTT)	3.0	mM
Buffer B	Tris-HCl, pH 8.0	50.0	mM
	Triton X-100	0.1	% (v/v)
	dithiothreitol (DTT)	3.0	mM
	NaCl	2.0	M

2.6.2 Recombinant Production and Purification of *Escherichia coli* HemZ

2.6.2.1 Cell Growth for Protein Production

6 x 500 ml of vapour sterilized LB medium containing 100 µg/ml ampicillin in 1 l Erlenmeyer flasks were each inoculated with 5 ml of an overnight culture of *E. coli* BL21(DE3) carrying pGEX-hemZ. Cultures were grown at 37 °C and 180 rpm to an OD_{578} of 0.7 and expression of *hemZ* was induced by addition of IPTG to a final concentration of 100 µM. Incubation was continued overnight at 25 °C and 180 rpm. Cells were then harvested by centrifugation (15 min at 4000 g and 4°C).

In this case, cells were grown and harvested under aerobic conditions. Starting with the resuspension of the sediment in anaerobic buffer, all subsequent steps were then carried out under strictly anaerobic conditions (compare 2.6.1.1).

2.6.2.2 Cell Disruption

The cell sediment obtained by centrifugation was resuspended in 10 ml PBS buffer (2.6.2.3). Cells were disrupted by a single anaerobic passage through a French Press at 1500 p.s.i.. Cell debris and the insoluble protein fraction were removed by centrifugation for 60 min at 50000 rpm and 4 °C (Beckman ultracentrifuge, Ti 70.1). The resulting supernatant was loaded onto a Glutathione Sepharose column.

2.6.2.3 First Affinity Chromatography Using Glutathione Sepharose

A 12 ml Glutathione Sepharose XK26 column (Amersham Biosciences) was equilibrated with 5 column volumes of PBS buffer. After loading the supernatant the column was washed with 10 column volumes of PBS to remove unbound proteins (flow rate 1 ml/min). The HemZ-GST fusion protein was then eluted with elution buffer at a flow rate of 1 ml/min. The eluate was collected in 4 ml fractions. Fractions containing HemZ-GST were identified by SDS-PAGE (2.6.9), pooled and concentrated by ultrafiltration (2.6.4). The chromatography was performed in an anaerobic chamber.

PBS buffer	NaCl	140.0 mM
	KCl	2.7 mM
	Na_2HPO_4	10.0 mM
	KH_2PO_4	1.8 mM
	DTT	5.0 mM
	pH 7.4	
Elution buffer	NaCl	140.0 mM
	KCl	2.7 mM
	Na_2HPO_4	10.0 mM
	KH_2PO_4	1.8 mM
	DTT	5.0 mM
	glutathione	10.0 mM
	pH 7.4	

2.6.2.4 PreScission™ Protease Cleavage and Second Affinity Chromatography

PreScission™ Protease (Amersham Biosciences) cleaves site-specifically at its recognition sequence between GST domain and target protein. 70 U of PreScission Protease were added

to the pooled and concentrated protein solution. The cleavage reaction proceeded overnight. At the same time, the protein solution was dialyzed three times against 500 ml of PBS buffer to remove the glutathione.

A second affinity chromatography with glutathione sepharose - also under anaerobic conditions - was then performed to remove the separated GST-tag, uncleaved HemZ-GST fusion protein and the PreScission Protease itself which is also a fusion with GST. A 12 ml Glutathione Sepharose XK16 column was equilibrated with 5 column volumes of PBS buffer and the protein solution was loaded onto the column. The column was washed with 5 column volumes of PBS buffer and HemZ was collected with the flow through. In a final step the column was treated with elution buffer, thereby eluting GST-tag, uncleaved fusion protein and PreScission Protease. All steps were controlled by SDS-PAGE (2.6.9). Fractions containing HemZ were again pooled and concentrated by ultrafiltration (2.6.4).

2.6.3 Recombinant Production and Purification of *Bacillus subtilis* HemZ2

As purification of *B. subtilis* HemZ2 as a His-tag fusion protein did not give satisfactory results, the His-tag was removed by insertion of a stop codon into plasmid pET-22b-$hemZ2_{B.s.}$ via site-directed mutagenesis (section 2.5.6). HemZ2 was then produced in *E. coli* BL21CodonPlus(DE3)-RIL carrying pET-22b-$hemZ2_{B.s.}$L502Stop and purified via Blue Sepharose affinity chromatography. Production and purification of *B. subtilis* HemZ2 were carried out exactly as described above for *E. coli* HemN (section 2.6.1), with the exception that 4 l of cells were grown and expression of *hemZ2* induced at an OD_{578} of 0.2 with a final IPTG concentration of 500 µM.

2.6.4 Concentrating Protein Solutions

Protein solutions were concentrated in a 50 ml or in a 10 ml stirred ultrafiltration cell with a YM30 membrane at 3 x 10^5 Pa until a protein concentration of 2-5 mg/ml was reached. *E. coli* HemN wild type and mutant proteins were stored at -20 °C, *E. coli* HemZ and *B. subtilis* HemZ2 were stored at 4 °C.

2.6.5 Determination of Protein Concentration

Concentrations of protein solutions were determined using the Bio-Rad Protein Assay, following the manufacturer's instructions. The assay is based on the colorimetric method

developed by Bradford (1976). Bovine serum albumin was used as a standard.

2.6.6 Determination of Iron Content

The iron content of recombinant, purified HemN, HemZ or HemZ2 was determined colorimetrically with *o*-phenanthroline (Lovenberg *et al.*, 1963).
To 100 µl of each protein solution 10 µl of HCl (37 %) and 390 µl H_2O were added. Samples were incubated at 80 °C for 10 min to denature the proteins and subsequently cooled on ice for 5 min. 100 µl of a 1 M hydroxylammonium chloride solution, 500 µl of an *o*-phenanthroline monohydrate solution (0.3 % (w/v) in 70 % (v/v) ethanol) and 500 µl H_2O were added to each sample. Samples were mixed and incubated at room temperature for 30 min. After centrifugation to precipitate the proteins (10 min, 7000 g) absorption of the supernatant at 512 nm was measured. The iron content of the samples was determined via a calibration curve obtained from a series of dilutions of an iron standard (Merck).

2.6.7 UV-Visible Light Absorption Spectroscopy

UV-visible light absorption spectra of purified recombinant proteins were recorded under anaerobic conditions using a Lambda 2 spectrophotometer (PerkinElmer). The presence of a [4Fe-4S] cluster was indicated by an absorption maximum at 410 nm.

2.6.8 Circular Dichroism Spectroscopy

For circular dichroism (CD) measurements protein solutions were dialyzed against 50 mM Na-phosphate buffer, pH 7.6, and 10 mM NaCl. CD spectra of protein samples (125 µg/ml) in quartz cuvettes of 1 mm path length were recorded as an average of ten scans with a Jasco J810 spectropolarimeter over a range of 200-250 nm on a millidegree ellipticity scale. For the investigation of thermal stability the temperature was raised from 20 °C to 100 °C (2 °C/min) and unfolding was monitored at 210 nm. Dialysis and measurements were carried out under strictly anaerobic conditions.

2.6.9 Discontinuous SDS Polyacrylamid Gel Electrophoresis (SDS-PAGE)

Proteins were analyzed by SDS-PAGE as described by Laemmli (1970) with modifications by Righetti *et al.* (1990) for discontinuous SDS-PAGE. Protein samples were prepared by

heating them to 95 °C for 10 min in SDS loading dye. Samples were loaded onto the gel which was run at 40 mA until the bromophenol blue reached the lower end of the gel. During electrophoresis, proteins were first focussed in the stacking gel and subsequently separated according to their relative molecular mass in the running gel. The size standards employed were Dalton Mark VII-L (Sigma) or Protein Molecular Weight Marker (MBI Fermentas). Gels were stained with Coomassie Brilliant Blue G-250 and destained until the protein bands were clearly visible.

	Running gel [12 % (v/v)]	*Stacking gel [6 % (v/v)]*
Acrylamide stock solution	2.0 ml	500.0 µl
Buffer for running gel	1.25 ml	-
Buffer for stacking gel	-	625.0 µl
$H_2O_{deion.}$	1.75 ml	1.375 ml
APS solution	5.0 µl	3.0 µl
TEMED (tetramethylen diamine)	50.0 µl	30.0 µl

Acrylamide stock solution	Rotiphorese® Gel 30 (37.5:1) (Roth)	
APS solution	ammonium peroxodisulfate	10 % (w/v) in H_2O
Buffer for running gel	Tris-HCl, pH 8.8	1.5 M
	SDS	0.4 % (w/v)
Buffer for stacking gel	Tris-HCl, pH 6.8	500.0 mM
	SDS	0.4 % (w/v)
Electrophoresis buffer	Tris-HCl, pH 8.4	3.03 g/l
	glycine	14.41 g/l
	SDS	1.0 g/l
SDS loading dye	Tris-HCl, pH 6.8	100.0 mM
	glyerol	40.0 % (v/v)
	β-mercaptoethanol	10.0 % (v/v)
	SDS	3.2 % (w/v)
	bromophenol blue	0.2 % (w/v)

Staining solution	ethanol	30.0	% (v/v)
	acetic acid	10.0	% (v/v)
	Coomassie Brilliant Blue G-250	2.5	g/l
Destaining solution	ethanol	30.0	% (v/v)
	acetic acid	10.0	% (v/v)

Dalton Mark VII-L (Sigma)

(indicated are approximate relative molecular weights)

albumin, bovine	66,000
albumin, egg	45,000
glyeraldehyde-3-phosphate dehydrogenase, rabbit muscle	36,000
carbonic anhydrase, bovine	29,000
trypsinogen, bovine pancreas	24,000
trypsin inhibitor, soybean	20,100
α-lactalbumin, bovine milk	14,200

Protein Molecular Weight Marker (MBI Fermentas)

(indicated are approximate relative molecular weights)

β-galactosidase, *E. coli*	116,000
albumin, bovine	66,200
albumin, egg	45,000
lactate dehydrogenase, porcine muscle	35,000
restriction endonuclease Bsp98I, *E. coli*	25,000
β-lactoglobulin, bovine milk	18,400
lysozyme, egg	14,400

2.6.10 Preparation of *Escherichia coli* Cell-free Extract and Other Cell Extracts

E. coli cell-free extract was required to restore activity of recombinant, purified *E. coli* HemN. To prepare the cell-free extract, 1 l of *E. coli* BL21(DE3) was anaerobically grown for 24 h in TB medium at 37 °C. Cells were harvested by centrifugation (15 min at 4000 g and 4°C). All further steps were carried out under strictly anaerobic conditions. The cell sediment

was resuspended in 5 ml of buffer C and cells were disrupted by a single passage through a French Press at 1500 p.s.i.. Cell debris and all insoluble components were removed by centrifugation for 90 min at 60000 rpm and 4 °C (Beckman ultracentrifuge, Ti 70.1). The resulting protein solution was stored at -20 °C.

An *E. coli* crude extract and a *B. subtilis* crude extract were prepared in an analogous manner but without the centrifugation step after cell disruption.

For the generation of crude extracts of *E. coli* strains overproducing different HemN and HemZ proteins, the strains bearing the respective plasmids were grown under standard conditions normally used to produce these proteins for purification, including addition of IPTG. After the normal incubation time, cells were simply harvested by centrifugation, disrupted by passage through the French Press and the resulting crude extracts used for enzyme activity assays (section 2.6.11.2). *E. coli* HemZ was produced in *E. coli* BL21(DE3) carrying plasmid pGEX-*hemZ*, *B. subtilis* HemZ2 in *E. coli* BL21CodonPlus(DE3)RIL carrying pET-22b-$hemZ2_{B.s.}$ and *E. coli* HemN in *E. coli* BL21(DE3) carrying pET-3a-*hemN*. The respective strains carrying gene-less plasmids pET-22b, pGEX-6P-1 and pET-3a served as blanks. Again all steps were carried out under strictly anaerobic conditions.

Buffer C	Tris-HCl, pH 8.0	50.0 mM
	DTT	3.0 mM

2.6.11 O_2-independent Corproporphyrinogen III Oxidase Activity Assay

2.6.11.1 Standard Assay

The O_2-independent corproporphyrinogen III oxidase activity assay was developed for *E. coli* HemN (Layer, 2001; modified in Layer *et al.*, 2002). In this assay - which is outlined in Figure 13 - the substrate corproporphyrinogen III is converted into protoporphyrinogen IX by the enzyme corproporphyrinogen III oxidase in the presence of *S*-adenosyl-L-methionine and additionally required components (e.g. electron donor and acceptor). Protoporphyrinogen IX is subsequently oxidized to protoporphyrin IX by the addition of H_2O_2. This can be fluorimetrically detected.

The assay was used to determine O_2-independent corproporphyrinogen III oxidase activity of *E. coli* HemN wild type and mutant enzymes, of *E. coli* HemZ and of *B. subtilis* HemZ2. It was performed under strictly anaerobic conditions. Reaction components were mixed in an anaerobic chamber. All solutions were saturated with N_2 prior to use. The standard assay

mixture contained, in a total volume of 300 µl assay buffer, 1.5 µM enzyme, 160 µg *E. coli* cell-free extract, 500 µM SAM, 500 µM NADH and 20 µM coproporphyrinogen III. Coproporphyrinogen III was prepared by reduction of coproporphyrin III (Paesel + Lorei) using sodium amalgam (Grandchamp and Nordmann, 1982). DTT (50 mM) was added to the coproporphyrinogen III solution, which was subsequently adjusted to pH 7-8 with 20 % (v/v) phosphoric acid. The coproporphyrinogen III solutions were stored in the dark at -20 °C.

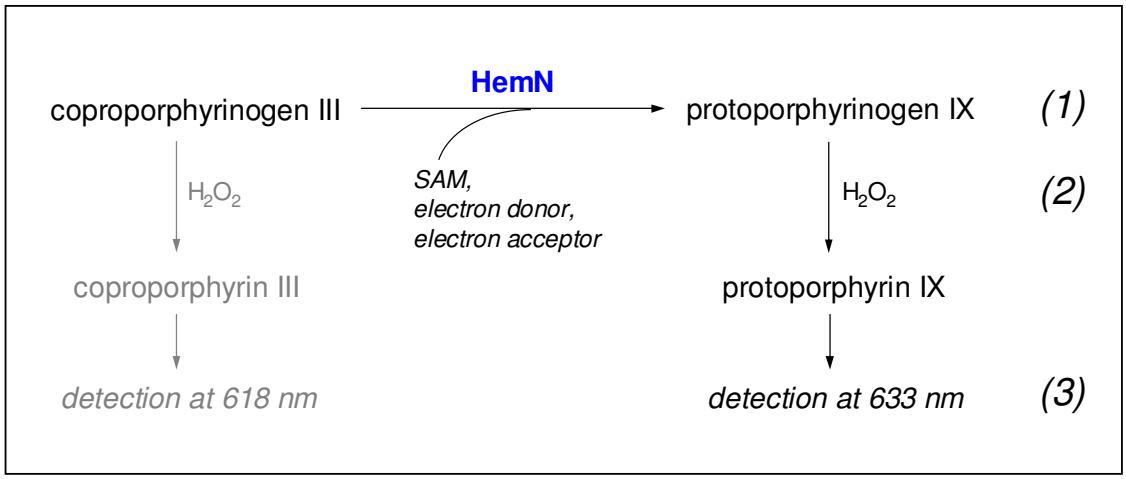

Figure 13: Overview of the O_2-independent coproporphyrinogen III oxidase activity assay. Successive steps are: *(1)* enzymatic conversion of coproporphyrinogen III into protoporphyrinogen IX, electron donor and acceptor are provided in an *E. coli* cell-free extract, *(2)* oxidation of the porphyrinogens to the corresponding porphyrins, *(3)* detection of porphyrins at their respective emission wavelengths. A detailed description is given in the text (2.6.11.1).

The enzymatic reaction was started by addition of the substrate to the assay mixture. For each assay mixture a corresponding blank was included in the test, containing all assay components except for the enzyme, to account for residual coproporphyrinogen III oxidase activity in the *E. coli* cell-free extract. After incubation at 37 °C in the dark for 90 min, the reaction was stopped and formed protoporphyrinogen IX oxidized for 15 min to protoporphyrin IX by adding 15 µl of 35 % (v/v) H_2O_2. Residual substrate was correspondingly oxidized to coproporphyrin III during this step. The oxidation and subsequent steps were carried out under aerobic conditions. The amount of enzymatically formed protoporphyrinogen IX was determined by fluorimetric detection of its oxidized form protoporphyrin IX using a fluorescence spectrometer (PerkinElmer) with an excitation wavelength of 409 nm, an emission scan range of 570-680 nm, a scan speed of 200 nm/min and a slit width of 5 nm for excitation and emission. Prior to measuring, appropriate dilutions of the samples were prepared using assay buffer II. Product concentrations were determined from the spectroscopic data via an experimentally obtained protoporphyrin IX calibration curve.

Assay buffer	Tris-HCl, pH 7.0	50.0	mM
	NaCl	300.0	mM
	Triton-X 100	0.3	% (v/v)
	DTT	3.0	mM
Assay buffer II	Tris-HCl, pH 8.0	500.0	mM
	Tween 80	2.0	% (v/v)

The assay was performed with modifications for the investigation of SAM cleavage during catalysis (2.6.12) and for the determination of the stoichiometry between SAM cleavage and protoporphyrinogen IX formation. Furthermore, concentrations of certain assay components were varied in tests with *E. coli* HemZ and of *B. subtilis* HemZ2. Details are given in the respective sections in RESULTS AND DISCUSSION.

The *E. coli* cell-free extract providing the physiological electron donor and electron acceptor can be replaced by the artificial electron donor and acceptor sodium dithionite (DT) and N-methylphenazonium methyl sulfate (PM). In this case, the assay composition was the following: 5 µM enzyme, 2 mM DT, 1 mM PM, 500 µM SAM and 20 µM coproporphyrinogen III in a total volume of 100 µl assay buffer.

2.6.11.2 Activity Assays with Different Cell Extracts

In the standard assay for *E. coli* HemN, addition of an *E. coli* cell-free extract is required for enzyme activity. This was in some cases replaced by an *E. coli* crude extract or a *B. subtilis* crude extract (25-100 µl). All other parameters remained unchanged (standard assay, see 2.6.11.1). Another modification of the standard assay was to use crude extracts instead of purified proteins (extract preparation, see 2.6.10). In this case the assay contained 40-100 µl of the crude extract, 500 µM SAM, 500 µM NADH and 20 µM coproporphyrinogen III in a total volume of 300 µl assay buffer. All subsequent steps encompassing H_2O_2 oxidation and fluorimetric detection remained unchanged.

2.6.11.3 Activity Assay Followed by Enzymatic Oxidation

For the comparison of enzymatic and H_2O_2 oxidation of protoporphyrinogen IX after HemN catalysis, standard enzyme assays (2.6.11.1) were carried out. After 90 min of incubation under anaerobic conditions at 37 °C in the dark, the assay mixture was divided. H_2O_2 (35 % (v/v)) was added to one aliquot (7.5 µl H_2O_2 to 150 µl) and purified recombinant proto-

porphyrinogen IX oxidase (PPO) from *Thermosynechococcus elongatus* was added to the second aliquot (final concentration 0.5 µM - 1.5 µM). Both samples were incubated for 15 min, the sample with H_2O_2 at room temperature, the sample containing PPO at 37 °C. Subsequently, formed protoporphyrin IX in both samples was detected fluorimetrically. In order to determine the optimal conditions for the assay with PPO, several parameters besides PPO concentration (concentration of SAM, NADH and substrate, duration of the oxidation step) were varied. However, standard assay conditions and 15 min incubation with PPO gave the best results.

For the determination of the stoichiometry between SAM cleavage and protoporphyrinogen IX formation [^{14}C]-SAM (*S*-adenosyl-L-[*methyl*-^{14}C]methionine with a specific activity of 53.6 mCi and 1.98 GBq per mmol) was used instead of non-labelled SAM. The concentrations in the assay mixture were 1.5 µM HemN, 160 µg *E. coli* cell-free extract, 20-30 µM [^{14}C]-SAM, 500 µM NADH and 20 µM coproporphyrinogen III in a total volume of 300 µl assay buffer. The mixtures were incubated anaerobically at 37°C in the dark. After 15, 30, 60 and 90 min of incubation 50 µl samples were taken from the assay mixture and divided into two aliquots for the determination of protoporphyrinogen IX and methionine formation. Enzymatically formed protoporphyrinogen IX was oxidized by addition of the enzyme PPO (final concentration 3 µM, incubation at 37 °C for 15 min) and the amount of protoporphyrinogen IX was determined by fluorimetric detection of its oxidized form protoporphyrin IX as described above. For the determination of methionine formation the proteins in the assay mixture were precipitated by addition of 10 % (w/v) PCA (perchloric acid) and removed by centrifugation. [^{14}C]-methionine formation was determined by HPLC analysis of the supernatant as described in section 2.6.12.2.

T. elongatus protoporphyrinogen IX oxidase was kindly provided by Ava Masoumi (Institut für Mikrobiologie, TU Braunschweig).

2.6.12 Assay for Cleavage of *S*-Adenosyl-L-Methionine (SAM)

2.6.12.1 Sample Preparation

HemN-mediated SAM cleavage was studied in the presence and absence of the terminal electron acceptor. The assay with electron acceptor was performed with *E. coli* cell-free extract as described in section 2.6.11.3. 20 µM [^{14}C]-SAM were used in a total volume of 50 µl. Alternatively, the assay was performed without *E. coli* cell-free extract. In this case sodium dithionite served as the reductant and concentrations were 10 µM HemN (wild type or

mutant HemN), 80 µM [^{14}C]-SAM, 2 mM dithionite and 100 µM coproporphyrinogen III in a total volume of 25 µl of assay buffer. This test was performed in the presence and absence of the substrate coproporphyrinogen III. Again, assay mixtures were incubated anaerobically at 37 °C in the dark for 90 min. After incubation the reaction was stopped by addition of 10 % (w/v) PCA and precipitated proteins were removed by centrifugation. Formation of [^{14}C]-methionine was determined by HPLC analysis of the supernatant.

2.6.12.2 High Performance Liquid Chromatography (HPLC) Analysis

The samples for HPLC analysis were prepared as described in section 2.6.12.1. After removal of the precipitated proteins the solution was filtered through a cellulose acetate membrane syringe filter with a pore width of 0.2 µm (Nalge Nunc International). 20 µl of the sample were loaded onto a 4.6 × 250 mm ODS Hypersil-C18 reversed phase column (Techlab) with a pore width of 120 Å. Separation was performed at 38°C at a flow rate of 500 µl/min using 50 mM $NH_4H_2PO_4$ (pH 2.5) as mobile phase. [^{14}C]-SAM and [^{14}C]-methionine were detected by measurement of radioactivity using a flow through scintillation counter (Raytest Isotopenmessgeräte) and in parallel by photometric diode array analysis at 200-650 nm. For the quantitation of the enzymatically formed methionine 250 µl fractions were collected and amounts of [^{14}C]-SAM and [^{14}C]-methionine were determined using a Liquid Scintillation Analyzer (PerkinElmer). The scintillation cocktail employed was OptiPhase HiSafe 2 (PerkinElmer). [^{14}C]-SAM and L-methionine (Sigma) were used as standards. Concentrations of [^{14}C]-SAM and [^{14}C]-methionine were determined via a calibration curve.

3. RESULTS AND DISCUSSION

3.1 Investigation of the Oxygen-independent Coproporphyrinogen III Oxidase HemN from Escherichia coli

3.1.1 Determination of the Stoichiometry between Protoporphyrinogen IX Formation and SAM Cleavage

The proposed HemN reaction mechanism suggests the generation of one 5'-deoxyadenosyl radical for the modification of each of the two propionate side chains to be decarboxylated (Layer *et al.*, 2002). Cleavage of two molecules of SAM would thus be required for the formation of one molecule of protoporphyrinogen IX. Consumption of SAM during HemN catalysis could previously be shown, indicating that SAM acts as a co-substrate rather than a true cofactor (Layer, 2004). However, a previous approach to quantify the ratio of SAM cleavage to protoporphyrinogen IX formation failed to yield clear results.

The source of these problems was probably the indirect detection method for protoporphyrinogen IX. As described in MATERIALS AND METHODS, only the oxidized form of protoporphyrinogen IX - protoporphyrin IX - can be detected fluorimetrically. Under standard assay conditions this oxidation was achieved by the addition of H_2O_2. The possibility had to be considered that oxidation was incomplete or that part of the product was destroyed during this treatment. An alternative oxidation method using HCl and UV irradiation has been described for the uroporphyrinogen III decarboxylase assay (Phillips and Kushner, 1999). HCl, on the other hand, interferes with the fluorescence emission spectrum of protoporphyrin IX.

Under these circumstances, the attempt to try an enzymatic oxidation of protoporphyrinogen IX to protoporphyrin IX seemed the most promising approach. Purification of recombinant oxygen-dependent protoporphyrinogen IX oxidase (HemY, PPO) from *Thermosynechococcus elongatus* had only recently been established by Ava Masoumi in our laboratory. Therefore, enzymatic oxidation of the reaction product using *T. elongatus* protoporphyrinogen IX oxidase was applied in assays for the determination of the stoichiometry between SAM cleavage and protoporphyrinogen IX formation during HemN catalysis after initial comparison with chemical oxidation.

3.1.1.1 Comparative Determination of the Amounts of Protoporphyrin IX Detectable after Enzymatic versus Chemical Oxidation of Protoporphyrinogen IX

A HemN activity assay was carried out under standard conditions with non-labelled SAM. After the 90 min of incubation to allow protoporphyrinogen IX formation, the assay mixture was divided. H_2O_2 was added to one aliquot and purified recombinant HemY was added to the second aliquot. Both samples were incubated for another 15 min to allow oxidation of protoporphyrinogen IX to protoporphyrin IX. Subsequently, formed protoporphyrin IX in both samples was detected fluorimetrically. Representative fluorescence spectra for both treatments are shown in Figure 14.

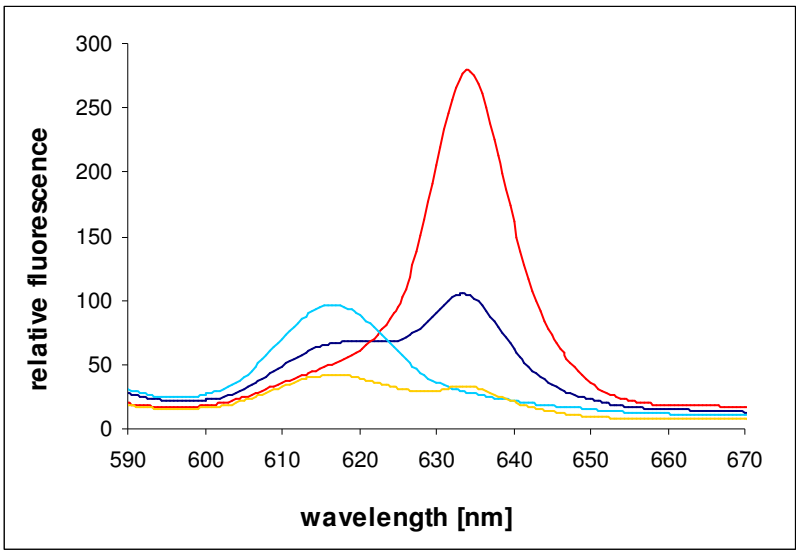

Figure 14: Comparison of the amounts of protoporphyrin IX detected after enzymatic and chemical oxidation of protoporphyrinogen IX. A standard activity assay was carried out as outlined in MATERIALS AND METHODS, containing 1.5 µM HemN, 0.5 µg/µl *E. coli* cell-free extract, 500 µM SAM, 500 µM NADH and 20 µM coproporphyrinogen III. After 90 min of incubation at 37 °C, aliquots of the assay mixture were subjected to oxidation with *T. elongatus* protoporphyrinogen IX oxidase (PPO) or H_2O_2 and amounts of protoporphyrin IX formed during each treatment were determined by fluorimetric detection at the characteristic emission wavelength of 633 nm. — HemN and PPO, — HemN and H_2O_2, — Blank with PPO, — Blank with H_2O_2.

Via a calibration curve, protoporphyrin IX concentrations were determined. On average, 6.6 µM protoporphyrin IX - representing protoporphyrinogen IX formed during HemN catalysis - were detected after enzymatic oxidation with HemY, whereas only 2 µM were detected after H_2O_2 oxidation. HemY concentration and the duration of the oxidation step were varied as were the concentrations of several assay components. However, these variations did not significantly change the amount of obtained product (6.4 - 6.7 µM with HemY vs. 1.7 - 2.2 µM with H_2O_2). By replacing H_2O_2 with the enzyme HemY, three times as much protoporphyrinogen IX as before was detected after HemN catalysis. This

improvement represented a good basis for the attempt to quantify the ratio between SAM cleavage and protoporphyrinogen IX formation.

3.1.1.2 The Ratio of SAM Cleavage to Protoporphyrinogen IX Formation of 2:1 Supports the Proposed Reaction Mechanism

In order to determine the ratio of SAM cleavage to protoporphyrinogen IX formation, three independent HemN activity assays were carried out - two with a final concentration of 20 µM [^{14}C]-SAM and one with 30 µM [^{14}C]-SAM. Apart from this difference, tests were carried out under identical conditions as described in MATERIALS AND METHODS. Samples were taken from each assay mixture after 15, 30, 60 and 90 minutes. Samples were divided and concentrations of formed protoporphyrinogen IX and [^{14}C]-methionine were determined by fluorimetric detection or scintillation counting after HPLC separation of [^{14}C]-SAM and [^{14}C]-methionine, respectively. Fluorescence spectra and HPLC chromatograms of one representative assay are shown in Figure 15, illustrating the increase in protoporphyrinogen IX formation and SAM cleavage over time.

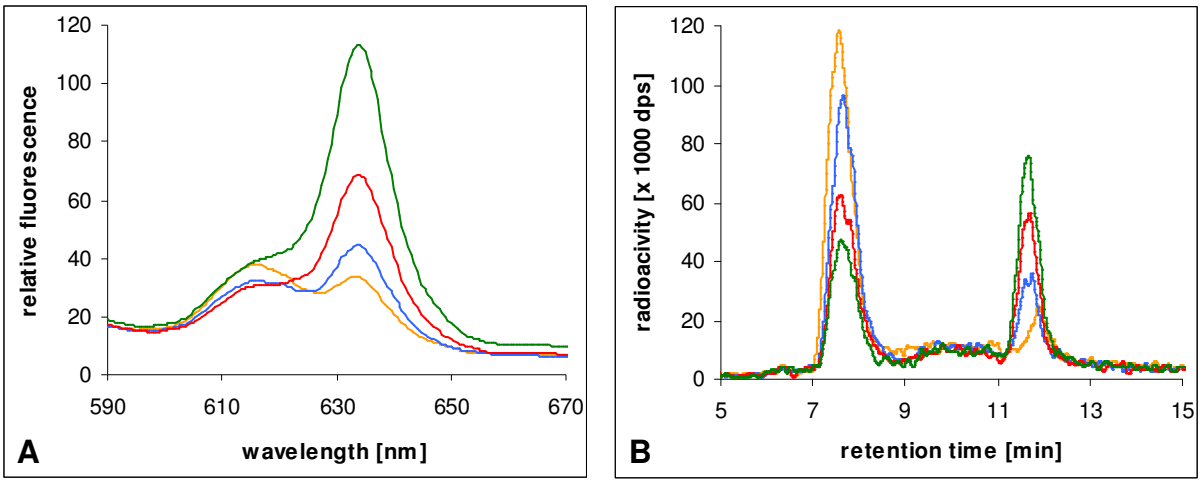

Figure 15: Increase in protoporphyrinogen IX formation and SAM cleavage over time. The assay was performed as outlined in MATERIALS AND METHODS in a standard reaction mixture containing 1.5 µM HemN and 20 µM [^{14}C]-SAM. Samples were taken after 15, 30, 60 and 90 min of incubation. Formed protoporphyrinogen IX was detected after enzymatic oxidation to protoporphyrin IX by its fluorescence emission spectrum (**A**). [^{14}C]-SAM (retention time 7-8 min) as well as its cleavage product [^{14}C]-methionine (retention time 11-12 min) were detected by HPLC analysis with a flow through scintillation counter (**B**). Blanks are not shown. Reaction times were — 15 min, — 30 min, — 60 min, — 90 min.

The data obtained from all three assays are summarized in Table 7. This table shows that very similar results were obtained in all tests. As expected, higher concentrations of proto-porphyrinogen IX and [^{14}C]-methionine were measured in the third assay which contained 30 µM instead of 20 µM [^{14}C]-SAM. However, the ratio of SAM cleavage to product

formation remained unchanged. For each of the three individual assays, quantitation of the amounts of formed protoporphyrinogen IX and methionine revealed an average methionine / protoporphyrinogen IX ratio of 1.9 (Table 7 and Figure 16). Considering the different results for each sampling time point between 15 and 90 minutes, similar average ratios were obtained, ranging between 1.7 and 2.3.

These results clearly indicate that two SAM molecules are cleaved during one catalytic cycle, i.e. for the formation of one molecule of protoporphyrinogen IX. This stoichiometry entirely agrees with the requirement for the decarboxylation of two propionate side chains of the substrate coproporphyrinogen III and consequently supports the previously proposed reaction mechanism (see INTRODUCTION). In addition, the need for two SAM molecules during one catalytic cycle is also interesting with regard to the observation of two SAM molecules bound in the HemN crystal structure.

Table 7: Quantitation of the ratio between methionine and protoporphyrinogen IX formation during HemN catalysis

Assay[1]	Reaction time [min]	Proto'gen[2] [µM][3]	[^{14}C]-Methionine [µM][4]	Methionine / proto'gen	Average ratio
1	15	0.99	2.0	2.0	1.9
	30	1.68	3.3	2.0	
	60	2.93	5.3	1.8	
	90	5.14	8.6	1.7	
2	15	0.57	1.5	2.6	1.9
	30	1.60	2.7	1.6	
	60	2.96	4.2	1.5	
	90	4.60	8.1	1.8	
3	15	0.80	1.8	2.3	1.9
	30	1.82	3.8	2.1	
	60	4.13	7.1	1.7	
	90	7.64	11.5	1.5	

[1] Assays were carried out as described in MATERIALS AND METHODS. Assays 1 and 2 contained 20 µM [^{14}C]-SAM, assay 3 contained 30 µM [^{14}C]-SAM.
[2] Proto'gen, protoporphyrinogen IX.
[3] Protoporphyrinogen IX concentrations were determined by fluorimetric detection of protoporphyrin IX after enzymatic oxidation as outlined in the text and in MATERIALS AND METHODS.
[4] [^{14}C]-methionine concentrations were determined by scintillation counting after HPLC separation of [^{14}C]-SAM and [^{14}C]-methionine (see MATERIALS AND METHODS).

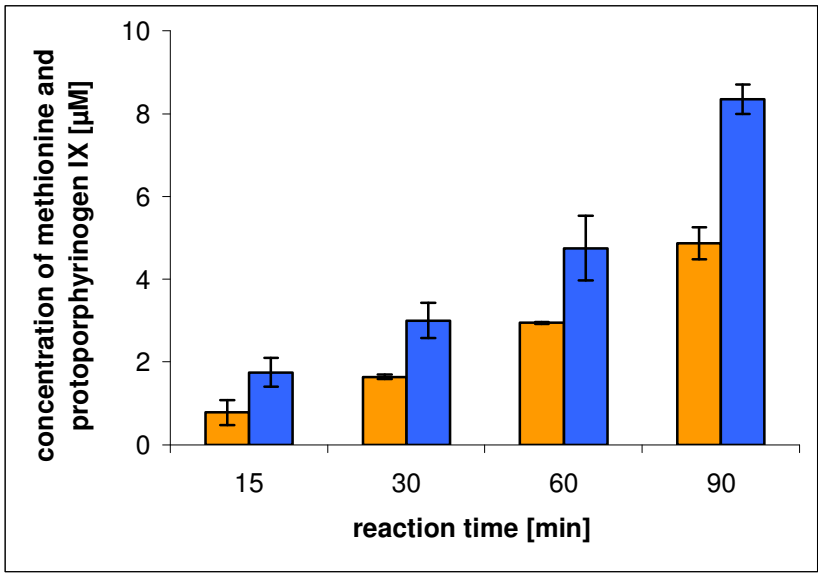

Figure 16: Quantitation of the methionine / protoporphyrinogen IX ratio at different time points during HemN catalysis. Assays were performed as outlined in MATERIALS AND METHODS in a standard reaction mixture containing 1.5 µM HemN and 20 µM [^{14}C]-SAM. After 15, 30, 60 and 90 minutes of incubation samples were taken. Formed protoporphyrinogen IX was oxidized enzymatically by addition of *T. elongatus* protoporphyrinogen IX oxidase and the amount of protoporphyrin IX was determined fluorimetrically. Cleavage of [^{14}C]-SAM was measured by separating the cleavage product [^{14}C]-methionine from [^{14}C]-SAM via HPLC and determining the amounts of both compounds in a Liquid Scinillation Analyzer. Orange, formed protoporphyrinogen IX, blue, released [^{14}C]-methionine. The values are averages of two independent measurements.

3.1.2 Investigation of the SAM2 Binding Site

As mentioned in the INTRODUCTION, the detection of two molecules of the co-substrate *S*-adenosyl-L-methionine (SAM) within the HemN crystal structure was entirely unexpected. One of these SAM molecules (SAM1) coordinates the fourth iron atom of the [4Fe-4S] cluster which is not coordinated by one of the three conserved cysteine residues. The physiological relevance of the second SAM molecule (SAM2) is still under discussion. Simultaneous binding of two molecules of SAM had not previously been observed for any of the other Radical SAM enzymes. However, in the HemN crystal structure SAM2 is located in the active site cleft in close proximity to SAM1, matches its binding pocket in size and shape and specifically interacts with a number of highly conserved amino acid residues. In order to study the potential functional role of SAM2 during HemN catalysis site-directed mutagenesis of the amino acid residues involved in SAM2 binding was performed.

3.1.2.1 Mutagenesis of Residues Tyr^{56}, Glu^{145}, Phe^{310}, Gln^{311} and Ile^{329}

According to the crystal structure of *E. coli* HemN (Layer *et al.*, 2003), amino acid residues Tyr^{56}, Glu^{145}, Phe^{310}, Gln^{311} and Ile^{329}, which are all highly conserved among different HemN enzymes, are adequately positioned to coordinate SAM2 (Figures 17 and 18). Tyr^{56} and Phe^{310} stack onto the adenine moiety of SAM2, Glu^{145} forms hydrogen bonds with the ribose, Gln^{311} contributes several hydrophilic interactions and Ile^{329} stabilizes SAM2 through hydrophobic interactions via its side chain and through hydrogen bonds via its back bone. Single amino acid exchanges were conducted, replacing Tyr^{56} and Phe^{310} by alanine and leucine, Glu^{145} by alanine and isoleucine, and Gln^{311} and Ile^{329} again by alanine.

The mutated enzymes were produced in *E. coli* BL21(DE3) and purified to apparent homogeneity under conditions identical to those established for the wild type enzyme (see MATERIALS AND METHODS). Interestingly, for some of the mutant proteins (Y56A and Y56L) binding to the Blue Sepharose column was affected. As Blue Sepharose is a resin for the purification of proteins with adenyl containing cofactors, this observation supports the previous assumption that binding of HemN to the Blue Sepharose might be achieved via the SAM2 binding site. All mutant proteins were analyzed for their iron-sulfur cluster content, their ability to cleave SAM and their overall coproporphyrinogen III oxidase activity.

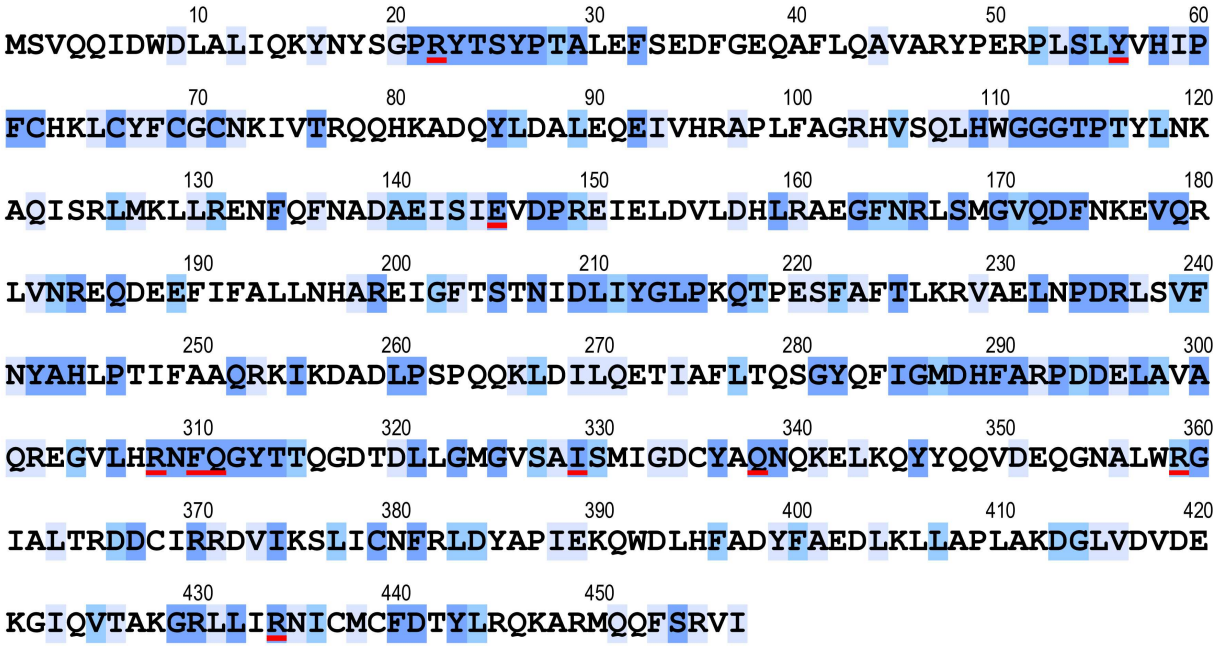

Figure 17: Amino acid sequence of *E. coli* HemN showing the distribution of conserved residues in HemN. 20 amino acid sequences were aligned with ClustalW. Conserved residues are underlaid in blue. Dark blue, conserved in > 80 % of sequences, mid blue, conserved in > 60 % of sequences, light blue, conserved in > 40 % of sequences. Residues subjected to mutagenesis are underlined in red.

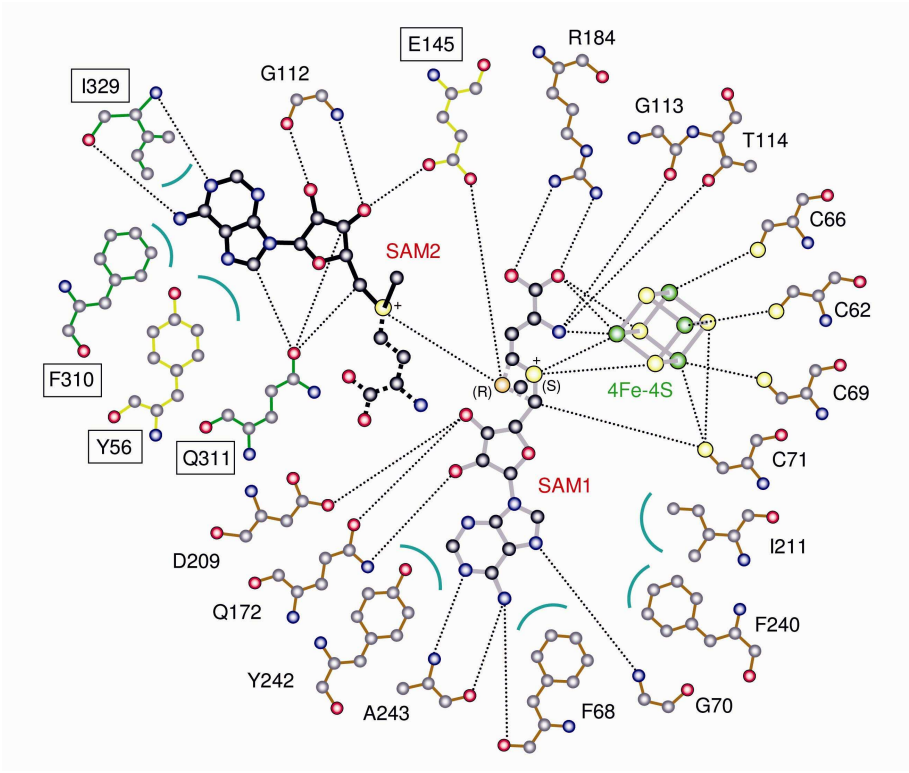

Figure 18: Schematic depiction of the active site of HemN showing the conserved amino acid residues involved in binding the [4Fe-4S] cluster and the two SAM co-substrates. Amino acids Tyr[56], Glu[145], Phe[310], Gln[311] and Ile[329] (boxed) involved in binding SAM2 were subjected to site-directed mutagenesis. Amino acid residues for which the mutant proteins were unable to cleave SAM are shown in yellow. Amino acid residues for which the mutant proteins exhibited residual SAM cleavage activity are shown in green. (modified from Layer *et al.*, 2003)

3.1.2.2 Iron-Sulfur Cluster Content of the HemN Mutant Proteins

For all proteins UV-visible light absorption spectra were recorded under strictly anaerobic conditions. An absorption maximum at 410 nm indicates the presence of a [4Fe-4S] cluster. In addition, the iron content was analyzed colorimetrically (Table 8). Both methods revealed that mutant proteins Q311A and I329A contained roughly the same amount of iron-sulfur cluster as wild type HemN. In all other enzyme variants the iron-sulfur cluster content was slightly reduced, but a [4Fe-4S] cluster was always detectable (Table 8). In all three cases (Tyr[56], Glu[145] and Phe[310]) the two different mutant proteins generated by exchange of the same amino acid exhibited very similar iron-sulfur cluster contents. The iron content was also reflected by the colour of the protein solutions: mutant proteins Y56A, Y56L, E145A and E145I appeared colourless, F310A and F310L were slightly yellow, and Q311A and I329A exhibited the same yellow-brown colour as wild type HemN.

Because of their very different iron-sulfur cluster contents, enzyme variants Y56A and Q311A were chosen as representative candidates to investigate whether the mutant proteins were properly folded. CD spectra in the far-UV region were recorded for the two mutant

proteins and wild type HemN and, in addition, their thermal stability was determined (data not shown). The spectra with their minima and maxima characteristic of certain secondary structure elements (e.g. α-helices) were basically identical for wild type and mutant enzymes and unfolding also occurred at very similar temperatures. These observations indicate overall structural integrity of the HemN mutant enzymes.

Table 8: Properties of HemN SAM2 binding site mutant proteins compared to the wild type enzyme

HemN protein	Total iron content [%][1]	[4Fe-4S] cluster by UV-Vis [%][2]	SAM cleavage [mol Met / mol HemN][3]		CPO activity [%][7]
			- Electron acceptor[4]	+ Electron acceptor[6]	
wild type	100	100	1.90	5.50	100
Y56A	43	30	n.d.[5]	n.d.	n.d.
Y56L	31	37	n.d.	n.d.	n.d.
E145A	27	20	n.d.	n.d.	n.d.
E145I	20	18	n.d.	n.d.	n.d.
F310A	58	45	0.36	0.40	1.5
F310L	40	45	0.20	0.13	n.d.
Q311A	95	86	0.95	0.47	n.d.
I329A	100	85	0.90	0.60	n.d.

[1] The iron content (mol iron / mol protein) was calculated after determination of protein and iron concentration of each sample (see MATERIALS AND METHODS). Protein concentrations were measured using the Bio-Rad Protein Assay, iron concentrations were measured colorimetrically with *o*-phenanthroline (see MATERIALS AND METHODS). The iron content of wild type HemN (max. 2 mol iron / mol protein) was set to 100 % and the iron contents of the mutant proteins were related to that.

[2] UV-visible light absorption spectra were recorded under anaerobic conditions for a protein concentration of 4 mg/ml. The presence of an iron-sulfur cluster was indicated by an absorption maximum at 410 nm. The height of this absorption maximum of wild type HemN was set to 100 % and all other maxima were related to that.

[3] SAM cleavage was determined using [^{14}C]-SAM and different electron acceptors. The amount of [^{14}C]-methionine formed during a reaction was determined after HPLC-separation of [^{14}C]-SAM and [^{14}C]-methionine. The methionine concentration was then related to the enzyme concentration in the assay mixture.

[4] SAM cleavage without the terminal electron acceptor was determined using [^{14}C]-SAM and dithionite as a reductant for the iron-sulfur cluster in the presence of substrate as described in MATERIALS AND METHODS. The assay mixture contained 10 µM HemN. The amount of determined methionine was related to the amount of enzyme employed. In the absence of substrate SAM cleavage was significantly reduced.

[5] n.d., not detectable.

[6] SAM cleavage with the terminal electron acceptor was determined using [^{14}C]-SAM and *E. coli* cell-free extract in the presence of substrate as described in MATERIALS AND METHODS. The assay mixture contained 1.5 µM HemN. As in the previous column, the amount of determined methionine was related to the amount of enzyme employed.

[7] CPO activity was determined using non-labelled SAM and *E. coli* cell-free extract as outlined in MATERIALS AND METHODS. Wild type CPO activity was set to 100 % and the activities of the mutant proteins were related to that.

3.1.2.3 SAM Cleavage Activity of the HemN Mutant Proteins

For all mutant proteins the ability to cleave SAM in the presence of substrate using dithionite as a reductant for the electron donating iron-sulfur cluster was determined (Table 8). Under these conditions wild type HemN cleaved two SAM molecules per molecule enzyme. This observation corresponded nicely to the two SAM molecules bound to the enzyme in the crystal structure. It should be noted that under these assay conditions there is no overall catalytic CPO activity since the final electron acceptor for the reaction is missing. SAM cleavage was also determined using *E. coli* cell-free extract. In the presence of the electron acceptor - provided in the *E. coli* cell-free extract - multiple rounds of SAM cleavage were observed for the wild type enzyme (Table 8). The mutant proteins with regard to their SAM cleavage function can be divided into two groups:

(1) For HemN Y56A, Y56L, E145A and E145I no detectable SAM cleavage was observed. Apparently, in these protein variants not only SAM2 binding was affected by the introduced mutation. According to the HemN crystal structure the side chain carboxyl group of Glu^{145} interacts with the ribose of SAM2, but also forms a salt bridge to the sulfonium sulfur of SAM1 in its R-configuration (Figure 18). Consequently, binding of both SAM molecules might be affected in mutant proteins E145A and E145I. Tyr^{56} is not located in close vicinity to SAM1. As described in section 3.1.2.2, both HemN Y56A and Y56L revealed relatively low iron contents. Possibly, the active site architecture in these mutants is more drastically disturbed than in others, although the overall structural integrity was shown by CD spectroscopy for Y56A (section 3.1.2.2). Another possibility is that the proteins folded properly but that subsequent insertion of the FeS cluster was hindered in some way by the introduced mutations. A HemN Y56F mutant protein investigated by Layer still exhibited reduced CPO activity (Layer *et al.*, 2002). Clearly, the introduced Phe was able to partially maintain the interaction between the aromatic side chain of the amino acid and the adenine of SAM2. Even in this case only a reduced amount of iron-sulfur cluster was detected. For other Radical SAM proteins the extreme lability of the [4Fe-4S] cluster has been discussed as well and was at least partly attributed to the unusual coordination of the cluster (Broderick *et al.*, 2000; Krebs *et al.*, 2000). Due to their complete lack of activity, the mutant proteins of this first group are only of limited use for a more detailed investigation of SAM2 function. Nevertheless, their behaviour demonstrates the importance of amino acid residues within the SAM2 binding site for enzyme activity and FeS cluster assembly.

(2) HemN F310A, F310L, Q311A and I329A represent the more interesting group of mutant proteins since they retained their ability to cleave SAM to a certain extent (Table 8). As

observed for wild type HemN (Layer, 2004) and other Radical SAM enzymes like anRNR-ae and BioB in assays with an artificial electron donor (Guianvarc'h *et al.*, 1997; Ollagnier *et al.*, 1997; Padovani *et al.*, 2001; Ollagnier-de Choudens *et al.*, 2002), SAM cleavage was found strongly increased in the presence of the substrate compared to assays without substrate (data not shown). Thus, substrate binding was not affected by the introduced mutations. The values given in Table 8 were measured in the presence of the substrate. As mentioned above, under these assay conditions (in the absence of the final electron acceptor) wild type HemN cleaved two SAM molecules per molecule enzyme (Table 8). The ratio of SAM cleavage with respect to the amount of enzyme was also determined for the mutant proteins. Between 0.20 and 0.95 molecules SAM per molecule HemN were measured (Table 8). Clearly, for the mutant proteins SAM cleavage never exceeded one molecule of SAM per molecule of enzyme. Most interestingly, mutant proteins Q311A and I329A which contained the full amount of iron-sulfur cluster also cleaved only one SAM molecule per molecule protein. In contrast to the wild type, addition of the electron acceptor (still in the presence of substrate) did not significantly change SAM cleavage of the mutant enzymes (Table 8). Under these conditions, wild type HemN performs multiple rounds of catalysis including SAM cleavage. One possible interpretation of these results is that in the mutant proteins within this second group SAM1 is still bound and thus can be cleaved upon reduction of the iron-sulfur cluster. In contrast, SAM2 binding is abolished due to the introduced mutations, and this explains the failure of the mutant proteins to cleave a second SAM molecule.

3.1.2.4 Coproporphyrinogen III Oxidase Activity of the HemN Mutant Proteins

The overall CPO activity of all mutant proteins was determined in assays using *E. coli* cell-free extract to provide electron donor and electron acceptor. Mutant enzymes F310A, F310L, Q311A and I329A were apparently still able to bind and cleave SAM1. Of these, the latter two proteins even exhibited a wild type-like iron content. At least for these two enzyme variants one would therefore expect either detectable CPO activity if SAM2 binding is not of functional importance or complete loss of CPO activity if SAM2 is of physiological significance.

With the exception of F310A, which carried traces of residual CPO activity, none of the generated mutant proteins revealed detectable protoporphyrinogen IX formation (Table 8). For the first group of mutant proteins this result is not surprising since these enzymes also failed to cleave SAM which is a prerequisite of HemN catalysis. More interestingly, the mutant proteins of the second group also did not show any CPO activity - although they were

obviously still able to bind and cleave SAM1. Therefore, one can conclude that the loss of enzyme activity can be attributed to the mutagenesis of the SAM2 binding site and the ensuing inability of these enzyme variants to bind SAM2.

3.1.2.5 Conclusions from the SAM2 Binding Site Mutagenesis Studies

The obtained results strongly imply that the second SAM molecule bound in the crystal structure of HemN (SAM2) is of physiological significance. The possibility that in wild type HemN both SAM molecules cleaved during one catalytic cycle consecutively bind to the SAM1 binding site cannot be entirely ruled out at this stage. However, if this was the case, at least mutant proteins Q311A and I329A should exhibit a wild type-like behaviour since their iron-sulfur cluster content and SAM1 binding were not affected. Altogether, the observed combination of strongly reduced SAM cleavage and complete lack of protoporphyrinogen IX formation is a valuable argument for a functional role of SAM2. If SAM cleavage was reduced for a different reason (irrespective of the presence or absence of SAM2), one would expect to observe at least some protoporphyrinogen IX formation.

HemN catalyzes the oxidative decarboxylation of two propionate side chains of the substrate coproporphyrinogen III and - as demonstrated in section 3.1.1 of this work - two molecules of SAM have to be cleaved during the reaction to generate the two 5'-deoxyadenosyl radicals needed for the two decarboxylation reactions. The presence of only one functional SAM binding site would require opening of the active site between the two decarboxylation reactions and (partly) release of the substrate intermediate to allow its re-orientation in the active site as well as replacement of the cleaved SAM (Layer *et al.*, 2003). In the case of uroporphyrinogen III decarboxylase, another tetrapyrrole modifying enzyme, a similar problem is solved by using a dimeric protein with two active sites localized at the dimer-dimer interface (Whitby *et al.*, 1998; Phillips *et al.*, 2003). Here, a catalytic mechanism has been proposed which includes movement of a reaction intermediate from the active site of one monomer to the other (Martins *et al.*, 2001). HemN, however, is a monomer. These structural prerequisites argue for the existence of two distinct locations for the two consecutive decarboxylation reactions.

The Radical SAM enzyme MiaB - a tRNA methylthiotransferase - also requires two SAM molecules, one for radical generation and subsequent thiolation and one as a methyl group donor for the methylation (Pierrel *et al.*, 2004). Although structural data is still lacking, the presence of two distinct SAM binding sites has been suggested for this enzyme. Other Radical SAM enzymes need only one SAM during one catalytic cycle or - like BioB - they need two,

but only have one SAM binding site (Escalettes *et al.*, 1999; Tse Sum Bui *et al.*, 2004). According to the crystal structure of BioB the two substrate carbons to be activated are both positioned in close vicinity to the one SAM molecule (Berkovitch *et al.*, 2004). These examples illustrate that - apart from the highly conserved process of radical generation - Radical SAM enzyme are quite variable as one would expect from their different substrates and catalytic functions.

For HemN, an interesting question is whether a reaction intermediate (hardero- or isohardero-porphyrinogen) would be detectable in assays with those SAM2 binding site mutant enzymes still cleaving SAM (F310A, F310L, Q311A, I329A). The detection of an intermediate with only one vinyl group would support the conclusion that both SAM1 and SAM2 are involved in the conversion of coproporphyrinogen III into protoporphyrinogen IX. However, would this also answer the question which SAM molecule is cleaved first? During the discussion of alternative mechanistic scenarios it was proposed that for a mutant protein which is still able to bind SAM1 but not SAM2 an intermediate should only be detectable in the case that SAM1 is cleaved prior to SAM2 (Layer, 2004). However, even if the order of cleavage was SAM2 before SAM1, SAM1 cleavage could still occur in the absence of SAM2, as this hypothetical mechanism comprises transfer of the electron from the iron-sulfur cluster to SAM2 via SAM1.

Nevertheless, if a reaction intermediate was detected for one of the HemN mutant enzymes only binding SAM1, this would at least provide an indication concerning the orientation of the substrate coproporphyrinogen III within the active site cleft, as the only vinyl group formed under these conditions should belong to the pyrrole ring (A or B) located closest to SAM1. For the O_2-dependent CPO HemF it has been demonstrated that the propionate side chain of ring A is decarboxylated prior to that of ring B (Kennedy *et al.*, 1970; Jackson *et al.*, 1980; see also INTRODUCTION). This results in the formation of harderoporphyrinogen as an intermediate. No experimental evidence has so far been obtained for an O_2-independent CPO reaction intermediate, but it might be justified to assume that the two decarboxylations proceed in the same order. It is, however, unclear at the moment whether any of the SAM2 binding site mutant enzymes would generate detectable amounts of an intermediate. One has to keep in mind that they cleave less than one molecule SAM per molecule enzyme.

3.1.3 Investigation of the Proposed Substrate Binding Site

Another task was the analysis of the proposed substrate binding site of HemN. The orientation of the substrate with regard to the cofactors - namely the two SAM molecules - is expected to contribute substantially to the understanding of the reaction mechanism. When the crystal structure of *E. coli* HemN was first published, an active site cavity accommodating the [4Fe-4S] cluster and the two SAM molecules was described (Layer *et al.*, 2003). Depending on the presence or absence of the SAM2 molecule, two alternative models for substrate binding were discussed. Already then, the need for a pocket large enough to accommodate the non-planar porphyrinogen molecule and the availability of possible interaction partners for the side chains of all four pyrrole rings argued in favour of the model containing both SAM molecules (Layer *et al.*, 2003). Additional support is now provided by the SAM2 binding site mutagenesis study which indicates a functional role for both SAM molecules during HemN catalysis (section 3.1.2).

3.1.3.1 Mutagenesis of Residues Arg^{22}, Arg^{308}, Arg^{359}, Arg^{434} and Gln^{338}

In order to further investigate the proposed substrate binding site of *E. coli* HemN, amino acid residues representing possible interaction partners for the substrate coproporphyrinogen III were subjected to site-directed mutagenesis. Several conserved arginines which are adequately positioned were considered as promising candidates since positive charges would be required to counterbalance the negative charges of the substrate propionate side chains (Figures 17 and 19). These amino acids contribute to the largely positively charged nature of the proposed substrate binding pocket of HemN, while the overall charge of the entire enzyme is significantly negative (61 Asp/Glu and 38 Arg/Lys). For other porphyrin(ogen) modifying enzymes, substrate propionate side chains and positively charged amino acid side chains (mostly arginines and lysines) have also been identified as main interaction partners, with the latter either orientating the substrate directly or ameliorating the charge of the substrate binding pocket (Schuller *et al.*, 1999; Phillips *et al.*, 2003).

Conserved residues Arg^{22}, Arg^{308}, Arg^{359}, Arg^{434} and Gln^{338} (Figures 17 and 19) were subjected to single amino acid exchanges, replacing Arg^{22} by alanine, Arg^{308} and Arg^{434} by alanine and lysine, Arg^{359} by lysine and Gln^{338} by alanine and asparagine. With the exception of Arg^{22} which is part of the N-terminal ‘trip-wire’, the exchanged residues are either positioned at the C-terminal end of the catalytic domain (Arg^{308}, Arg^{359} and Gln^{338}) or in the C-terminal domain (Arg^{434}). The mutated enzymes were produced in *E. coli* BL21(DE3) and

purified to apparent homogeneity under conditions identical to those established for the wild type enzyme (see MATERIALS AND METHODS). HemN R22A could not be purified in sufficient amounts and was therefore not characterized any further. All other mutant proteins were analyzed for their iron-sulfur cluster content, their ability to cleave SAM and their overall coproporphyrinogen III oxidase activity.

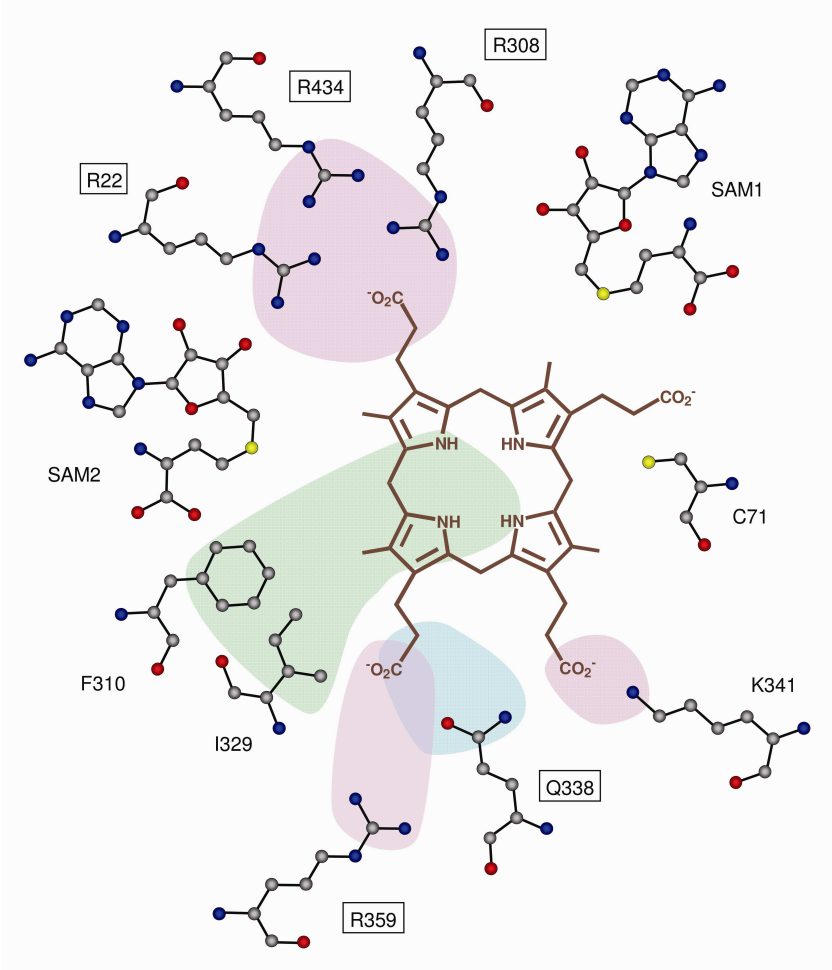

Figure 19: Schematic depiction of the proposed substrate binding site with modelled coproporphyrinogen III. Potential hydrophilic (light blue), hydrophobic (light green) and ionic (light pink) interactions between amino acid residues and the substrate are indicated by coloured shading. Highly conserved amino acid residues Arg^{22}, Arg^{308}, Gln^{338}, Arg^{359} and Arg^{434} (boxed) were subjected to site-directed mutagenesis. Conservation of Lys^{341} is considerably lower (compare Figure 17). Phe^{310} and Ile^{329} were mutated in connection with their role in SAM2 binding.

3.1.3.2 Iron-Sulfur Cluster Content of the HemN Mutant Proteins

As for the SAM2 binding site mutants, UV-visible light absorption spectra were recorded for all mutant proteins under strictly anaerobic conditions and, in addition, the iron content was analyzed colorimetrically (Table 9). Both methods revealed that the capacity of the mutant proteins to form the iron-sulfur cluster was largely retained (Table 9). Enzyme variants

R308A and R434A exhibited the lowest absorption maxima at 410 nm, the wavelength indicating the presence of a [4Fe-4S] cluster. However, the height of their absorption maxima still indicated 50 % of the FeS cluster measured for wild type HemN. The slightly reduced iron content of mutant protein Q308A correlated with a slightly less intense yellow-brown colour of the protein solution. The total iron content and colour of the protein solution did not significantly differ from wild type HemN in the case of R434A. In conclusion, the detection of a [4Fe-4S] cluster in all mutant proteins confirms that the introduced mutations did not affect the structural integrity of the active site.

Table 9: Properties of HemN mutant proteins carrying amino acid exchanges in the proposed substrate binding site compared to the wild type enzyme

HemN protein	Total iron content [%][1]	[4Fe-4S] cluster by UV-Vis [%][2]	SAM cleavage [%][3]	CPO activity [%][5]
wild type	100	100	100	100
R359K	100	86	100	100
Q338A	100	86	17	12.3
Q338N	100	100	9.5	7.7
R308A	65	52	n.d.[4]	n.d.
R308K	85	71	n.d.	n.d.
R434A	94	55	n.d.	n.d.
R434K	100	86	n.d.	n.d.

[1] The iron content (mol iron / mol protein) was calculated after determination of protein and iron concentration of each sample (see MATERIALS AND METHODS). The iron content of wild type HemN (max. 2 mol iron / mol protein) was set to 100 % and the iron contents of the mutant proteins were related to that.
[2] UV-visible light absorption spectra were recorded under anaerobic conditions for a protein concentration of 4 mg/ml. The presence of an iron-sulfur cluster was indicated by an absorption maximum at 410 nm. The height of this absorption maximum of wild type HemN was set to 100 % and all other maxima were related to that.
[3] SAM cleavage was determined using [^{14}C]-SAM and *E. coli* cell-free extract in the presence of substrate as described in MATERIALS AND METHODS. The amount of methionine obtained for the wild type was set to 100 % and all other values were related to that.
[4] n.d., not detectable.
[5] CPO activity was determined using non-labelled SAM and *E. coli* cell-free extract as outlined in MATERIALS AND METHODS. Wild type CPO activity was set to 100 % and the activities of the mutant proteins were related to that.

3.1.3.3 Catalytic Activity of the HemN Mutant Proteins

For all mutant proteins the ability to cleave SAM and to generate the reaction product protoporphyrinogen IX was determined in the presence of substrate in a standard assay using *E. coli* cell-free extract (Table 9). Both activities correlated for each mutant protein. Three

groups of mutants were distinguished on the basis of activity:

(1) HemN R359K showed full CPO activity and 100 % SAM cleavage compared to wild type HemN (Table 9). This mutant protein reached wild type levels in all the parameters investigated, leading to the conclusion that Arg^{359} is not essential for enzyme activity and obviously not directly involved in substrate binding.

(2) Mutant proteins R308A, R308K, R434A and R434K revealed neither detectable CPO activity nor detectable ability to cleave SAM (Table 9). The amino acid residues (Arg^{308} and Arg^{434}) are obviously indispensable for enzyme activity. According to the HemN crystal structure the two residues are not involved in coordinating either of the two SAMs. These observations suggest an important role of Arg^{308} and Arg^{434} in providing interaction partners for the substrate coproporphyrinogen III, either via salt bridges or hydrogen bonds. Interestingly, not even lysine can maintain these interactions to a sufficient extent.

(3) HemN Q338A and Q338N exhibited strongly reduced but still detectable CPO activity and SAM cleavage (about 10-15 % of the respective wild type activities; Table 9), indicating that Gln^{338} is apparently also involved in coordinating the substrate, but makes a smaller contribution to its stabilization compared to Arg^{308} or Arg^{434}. For Q338N an alternative interpretation of the remaining catalytic activity would be that asparagine partly maintains the interaction of glutamine, but this is improbable for Q338A.

The observed correlation between protoporphyrinogen IX formation and SAM cleavage (both either abolished or similarly reduced) supports a role of Arg^{308}, Arg^{434} and Gln^{338} in substrate binding, as it has previously been demonstrated for HemN that SAM cleavage occurs only in the presence of substrate when the physiological electron donor is used (Layer, 2004). Similar observations have also been reported for other Radical SAM enzymes and their respective substrates (Guianvarc'h *et al.*, 1997; Ollagnier *et al.*, 1997; Padovani *et al.*, 2001; Pierrel *et al.*, 2004). As a consequence, when the substrate cannot bind - as in these mutant proteins - SAM cleavage does not take place either. For biotin synthase it has been suggested that the observed cooperative binding of SAM and substrate might provide a mechanism to limit the generation of 5'-deoxyadenosyl radicals in the absence of the correct substrate, thus avoiding harmful side reactions (Ugulava *et al.*, 2003).

As mentioned above in section 3.1.3.1 all amino acid residues chosen for mutagenesis are conserved among different HemN proteins. However, as illustrated in Figure 17, the degree of conservation is indeed higher for Arg^{308}, Arg^{434} and Gln^{338} than for Arg^{359} which could be mutated without detectable effect on enzyme function. One might argue that replacing Arg^{359} with lysine is a conservative exchange and that lysine might be able to maintain the assumed

ionic interaction of arginine with the substrate propionate side chain. However, identical conservative exchanges were carried out for the other two arginines (Arg^{308} and Arg^{434}) and caused the same loss of activity as the exchange for alanine (see above).

3.1.3.4 Conclusions from the Mutagenesis of the Proposed Substrate Binding Site

The mutagenesis study presented here provides first experimental data supporting the proposed substrate binding site of *E. coli* HemN. Two conserved arginines (Arg^{308} and Arg^{434}) were identified which were absolutely essential for enzyme activity. Gln^{338} was also found to be important.

With the exception of Arg^{22} the amino acid residues mutated in this study are located in or near the C-terminal domain of HemN. This is in good agreement with a recent bioinformatics study analyzing a structure-based alignment of different subclasses of Radical SAM proteins (Nicolet and Drennan, 2004). This analysis revealed that conserved domains were mostly found in the N-terminal regions of the proteins and were e.g. associated with SAM coordination. The C-terminal region, on the other hand, was found to be quite divergent between the subclasses, thus allowing the binding of a variety of very different substrates. The alignment did not include the N-terminal 35 amino acid residues of *E. coli* HemN, the so-called N-terminal 'trip-wire', which does not belong to either of the two domains.

In the present 'substrate-less' conformation of HemN - as depicted by the crystal structure - binding to the investigated amino acid residues does not place the substrate in immediate vicinity to the iron-sulfur cluster and the two SAM co-substrates. *In vivo*, however, conformational rearrangements of the C-terminal domain and the N-terminal 'trip-wire' are expected to take place upon substrate binding (Layer *et al.*, 2003). The C-terminal domain may play a role in covering the active site cavity and thus shielding the bound substrate from the solvent. The N-terminal 'trip-wire' adopts an extended conformation without pronounced secondary structure in the HemN crystal structure but contains a stretch of nine highly conserved residues (Figure 17). It may stabilize upon substrate binding and possibly induce rearrangement of the C-terminal domain. During such rearrangements distances between substrate and cofactors could certainly be modified. Alternatively, the investigated amino acids could be involved in positioning the substrate, meaning that the model would reflect just a transitory state and not the final orientation. However, the striking accumulation of suitable interaction partners at the present binding site makes it difficult to envisage the substrate moving further. In any case, one has to consider that the substrate binding model for *E. coli* HemN depicts the interaction of two not clearly defined partners (the enzyme is expected to

alter its conformation; the substrate coproporphyrinogen III is not entirely rigid either due to its non-conjugated backbone) and is therefore only an approximation. Nevertheless, the support of the proposed substrate binding site provided by this mutagenesis approach represents a good basis for further studies.

3.2 Investigation of Proposed Alternative Oxygen-independent Coproporphyrinogen III Oxidases

3.2.1 Two Distinct Types of HemZ and Approaches for their Characterization

The initial goal of this project was to provide final evidence for the postulated O_2-independent CPO activity of the enzyme HemZ by purifying and biochemically characterizing a representative of the group. Since the designations HemN and HemZ have been used inconsistently throughout the literature (compare INTRODUCTION) and not even only for (potential) O_2-independent CPOs, it was first necessary to get an overview of the distribution of both enzymes in bacteria and to select suitable canditates for a characterization. Database searches were performed, amino acid sequences assigned to the correct groups and the groups compared. While an alignment of 18 HemZ and 10 HemN amino acid sequences illustrated the overall sequence conservation among the different proteins, a phylogenetic tree created on the basis of this sequence alignment revealed that two subgroups of HemZ can clearly be distinguished. Figures 20 and 21 show part of an alignment of 10 HemZ and 6 HemN sequences and the corresponding phylogenetic tree; the complete alignment and tree of all 28 sequences can be found in Appendices 1 and 2.

The two subgroups of HemZ were designated HemZ and HemZ2. The two HemZ proteins of *B. subtilis* mentioned in the INTRODUCTION do indeed belong to the different groups. According to the sequence data presently available *hemZ* is more widely distributed than *hemZ2*. Unlike *hemN*, it is even present in some eukaryotic genomes. *hemZ2* has so far only been found in relatively few organisms and exclusively in Gram-positive bacteria. Interestingly, in these Gram-positive bacteria no homologues of the known CPOs HemF or HemN have been identified. Apart from their sequence conservation the two HemZ subgroups can be distinguished by protein length. HemZ2 proteins are on average about 100 amino acids longer than HemZ proteins (HemZ about 370 - 400 amino acids, HemZ2 about 480 - 500 amino acids; compare alignment in Appendix 1). As this distiction of two groups of potential alternative CPOs raised the possibility that they have different activities, it was decided to characterize a representative of each group.

First, HemZ from *E. coli* was chosen for recombinant production, purification and enzymatic characterization because the O_2-independent CPO acivity assay has been established for HemN from the same organism (Layer, 2001; Layer *et al.*, 2002). However, no detectable CPO activity was demonstrated for *E. coli* HemZ. Second, HemZ2 from *B. subtilis* was also

purified and tested for activity. In addition, the ability of *hemZ* and *hemZ2* to complement two CPO-deficient mutant strains - a *S. typhimurium hemF hemN* mutant and an *E. coli hemN* mutant - was examined.

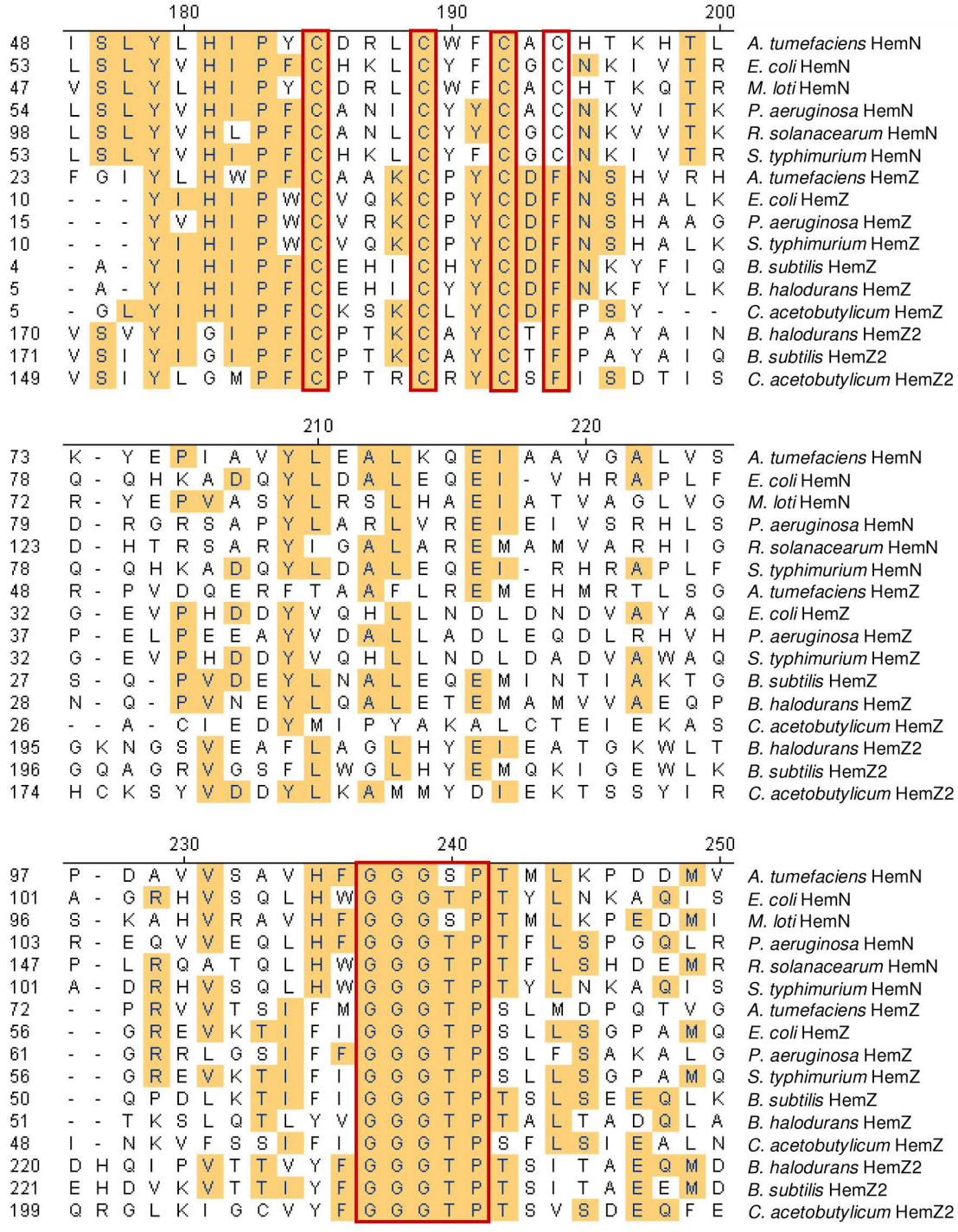

Figure 20: Section of an amino acid sequence alignment of the different HemN, HemZ and HemZ2 proteins showing the two most characteristic conserved regions. Boxed in red are the conserved CxxxCxxCxC/F motif (CxxxCxxCxC in HemN, CxxxCxxCxF in HemZ and HemZ2) and the glycin-rich motif. Numbers on the left indicate amino acid positions of the individual sequences, numbers on top refer to the length of the entire alignment. The alignment was generated with the program DNASTAR MegAlign™ by the Clustal method.

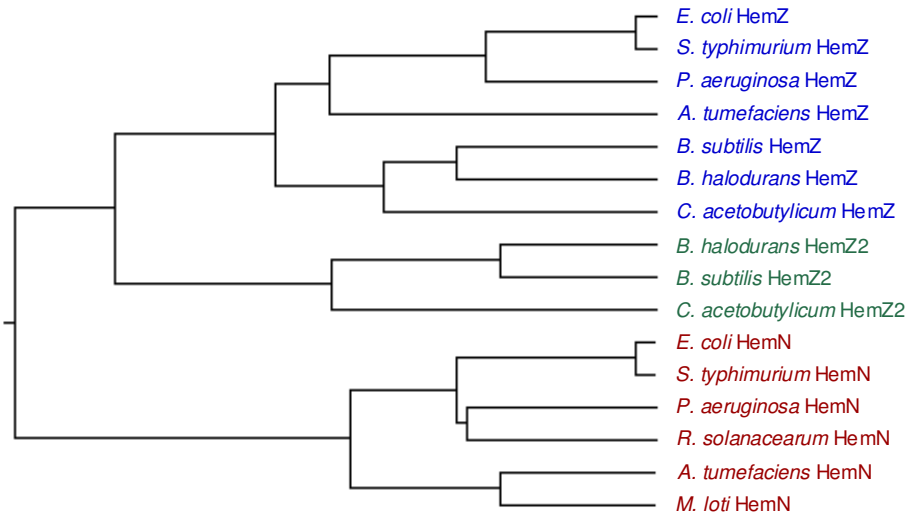

Figure 21: Phylogenetic tree showing the different groups of HemN, HemZ and HemZ2 proteins. The tree was created with the program DNASTAR MegAlign™ on the basis of the amino acid sequence alignment in Figure 20. Despite the apparent high overall homology seen in the alignment, three individual groups - depicted in different colours - are clearly distinguishable.

3.2.2 Biochemical Approach: Purification and Functional Investigation of *Escherichia coli* HemZ and *Bacillus subtilis* HemZ2

3.2.2.1 Purification and Characterization of *Escherichia coli* HemZ

The 1134 bp long gene *hemZ* from *E. coli* was cloned into plasmid pGEX-6P-1, resulting in plasmid pGEX-*hemZ*. The protein was produced in *E. coli* BL21(DE3) and purified to apparent homogeneity under anaerobic conditions using Glutathione Sepharose. In a first chromatographic step, the fusion protein consisting of HemZ and the N-terminal GST-tag was isolated. After PreScission Protease cleavage of the GST-HemZ fusion, recombinant HemZ was separated from the released GST-tag and the GST-tagged protease by a second affinity chromatography. Figure 22 provides documentation of the purification procedure. SDS-PAGE analysis of the purified protein (lane 8 in Figure 22) revealed a single band corresponding to a protein with a molecular weight of about 40 kDa, which is in good agreement with the calculated molecular mass of 42584.3 Da.

Protein and iron concentration of the concentrated HemZ solution were determined and an iron content of 0.3 mol iron / mol protein was calculated from these concentrations. The obtained iron content was very low for a protein which was expected to contain an iron-sulfur cluster. For *E. coli* HemN, a protein containing one [4Fe-4S] cluster, the experimentally

measured iron content in general ranges between 1.2 and 2.0 mol iron / mol protein. The low iron content of *E. coli* HemZ was also reflected by the absence of the characteristic yellow-brown colour of the protein solution and by the UV-visible light absorption spectrum recorded under anaerobic conditions (data not shown). A slight peak at 410 nm was detectable, indicating the presence of a [4Fe-4S] cluster in the protein. However, this peak was nearly negligible when compared to the spectrum of *E. coli* HemN (about 15-20 % of the HemN peak height).

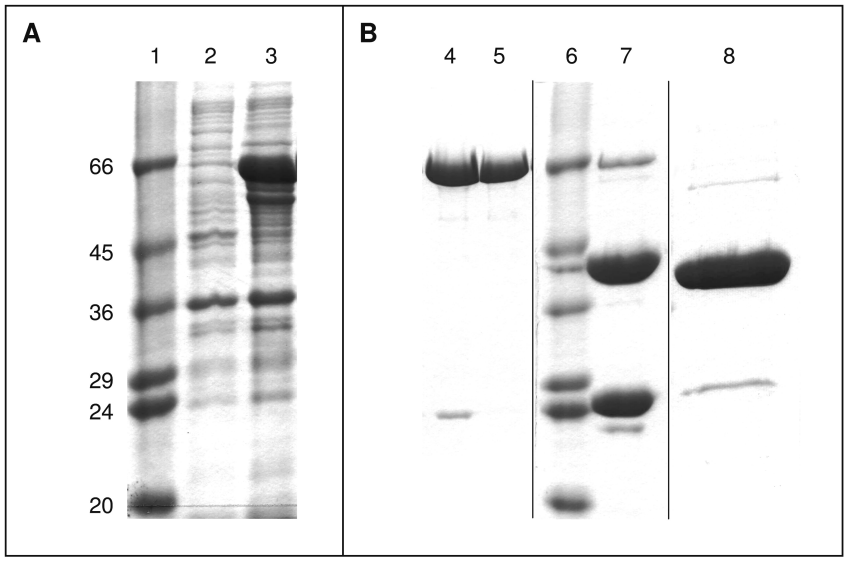

Figure 22: Production and purification of recombinant *E. coli* HemZ. Proteins were separated by 0.1 % SDS - 12 % PAGE as described in MATERIALS AND METHODS and visualized by staining with Coomassie Brilliant Blue. **A**, induction of protein production. **B**, protein purification. Lanes 1 and 6 show the proteins of the molecular weight marker, the respective relative molecular masses [x 10^3] are indicated. Lanes 2 and 3 show the crude extract of *E. coli* BL21(DE3) carrying pGEX-*hemZ* before (lane 2) and after (lane 3) induction with 100 µM IPTG. Lanes 4 and 5 contain the purified GST-HemZ fusion protein after the first Glutathione Sepharose affinity chromatography, lane 7 the same sample after PreScission Protease cleavage and lane 8 pure recombinant HemZ after removal of the GST-tag via a second Glutathione Sepharose affinity chromatography.

Because of the relatively high sequence homology between *E. coli* HemN and HemZ (31 % sequence identity), similar requirements with regard to assay conditions were expected. For this reason, first activity assays with purified recombinant *E. coli* HemZ were carried out under standard conditions for *E. coli* HemN, using purified recombinant HemN as a positive control. As shown in Figure 23, no O_2-independent CPO activity was detected for *E. coli* HemZ under these conditions. Tests were repeated with increased HemZ concentrations, with NADPH instead of NADH and with an *E. coli* crude extract instead of cell-free extract (see MATERIALS AND METHODS). However, also under modified assay conditions no O_2-independent CPO activity was detected for *E. coli* HemZ.

In addition to the activity assays with purified HemZ, a crude extract was prepared from the *E. coli* strain overproducing *E. coli* HemZ and used for activity assays without prior purification. The same was done for *E. coli* HemN. Crude extracts were added to standard assay mixtures instead of the purified proteins. As in the tests with purified protein no CPO activity was detected for *E. coli* HemZ while protoporphyrinogen IX was formed in the assay with HemN (Table 10). The results of all activity assays are summarized in Table 10.

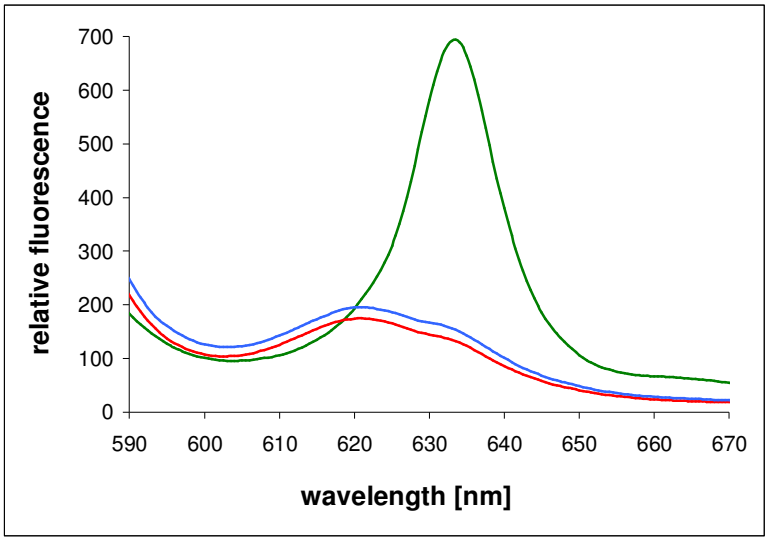

Figure 23: O_2-independent CPO activity assay for *E. coli* HemZ. Assays were carried out as described in MATERIALS AND METHODS. After oxidation of the formed reaction product protoporphyrinogen IX to protoporphyrin IX, this oxidized form was identified at its fluorescence emission wavelength of 633 nm. — sample containing *E. coli* HemZ, — sample containing *E. coli* HemN (positive control), — sample containing all assay components except enzyme (blank)

3.2.2.2 Purification and Characterization of *Bacillus subtilis* HemZ2

The 1503 bp long gene *hemZ2* from *B. subtilis* was cloned into pET-22b, resulting in plasmid pET-22b-$hemZ2_{B.s.}$. The vector pET-22b was initially chosen to allow production of HemZ2 as a His-Tag fusion protein. HemZ2 was produced in *E. coli* BL21 CodonPlus(DE3)-RIL carrying pET-22b-$hemZ2_{B.s.}$ and the fusion protein was purified to apparent homogeneity via Ni^{2+} affinitiy chromatography under anaerobic conditions (data not shown). However, a component present in the protein solution after the purification procedure interfered with the activity assay and/or the fluorimetric detection (data not shown). This was unexpected because several other enzymes of the tetrapyrrole biosynthetic pathway - e.g. uroporphyrinogen decarboxylase (Whitby *et al.*, 1998; Phillips *et al.*, 2003) and protoporphyrinogen IX oxidase (Hansson *et al.*, 1997) - have also been purified via Ni^{2+} affinitiy chromatography and similar problems have never been reported. Imidazole, β-

mercaptoethanol or nickel were identified as possible candidates for the interfering substance which could not be entirely removed by dialysis or buffer exchange via PD-10 columns. For this reason, an alternative purification system was used.

In order to remove the C-terminal His-Tag, a stop codon was inserted by site-directed mutagenesis into its original position behind the gene *hemZ2* on plasmid pET-22b-*hemZ2*$_{B.s.}$. The resulting plasmid pET-22b-*hemZ2*$_{B.s.}$L502Stop was subsequently expressed in *E. coli* BL21CodonPlus(DE3)-RIL for purification of recombinant HemZ2 via Blue Sepharose affinity chromatography analogous to *E. coli* HemN. Prior to purification, successful removal of the His-Tag was confirmed by Western Blot analysis of cells overproducing HemZ2 using an Anti-His antibody (data not shown). *B. subtilis* HemZ2 bound to Blue Sepharose and eluted at approximately 300 mM NaCl. *E. coli* HemN elutes at a similar NaCl concentration. SDS-PAGE analysis of the purified protein (Figure 24, lanes 7 and 8) revealed a predominant band similar in size to the overproduced protein in the crude extract in lane 3 and corresponding to a protein with a molecular weight of about 55 kDa. This is in good agreement with the calculated molecular mass of 57357.2 Da.

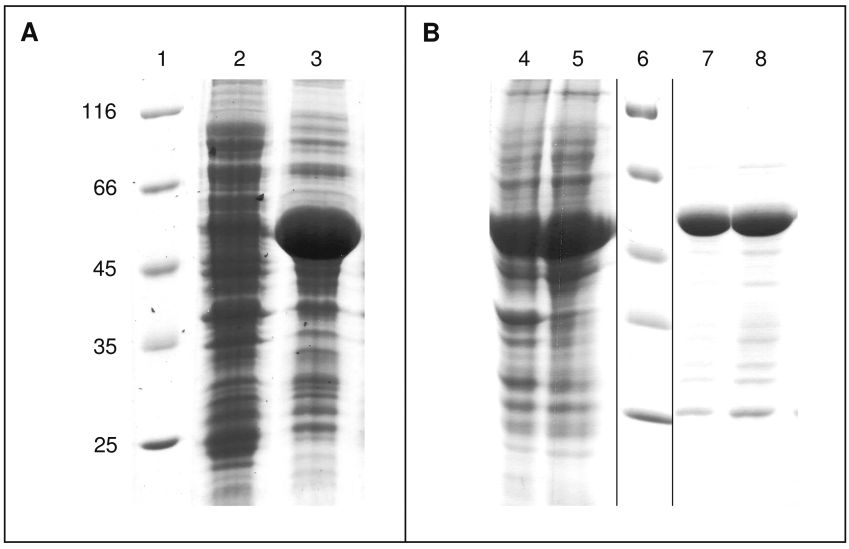

Figure 24: Production and purification of recombinant *B. subtilis* HemZ2. Proteins were separated by 0.1 % SDS - 12 % PAGE as described in MATERIALS AND METHODS and visualized by staining with Coomassie Brilliant Blue. **A**, induction of protein production. **B**, protein purification. Lanes 1 and 6 show the proteins of the molecular weight marker, the respective relative molecular masses [x 10^3] are indicated. Lanes 2 and 3 show the crude extract of *E. coli* BL21CodonPlus(DE3)-RIL carrying pET-22b-*hemZ2*$_{B.s.}$ before (lane 2) and after (lane 3) induction with 500 µM IPTG. Lanes 4 and 5 compare total crude extract (lane 4) and its soluble fraction (lane 5). Lanes 7 and 8 contain recombinant HemZ2 after purification via Blue Sepharose affinity chromatography.

As it was the case for *E. coli* HemZ, also *B. subtilis* HemZ2 appeared colourless. The iron content of HemZ2, calculated after protein and iron concentration of the protein solution had been determined, was 0.35 mol iron / mol protein. This is also similar to the data obtained for

E. coli HemZ (section 3.2.2.1). The UV-visible light absorption spectrum recorded for *B. subtilis* HemZ2 gave only weak indication of a [4Fe-4S] cluster (about 5-10 % of the 410 nm peak height of *E. coli* HemN). Purified recombinant HemZ2 was tested for O_2-independent CPO activity under standard conditions used for *E. coli* HemN (see MATERIALS AND METHODS). Further assays were carried out with increased enzyme and substrate concentrations. No CPO activity of *B. subtilis* HemZ2 could be detected in any of these assays (spectra identical to those shown for *E. coli* HemZ in Figure 23).

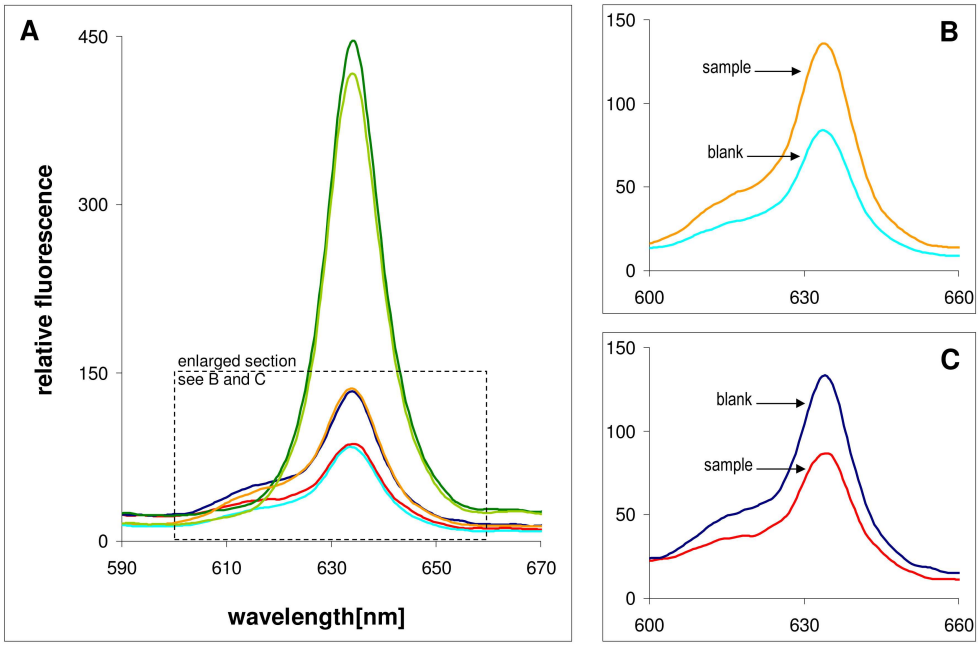

Figure 25: Illustration of the varying results obtained in activity assays with *B. subtilis* HemZ2 using PPO for product oxidation. Assays contained 3 µM enzyme and 60 µM substrate. The assay with *E. coli* HemN was carried out using only 1.5 µM enzyme and 30 µM substrate. After incubation (90 min at 37 °C under anaerobic conditions) formed protoporphyrinogen IX in each sample was oxidized to protoporphyrin IX by addition of 7.5 µM PPO. This oxidized form of the reaction product was identified at its fluorescence emission wavelength of 633 nm. **A**, fluorescence spectra of HemZ2, HemN and Blank of two different tests series. Test 1, — sample containing HemZ2, — sample containing HemN (positive control), — sample containing all assay components except enzyme (blank). Test 2, — sample containing HemZ2, — sample containing HemN (positive control), — blank. **B**, detail of A, showing only spectra of HemZ2 (—) and blank (—) of test 1. **C**, detail of A, showing only spectra of HemZ2 (—) and blank (—) of test 2.

As enzymatic protoporphyrinogen IX oxidation with *T. elongatus* PPO had allowed a more realistic detection of the reaction product in the case of *E. coli* HemN, assays with *B. subtilis* HemZ2 were repeated using PPO instead of H_2O_2. HemZ2 concentration (1.5 µM - 6 µM), PPO concentration (0.75 µM - 7.5 µM) and duration of the oxidation step (15 - 30 min) were varied. Also these tests did not reveal O_2-independent CPO activity for HemZ2. For some assays obtained results were difficult to interpret, because blank and sample alternately produced a slightly higher fluorescence peak at 633 nm (Figure 25). These results were never

reproducible and peaks were hardly above the background, which indicates that all measured values were within the error range of the method.

Possibly different cofactor requirements of the *E. coli* and *B. subtilis* enzymes were taken into account and the *E. coli* cell-free extract - which supplies the so far unidentified physiological electron donor and electron acceptor in the HemN activity assay - replaced accordingly. First, sodium dithionite (DT) and N-methylphenazonium methyl sulfate (PM) were used instead. These substances have been shown to function as artificial electron donor and acceptor for *E. coli* HemN, although with lower yield of the reaction product. Alternatively, the *E. coli* cell-free extract was replaced by a *B. subtilis* crude extract. Both approaches did not reveal O_2-independent CPO activity for *B. subtilis* HemZ2 (Table 10). Interestingly, *E. coli* HemN also showed no activity in the assay with *B. subtilis* crude extract. This points to a high degree of - possibly genus-dependent - specificity of the O_2-independent CPOs.

Table 10: Summary of the different assay conditions and obtained results for *E. coli* HemZ and *B. subtilis* HemZ2

Assay system[1]	*E. coli* HemZ	*B. subtilis* HemZ2	*E. coli* HemN (positive control)
E. coli cell-free extract and H_2O_2	–[4]	–	+[7]
E. coli cell-free extract and PPO	n.t.[5, 6]	–	+
E. coli crude extract	–	n.t.	+
B. subtilis crude extract and H_2O_2 or PPO	n.t.	–	–[8]
DT/PM[2]	n.t.[6]	–	+
Overproduced protein in crude extract[3]	–	–	+

[1] Unless specifically stated, H_2O_2 was used to oxidize the reaction product protoporphyrinogen IX to protoporphyrin IX.
[2] DT, sodium dithionite, PM, N-methylphenazonium methyl sulfate
[3] Proteins were overproduced in the respective strains and crude extracts were prepared and used for activity assays without prior purification of the proteins.
[4] –, no activity detectable
[5] n.t., not tested
[6] Test systems with PPO and DT/PM had not yet been established when the activity of *E. coli* HemZ was investigated.
[7] +, CPO activity shown
[8] The observed catalytic inactivity of *E. coli* HemN upon replacement of the *E. coli* cell-free extract with a *B. subtilis* crude extract points to a high degree of specificity of the O_2-independent CPOs.

As described in section 3.2.2.1 for *E. coli* HemZ, a crude extract was prepared from the

E. coli strain overproducing *B. subtilis* HemZ2 and used for activity assays without prior purification. Crude extracts were added to standard assay mixtures instead of the purified proteins, either with or without additional *B. subtilis* crude extract. As before, no CPO activity was detected for *B. subtilis* HemZ2 (Table 10).

3.2.3 Genetic Approach: Functional Complementation of CPO-deficient Mutants

Although no O_2-independent CPO activity was observed in assays with purified recombinant HemZ and HemZ2 or in assays with crude extracts, one cannot rule out the possibility that - e.g. due to the assay conditions - activities were too low to be detected. For this reason, a more sensitive method was used to verify the results of the biochemical approach. Functional complementation normally allows detection of low levels of gene expression and of activity of the respective gene product because there only has to be enough activity to support growth.

E. coli hemZ and both *hemZ* and *hemZ2* from *B. subtilis* were tested for their ability to complement heme-requiring mutants defective in the CPO encoding gene(s). Initially, the strain *Salmonella typhimurium* TE3006 was used for these functional complementation experiments. This strain lacks a functional CPO due to a disruption of both the *hemF* and the *hemN* gene and can therefore only grow when the medium is supplemented with hemin (Xu *et al.*, 1992). A similar *hemF hemN* mutant had so far not been generated in *E. coli* because the *E. coli* K12 derived strains normally used in the laboratory today are unable to transport externally supplied hemin into the cell. However, as transformation efficiencies obtained for *S. typhimurium* are generally low (e.g. Wirth *et al.*, 1989) and turned out to be very low for mutant strain TE3006, an *E. coli hemN* mutant was generated and used for further complementation experiments. The idea behind this approach was that for an *E. coli hemN* mutant - in contrast to a *hemF hemN* double mutant - growth under aerobic conditions should not be affected and external hemin supply should not be necessary, because the mutant still has a functional O_2-dependent CPO (HemF). Under anaerobic conditions, on the other hand, growth of an *E. coli hemN* mutant should be significantly reduced. Such a mutant strain could then be grown without difficulties under aerobic conditions and be used for functional complementation tests under anaerobic conditions.

3.2.3.1 Functional Complementation of a *Salmonella typhimurium hemF hemN* Double Mutant

S. typhimurium TE3006 was transformed with different plasmids carrying the genes to be tested for their ability to complement the mutant as well as plasmids serving as positive and negative controls. The genes to be tested were *E. coli hemZ* (pGEX-*hemZ*), *B. subtilis hemZ* (pBlue-$hemZ_{B.s.}$) and *B. subtilis hemZ2* (pBlue-$hemZ2_{B.s.}$); plasmid designations are given in parentheses. *E. coli hemF* (pBlue13) and *E. coli hemN* (pBlueN7) were included as positive controls, plasmids pGEX-6P-1 and pBlueskript SK^+ without inserts as negative controls. Colonies growing on hemin-supplied medium after transformation of *S. typhimurium* TE3006 were subsequently streaked in parallel on plates with and without hemin. If the ability of the mutant to grow without hemin addition was restored, this provided evidence that the gene on the plasmid encoded a protein with CPO activity. Different antibiotics were used as described in MATERIALS AND METHODS.

Both *E. coli hemZ* and *B. subtilis hemZ* did not complement the mutant, while both genes used as positive controls (*E. coli hemF* and *hemN*) did restore hemin-independent growth of *S. typhimurium* TE3006 (Figure 26). Due to the poor transformation efficiency of *S. typhimurium* TE3006, the ability of *B. subtilis hemZ2* to complement this strain could not be investigated. For this reason, an *E. coli hemN* mutant was generated to be used for further experiments instead of the *S. typhimurium hemF hemN* mutant. The results of all complementation experiments are summarized in Table 11.

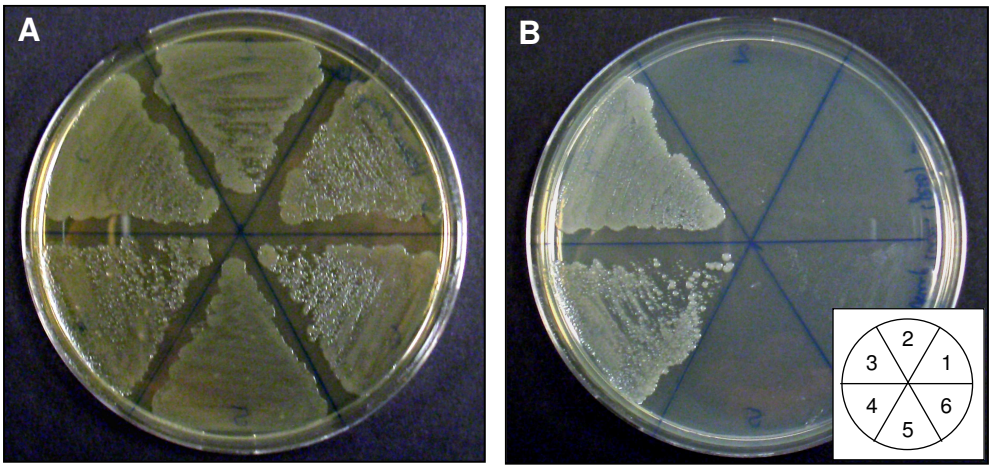

Figure 26: Functional complementation of heme-requiring *hemF hemN* mutant strain *S. typhimurium* TE3006. A, Growth on medium supplemented with hemin. **B**, Growth on medium not containing hemin. Streaked out are: 1, TE3006 carrying plasmid pBlue-$hemZ_{B.s.}$ (*B. subtilis hemZ*), 2, TE3006 with plasmid pGEX-*hemZ* (*E. coli hemZ*), 3, TE3006 with plasmid pBlueN7 (*E. coli hemN*), 4, TE3006 with plasmid pBlue13 (*E. coli hemF*), 5, TE3006 carrying pBlueskript SK^+ without insert, 6, TE3006 carrying pGEX-6P-1 without insert.

3.2.3.2 Generation of an *Escherichia coli hemN* Mutant

Using the method of Datsenko and Wanner (2000) described in detail in MATERIALS AND METHODS, the chromosomal *hemN* gene of *E. coli* wild type strain MC4100 was replaced by a kanamycin resistance (kan^r) gene. The successful replacement was verified by PCR amplification of both new junction fragments. Using two different primer pairs, each consisting of one primer complementary to the kan^r gene and one primer complementary to the region upstream or downstream of *hemN*, fragments of the expected size were amplified (1400 bp with primers kt and controlhemN-rev, 1100 bp with primers controlhemN-fwd and k2; compare Figure 12 D in section 2.5.10) (data not shown).

Growth curves of the *E. coli hemN* mutant strain in comparison to the *E. coli* MC4100 wild type were recorded under aerobic and anaerobic conditions. As mentioned above (section 3.2.3), normal aerobic growth was expected because the mutant strain still has a functional *hemF* gene, coding for the O_2-dependent CPO. Under anaerobic conditions, on the other hand, the *hemN* mutant was expected to exhibit reduced growth compared to the wild type.

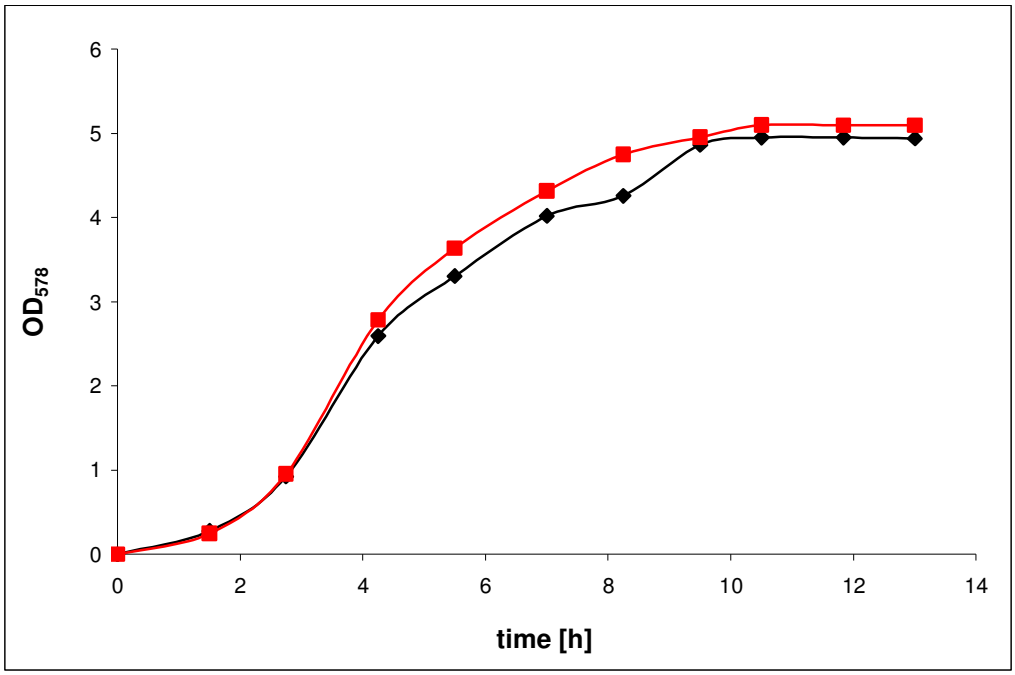

Figure 27: Growth of *E. coli* MC4100 *hemN* mutant and wild type under aerobic conditions. Cells were grown at 37 °C in LB medium without antibiotics. Values for each strain are averages of three parallel cultures. — Δ*hemN*, — wild type.

The growth curves shown in Figures 27 and 28 illustrate that growth of *E. coli* Δ*hemN* under anaerobic conditions was indeed clearly reduced in comparison to the wild type (Figure 28), while growth of both strains was identical under aerobic conditions (Figure 27). This growth

phenotype represented an additional verification of the successful *hemN* disruption and furthermore indicated that the newly generated *E. coli* mutant strain was suited for functional complementation experiments under anaerobic conditions.

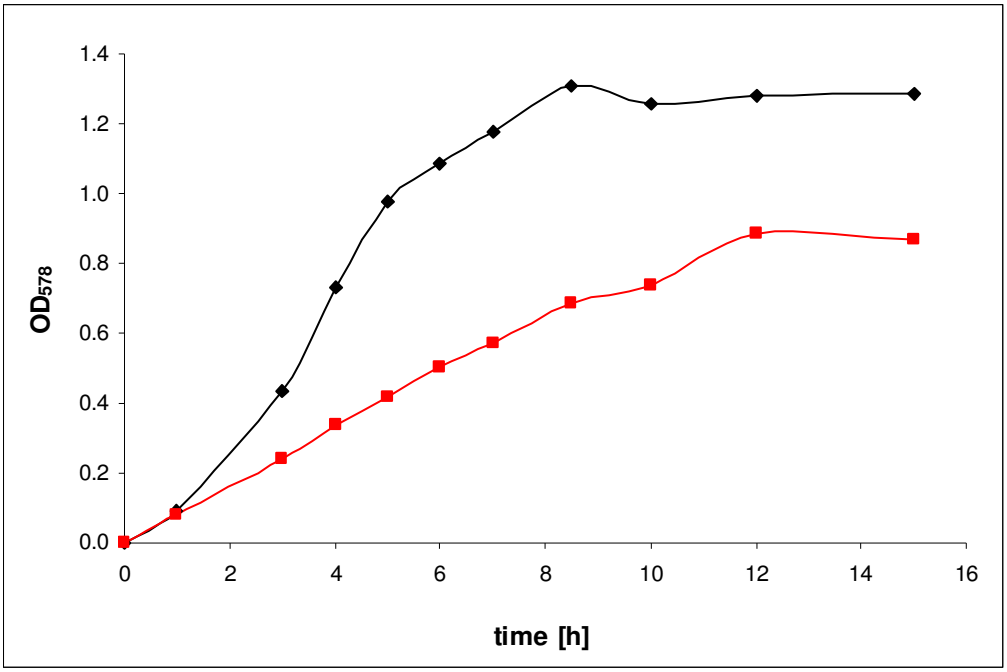

Figure 28: Growth of *E. coli* MC4100 *hemN* mutant and wild type under anaerobic conditions. Cells were grown at 37 °C in LB medium containing 10 mM $NaNO_3$ and no antibiotics in tightly sealed anaerobic flasks. Values for each strain are averages of three parallel cultures. — Δ*hemN*, — wild type.

3.2.3.3 Functional Complementation of an *Escherichia coli hemN* Mutant

The *E. coli hemN* mutant was transformed with different plasmids carrying the genes to be tested for their ability to complement the mutant as well as plasmids serving as positive and negative controls. The genes to be tested were *E. coli hemZ* (pGEX-*hemZ*, pET-21b-*hemZ*) and *B. subtilis hemZ2* (pET-22b-$hemZ2_{B.s.}$L502Stop); plasmid designations are again given in parentheses. *E. coli hemN* (pET-3a-*hemN*) was included as positive control, plasmids pET-22b and pGEX-6P-1 without inserts as negative controls. The *E. coli* MC4100 wild type was also transformed with the insert-less vectors to serve as an additional control. Subsequently, parallel growth curves were recorded under anaerobic conditions for all strains carrying a pET-vector and for all strains with a pGEX-vector, respectively.

First of all, both *E. coli* wild type and mutant strain bearing insert-less plasmids pET-22b or pGEX-6P-1 exhibited the same growth phenotype as outlined before in section 3.2.3.2 (Figures 29 and 30). In contrast, *E. coli* Δ*hemN* carrying pET-3a-*hemN* reached cell densities comparable to the wild type (Figure 29). Clearly, *E. coli hemN* - the postitive control - was

able to restore wild type-like growth of the mutant strain. This successful complementation of the *E. coli hemN* mutant demonstrates the validity of the experimental approach. Growth curves of *E. coli* Δ*hemN* carrying plasmids with *E. coli hemZ* or *B. subtilis hemZ2* (pGEX-*hemZ*, pET-21b-*hemZ* or pET-22b-$hemZ2_{B.s.}$L502Stop) were identical to the growth curves of the negative controls, i.e. *E. coli* Δ*hemN* with the corresponding insert-less plasmids (Figures 29 and 30). Unlike *E. coli hemN*, both genes *E. coli hemZ* and *B. subtilis hemZ2* did not restore wild type-like growth of the mutant. These are the first experimental results concerning the question whether *B. subtilis hemZ2* is able to complement a heme-requiring mutant. In the case of *E. coli hemZ* these experiments confirm the results obtained with the *Salmonella* mutant (section 3.2.3.1). For both genes one can summarize that they failed to complement the *E. coli hemN* mutant.

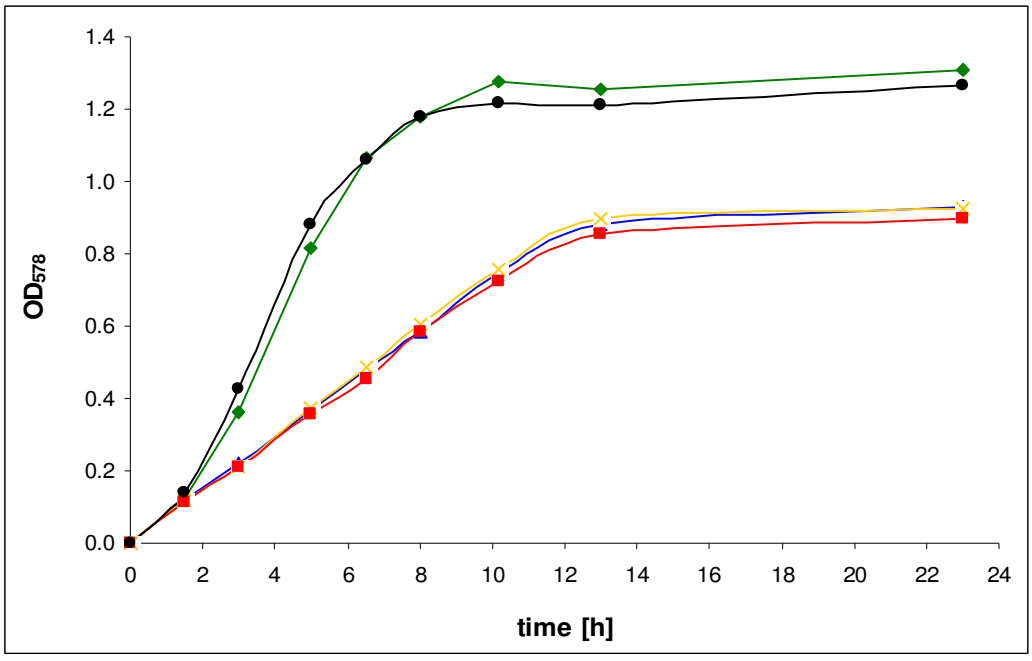

Figure 29: Comparison of the growth under anaerobic conditions of *E. coli* wild type and *hemN* mutant carrying different pET-constructs to test for functional complementation. Cells were grown at 37 °C in LB medium containing 10 mM $NaNO_3$ and no antibiotics in tightly sealed anaerobic flasks. Values for each strain are averages of three parallel cultures. — wild type with gene-less pET-22b, — Δ*hemN* with gene-less pET-22b, — Δ*hemN* with pET-3a-*hemN* (*E. coli hemN*), — Δ*hemN* with pET-21b-*hemZ* (*E. coli hemZ*), — Δ*hemN* with pET-22b-$hemZ2_{B.s.}$L502Stop (*B. subtilis hemZ2*).

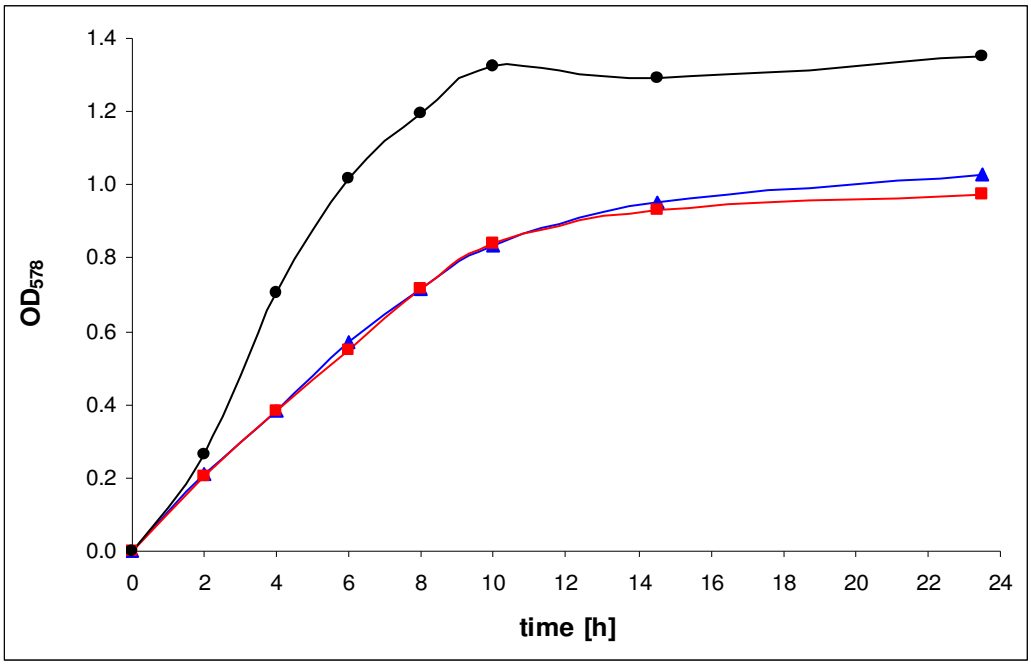

Figure 30: Comparison of the growth under anaerobic conditions of *E. coli* wild type and *hemN* mutant carrying different pGEX-constructs to test for functional complementation. Cells were grown at 37 °C in LB medium containing 10 mM $NaNO_3$ and no antibiotics in tightly sealed anaerobic flasks. Values for each strain are averages of three parallel cultures. — wild type with gene-less pGEX-6P-1, — Δ*hemN* with gene-less pGEX-6P-1, — Δ*hemN* with pGEX-*hemZ* (*E. coli hemZ*).

Table 11: Summary of the functional complementation experiments with *S. typhimurium* TE3006 and *E. coli* Δ*hemN*

Gene	CPO-deficient strain	
	TE3006[1]	Δ*hemN*[9]
E. coli hemZ	–[2, 3]	–[10]
B. subtilis hemZ	–[4]	n.t.
B. subtilis hemZ2	n.t.[5]	–[11]
E. coli hemF	+[6, 7]	n.t.
E. coli hemN	+[8]	+[12]

[1] TE3006, *S. typhimurium* TE3006
[2] pGEX-*hemZ*
[3] –, no complementation
[4] pBlue-$hemZ_{B.s.}$
[5] n.t., not tested
[6] pBlue13 (positive control)
[7] +, complementation successful
[8] pBlueN7 (positive control)
[9] Δ*hemN*, *E. coli* MC4100 Δ*hemN*
[10] pGEX-*hemZ* , pET-21b-*hemZ*
[11] pET-22b-$hemZ2_{B.s.}$L502Stop
[12] pET-3a-*hemN* (positive control)

Originally, plasmid pGEX-$hemZ_{B.s.}$ carrying *B. subtilis hemZ* was supposed to be included in these experiments. However, sequencing after cloning the gene into vector pGEX-6P-1 revealed that the sequence of *B. subtilis hemZ* available in the databases (and first determined by Homuth *et al.*, 1996) apparently contains a deletion of one nucleotide. The ‘new’ sequence

obtained during this work contains an additional G after position 1091 (see Appendix 3). Due to this 'frame shift' the translated protein is 11 amino acids longer. This hypothetical new C-terminus of *B. subtilis* HemZ is highly similar to the HemZ sequences from several other *Bacillus* species and from other bacterial genera, indicating that the longer sequence is in fact the correct one (see Appendix 3). In this case, the *hemZ* gene cloned into vector pGEX-6P-1 would be too short, as the original database sequence was used for primer design. Plasmid pBlue-$hemZ_{B.s.}$, on the other hand, and the results of the functional complementation experiments with *S. typhimurium* TE3006 are not concerned because longer DNA fragments were cloned into pBlueskript SK^+. The results of all complementation experiments are summarized in Table 11.

3.2.4 Conclusions from the Investigation of the Proposed Alternative Coproporphyrinogen III Oxidases

3.2.4.1 HemZ and HemZ2 do not Carry Detectable O_2-independent CPO Activity

E. coli hemZ was tested for its ability to complement both heme-requiring mutants *S. typhimurium* TE3006 and *E. coli* MC4100 Δ*hemN* and, in addition, activity assays with purified recombinant HemZ were carried out. A second *hemZ* - the *B. subtilis* gene - was also used in complementation tests with the *S. typhimurium* mutant. *B. subtilis hemZ2* was tested for its ability to complement the *E. coli hemN* mutant and - like *E. coli* HemZ - *B. subtilis* HemZ2 was subjected to a variety of activity assays. None of the approaches revealed O_2-independent CPO activity for HemZ or HemZ2. Although the present data is not interpreted as final evidence, all results consistently indicate that neither *hemZ* nor *hemZ2* encodes an O_2-independent coproporphyrinogen III oxidase.

As pointed out in section 3.2.3, absence of detectable enzyme activity alone would not be sufficient to support this conclusion, as it cannot be entirely ruled out that the assay conditions did not meet the requirements of the investigated enzyme. As far as the iron-sulfur cluster content of purified recombinant *E. coli* HemZ and *B. subtilis* HemZ2 is concerned, one can state that they have both been assigned to the Radical SAM protein family (Sofia *et al.*, 2001) and contain the characteristic CxxxCxxC motif. For this reason, the proteins were expected to contain a [4Fe-4S] cluster. Overproduction of recombinant proteins often causes incomplete iron-sulfur cluster incorporation. Purified recombinant *E. coli* HemN, for example, contains

maximal two instead of the theoretical four mol iron / mol protein. Both *E. coli* HemZ and *B. subtilis* HemZ2 had a similar iron content, indicating no specific problems with the synthesis of a *Bacillus* iron-sulfur protein in an *E. coli* host. For *B. subtilis* Fnr such problems were also not observed (Reents, unpublished data). In conclusion, one simply does not know what would be the minimum FeS cluster content to 'theoretically' support enzyme activity. Furthermore, even if this was known, one would still not be able to draw definite conclusions in the absence of detectable activity. If an enzyme does not have the expected function, data from activity assays can never suffice as final evidence.

The successful complementation of the *E. coli hemN* mutant with pET-3a-*hemN* demonstrated that the plasmid-borne gene was expressed in strain *E. coli* MC4100 Δ*hemN* although this strain does not contain T7 RNA polymerase. Repetition of the these complementation experiments in the presence of plasmid-encoded T7 RNA polymerase was intended. However, obtained growth curves did not allow conclusions to be drawn (data not shown). Plasmid pGP1-2 contains the T7 RNA polymerase gene under the control of a heat-inducible promoter (Tabor and Richardson, 1985) and the necessary shifts in incubation temperature and/or the protein overproduction might have caused the growth curve problems.

For *hemZ* additional evidence supporting the conclusion that the gene does not encode a CPO comes from other strains. For example, a *hemZ* homologue has also been identified in *S. typhimurium*. Nevertheless, the *hemF hemN* mutant strain TE3006 used in this and other studies is definitely CPO deficient (Xu *et al.*, 1992) and sequence conservation between *S. typhimurium* and *E. coli* is extremely high (92 % amino acid sequence identity for HemZ). For *Bradyrhizobium japonicum* experimental evidence also indicates that only hemN ('hemN2' in the original publication) and not hemZ ('hemN1' in the original publication) is functional (Fischer *et al.*, 2001). For *hemZ2* no such additional evidence was found and, furthermore, the gene is present only in organisms which possess neither *hemF* nor *hemN*. Consequently, the possibility was temporarily considered that *hemZ2* might encode an O_2-independent CPO even though *hemZ* does not. However, as pointed out above, the entirety of experimental data obtained for both genes points to the same conclusion, i.e. that both *hemZ* and *hemZ2* do not code for enzymes with CPO activity.

3.2.4.2 Implications for Heme Biosynthesis in *Bacillus subtilis* and Related Genera

The results presented here for *hemZ* and *hemZ2* and the conclusions these results point to raise two central questions:

(1) How can these findings be reconciled with previous studies of other researchers in our

laboratory who came to the conclusion that both *B. subtilis* HemZ and HemZ2 are O_2-independent CPOs (Hippler *et al.*, 1997; Homuth *et al.*, 1999)?

(2) How do organisms like *B. subtilis* accomplish the conversion of coproporphyrinogen III into protoporphyrinogen IX?

As far as the first question is concerned, the results obtained in this work cannot at present be entirely reconciled with those presented earlier by Hippler, Homuth and co-workers. In their publications, successful complementation of a CPO-deficient *S. typhimurium* mutant strain with both *B. subtilis hemZ* and *hemZ2* was reported. In addition, coproporphyrin III was shown to accumulate under anaerobic conditions in a *B. subtilis hemZ* and in a *B. subtilis hemZ2* mutant. For the functional complementation experiments with *B. subtilis hemZ* *S. typhimurium* TE3006 and another mutant strain, *S. typhimurium* TE2849, were used (Hippler *et al.*, 1997). Both strains are kan^r. The *hemZ* gene was cloned into plasmid pOK12 which is also kan^r. This leaves only heme sufficiency vs. heme requirement to select for transformed cells. In addition, only the *hemN* gene of strain TE2849 has been disrupted by a transposon, *hemF* has only been inactivated by a point mutation (Xu *et al.*, 1992). While there might be one or two potentially critical aspects, it is in no way intended to question the experimental work of Hippler and co-workers. For the corresponding experiments with *hemZ2* exclusively *S. typhimurium* TE3006 and an amp^r plasmid (pBlueskript SK^+) were used (Homuth *et al.*, 1999).

However, another result of those older studies - which does not indicate that the investigated genes encode CPOs - is that for both the *B. subtilis hemZ* and the *hemZ2* single mutant and even for a *hemZ hemZ2* double mutant growth was not affected compared to the *B. subtilis* wild type (Hippler *et al.*, 1997; Homuth *et al.*, 1999). The observed accumulation of coproporphyrin III and uroporphyrin III (autooxidized forms of the corresponding porphyrinogens) in the *B. subtilis hemZ* and *hemZ2* mutants under anaerobic conditions indicates that the two genes are in some way involved in the conversion of coproporphyrinogen III into protoporphyrinogen IX or in heme biosynthesis in general. They could play a regulatory role, e.g. related to oxygen.

The second question was already discussed before the *hemZ* genes were discovered in *B. subtilis*. The enzyme for the conversion of coproporphyrinogen III into protoporphyrinogen IX is the only one of the entire pathway that has not been identified in *B. subtilis*. The other genes are organized in two gene clusters on the *B. subtilis* genome, the *hemAXCDBL* operon encoding the enzymes required for the synthesis of uroporphyrinogen III from glutamyl-tRNA (Hansson *et al.*, 1991) and the *hemEHY* operon containing the genes for

uroporphyrinogen III decarboxylase, protoporphyrinogen IX oxidase and ferrochelatase (Hansson and Hederstedt, 1992).

After the identification of the *hemEHY* operon it was considered for some time that *hemY* might encode a bifunctional protein with both CPO and PPO activity (Hansson and Hederstedt, 1992). HemY then turned out to be a protoporphyrinogen IX oxidase, but it was also observed that the enzyme catalyzed the oxidation of coproporphyrinogen III to coproporphyrin III (Dailey *et al.*, 1993; Hansson and Hederstedt, 1994; Hansson *et al.*, 1997). The absence of a CPO-encoding gene within the two gene clusters together with the coproporphyrinogen III to coproporphyrin III oxidase activity of HemY gave rise to the idea that *B. subtilis* might synthesize protoporphyrinogen IX by an alternative pathway, leading from coproporphyrinogen III via coproporphyrin III to protoporphyrin IX (Hansson *et al.*, 1997). In this case, *B. subtilis* would have to possess a still unidentified enzyme for the conversion of coproporphyrin III into protoporphyrin IX.

It is possible that such an alternative pathway exists - but rather as an additional pathway besides a main pathway within one organism. (If HemY indeed oxidizes coproporphyrinogen III to coproporphyrin III in cells *in vivo*, this will otherwise be a dead-end product which is probably harmful and removes coproporphyrinogen III from the heme biosynthetic pathway.) Rescue of an *E. coli* Δ*hemG* mutant by overexpression of *hemF* has been reported which suggests that HemF can also catalyze the oxidation of protoporphyrinogen IX to protoporphyrin IX (Narita *et al.*, 1999). It therefore does not seem to be unusual - but also not more than a side-effect - that one enzyme recognizes and oxidizes both porphyrinogens. In addition, one has to keep in mind that the conversion of coproporphyrinogen III into protoporphyrinogen IX has been shown to be a major target of regulation of heme biosynthesis (Jahn, 1996; Rompf *et al.*, 1998; Schobert and Jahn, 2003). Under these circumstances, regulation of the two different activities of a bifunctional enzyme responsible for almost directly consecutive reactions would be difficult to accomplish.

The other possibility is the existence of a different, so far unrecognized enzyme catalyzing the oxidative decarboxylation of coproporphyrinogen III to protoporphyrinogen IX. This hypothetical third coproporphyrinogen III oxidase apparently does not have detectable sequence similarity to either the O_2-dependent CPO HemF or the O_2-independent CPO HemN. HemF and HemN are also not structurally related, but this can be explained by their different relationship to oxygen and ensuing cofactor requirements. The occurrence of the hypothetical third CPO could e.g. be limited to Gram-positive bacteria.

4. SUMMARY

The Radical SAM enzyme coproporphyrinogen III oxidase (CPO) catalyzes the oxidative decarboxylation of coproporphyrinogen III to protoporphyrinogen IX during heme and chlorophyll biosynthesis. This work included further characterization of the oxygen-independent CPO HemN from *E. coli* and the investigation of two proposed alternative oxygen-independent CPOs, designated HemZ and HemZ2.

Based on the crystal structure of *E. coli* HemN, single amino acid residues were exchanged by site-directed mutagenesis to investigate the functional role of the second SAM molecule bound in the HemN crystal structure (SAM2) and its proposed substrate binding site. All mutant proteins were tested for various catalytic properties, namely their ability to cleave SAM and to form the reaction product protoporphyrinogen IX. In the SAM2 binding site mutagenesis study no significant protoporphyrinogen IX formation was detected for any of the mutant enymes. Unlike wild type HemN, those enzyme variants which still exhibited reduced SAM cleavage never cleaved more than one molecule of SAM per molecule of enzyme. These observations indicate that SAM1 can still be bound and cleaved, but that no product is formed due to the absence of SAM2. A functional role of SAM2 in HemN catalysis is apparent. Mutational analysis of the proposed substrate binding site led to the identification of two highly conserved arginines and one equally conserved glutamine which were essential for HemN activity. A role of these amino acid residues in substrate binding was deduced. These are the first experimental results supporting the proposed substrate binding site of *E. coli* HemN. In addition, the ratio of SAM cleavage to product formation was quantified for wild type HemN. It was shown that two molecules of SAM are consumed during the formation of one molecule of protoporphyrinogen IX. This stoichiometry is compatible with the catalyzed reaction - the oxidative decarboxylation of two propionate side chains of the substrate - and supports the previously proposed reaction mechanism.

Some organisms possess neither the O_2-dependent CPO HemF nor the O_2-independent enzyme HemN. The genes *hemZ* and *hemZ2* which were first identified in *B. subtilis* have been proposed to encode alternative O_2-independent CPOs. In this work HemZ from *E. coli* and HemZ2 from *B. subtilis* were purified and biochemically characterized. In addition, the *hemZ* gene from *E. coli* and the genes *hemZ* and *hemZ2* from *B. subtilis* were tested for their ability to complement two CPO-deficient mutants, a *S. typhimurium hemF hemN* mutant and an *E. coli hemN* mutant. Both approaches revealed no CPO activity for either HemZ or HemZ2, indicating that the two types of enzymes have different functions.

5. OUTLOOK

E. coli HemN

For HemN, the focus of this work lay on the structure-based mutagenesis studies. Structural information on HemN with bound substrate could help to confirm the results of these studies and, in addition, promote a more detailed understanding of the reaction mechanism. As pointed out in the discussion of the SAM2 binding site mutants, one step towards this better understanding of the HemN reaction would be to find out which SAM is cleaved first.

Co-crystallization and structure determination of wild type HemN with bound substrate could e.g. provide further evidence for the functional role of SAM2 by showing whether SAM2 is adequately positioned to be involved in transfer of an electron from the iron-sulfur cluster to the substrate. According to the substrate model a suitable orientation is possible, but not simultaneously for SAM1 and SAM2 (Layer *et al.*, 2003). Nevertheless, this model could not consider aspects like the exact conformation of bound coproporphyrinogen III and possible structural rearrangements of HemN upon substrate binding.

Furthermore, a co-crystal is expected to reveal the orientation of the substrate pyrrole rings A and B towards SAM1 and SAM2. If one then assumes that the propionate side chain of ring A is decarboxylated first as observed for HemF, one will be able to conclude which SAM is cleaved first. If, in addition, detection of a reaction intermediate with only one vinyl group is possible for wild type HemN, this - in combination with the structural data - will provide more solid evidence for the sequence of reaction steps.

With regard to substrate binding itself, co-crystallization will be indispensable to identify beyond doubt the involved amino acids and also to find out about possible conformational rearrangements upon substrate binding. Here, the SAM2 binding site mutants still cleaving SAM might be useful candidates for crystallization. Their inability to cleave more than one SAM gave rise to the idea that they might be unable to replace SAM1 without completing their catalytic cycle. In this case the substrate might also get trapped in the active site.

First attempts to co-crystallize HemN with coproporphyrinogen III generated by chemical reduction of coproporphyrin III were unsuccessful (Layer, unpublished data). Similar observations were reported for uroporphyrinogen III decarboxylase (URO-D) and the problems attributed to the sodium amalgam-mediated reduction of uroporphyrin III (Phillips *et al.*, 2003). In the case of URO-D co-crystallization was instead achieved with enzymatically *in situ* synthesized substrate (Phillips *et al.*, 2003). Parallel approaches with both chemically and enzymatically synthesized coproporphyrinogen III should be pursued for

HemN.

The physiological electron donor and electron acceptor of the HemN reaction also remain to be identified. Were they known, a more defined assay system - not requiring the *E. coli* cell-free extract - could be established.

Alternative CPO

For the proposed alternative O_2-independent CPOs HemZ and HemZ2 the data presented in this work indicate that both do not catalyze the oxidative decarboxylation of coproporphyrinogen III to protoporphyrinogen IX. Further investigation of the two genes or proteins themselves is not expected to provide substantial new or more definite evidence. Rather, a new approach should be undertaken to search for the still unidentified CPO in e.g. *Bacillus subtilis*. This would involve construction of a plasmid library of the *B. subtilis* genome and subsequent screening of this library for clones with the ability to complement a CPO-deficient mutant strain. With regard to this mutant strain the same problems as in this work would be faced, i.e. low transformation efficiency of *S. typhimurium* TE3006 and constriction to anaerobic growth conditions when using *E. coli* Δ*hemN*. To circumvent these problems one could e.g. try to generate an *E. coli hemF hemN* mutant using the plasmid-encoded heme utilization locus from *Shigella dysenteriae* (Mills and Payne, 1995). This additional plasmid would have to be compatible with both the mutagenesis system and the plasmid library.

6. REFERENCES

Akhtar, M. (1991) Mechanism and stereochemistry of the enzymes involved in the conversion of uroporphyrinogen III into haem. In *Biosynthesis of tetrapyrroles*. (Jordan, P. M., ed.) Elsevier Science Ltd., Amsterdam, pp. 67-99.

Al-Karadaghi, S., Hansson, M., Nikonov, S., Jonsson, B. and Hederstedt, L. (1997) Crystal structure of ferrochelatase: the terminal enzyme in heme biosynthesis. *Structure* **5**, 1501-1510.

Ballinger, M. D., Reed, G. H. and Frey, P. A. (1992a) An organic radical in the lysine 2,3-aminomutase reaction. *Biochemistry* **31**, 949-953.

Ballinger, M. D., Frey, P. A. and Reed, G. H. (1992b) Structure of a substrate radical intermediate in the reaction of lysine 2,3-aminomutase. *Biochemistry* **31**, 10782-10789.

Battersby, A. R. and Leeper, F. J. (1990) Biosynthesis of the pigments of life: mechanistic studies on the conversion of porphobilinogen to uroporphyrinogen III. *Chem. Rev.* **90**, 1261-1274.

Battersby, A. R. (2000) Tetrypyrroles: the pigments of life. *Nat. Prod. Rep.* **17**, 507-526.

Beale, S. I. and Castelfranco, P.A. (1973) ^{14}C incorporation from exogenous compounds into δ-aminolevulinic acid by greening cucumber cotyledons. *Biochem. Biophys. Res. Commun.* **52**, 143-149.

Beale, S. I. and Weinstein, J. D. (1990) Tetrapyrrole metabolism in photosynthetic organisms. In *Biosynthesis of heme and chlorophylls.* (Dailey, H. A., ed.) McGraw-Hill Publishing, New York, pp. 287-392.

Beale, S. I. and Weinstein, J. D. (1991) Biochemistry and regulation of photosynthetic pigment formation in plants and algae. In *Biosynthesis of tetrapyrroles*. (Jordan, P. M., ed.) Elsevier Science Ltd., Amsterdam, pp. 155-235.

Beale, S. I. (1993) Biosynthesis of phycobilins. *Chem. Rev.* **93**, 785-802.

Beale, S. I. and Yeh, J. I. (1999) Deconstructing heme. *Nature Struct. Biol.* **6**, 903-905.

Beinert, H., Kennedy, M. C. and Stout, C. D. (1996) Aconitase as iron-sulfur protein, enzyme and iron-regulated protein. *Chem. Rev.* **96**, 2335-2374.

Beinert, H., Holm, R. H. and Münck, E. (1997) Iron-sulfur clusters: nature's modular, multipurpose structures. *Science* **277**, 653-659.

Beinert, H. (2000) Iron-sulfur proteins: ancient structures, still full of surprises. *J. Biol. Inorg. Chem.* **5**, 2-15.

Berkovitch, F., Nicolet, Y., Wan, J. T., Jarrett, J. T. and Drennan, C. L. (2004) Crystal structure of biotin synthase, an *S*-adenosylmethionine-dependent radical enzyme. *Science*,

303, 76-79.

Bradford, M. M. (1976) A rapid and sensitive method for the quantitation of microgram quantities of protein utilizing the principle of protein dye-binding. *Anal. Biochem.* **72**, 248-254.

Breckau, D., Mahlitz, E., Sauerwald, A., Layer, G. and Jahn, D. (2003) Oxygen-dependent coproporphyrinogen III oxidase (HemF) from *Escherichia coli* is stimulated by manganese. *J. Biol. Chem.* **278**, 46625-46631.

Broderick, J. B., Henshaw, T. F., Cheek, J., Wojtuszewski, K., Smith, S. R., Trojan, M. R., McGhan, R. M., Kopf, A., Kibbey, M. and Broderick, W. E. (2000) Pyruvate formate-lyase-activating enzyme: strictly anaerobic isolation yields active enzyme containing a $[3Fe\text{-}4S]^{+}$ cluster. *Biochem. Biophys. Res. Commun.* **269**, 451-456.

Casadaban, M. J. (1976) Transposition and fusion of the *lac* genes to selected promoters in *Escherichia coli* using bacteriophage λ and Mu. *J. Mol. Biol.* **104**, 541-555.

Chang, C. K. (1994) Haem d_1 and other haem cofactors from bacteria. In *The biosynthesis of tetrapyrrole pigments; Ciba Foundation Symposium 180*. (Chadwick, D. J. and Ackrill, K., eds.) Wiley, Chichester, pp. 228-246.

Cheek, J. and Broderick, J. B. (2001) Adenosylmethionine-dependent iron-sulfur enzymes: versatile clusters in a radical new role. *J. Biol. Inorg. Chem.* **6**, 209-226.

Cheek, J. and Broderick, J. B. (2002) Direct H atom abstraction from spore photoproduct C-6 initiates DNA repair in the reaction catalyzed by spore photoproduct lyase: evidence for a reversibly generated adenosyl radical intermediate. *J. Am. Chem. Soc.* **124**, 2860-2861.

Chenna, R., Hideaki, S., Koike, T., Lopez, R., Gibson, T. J., Higgins, D. G. and Thompson, J. D. (2003) Multiple sequence alignment with the Clustal series of programs. *Nucleic Acids Res.* **31**, 3497-3500.

Cosper, M. M., Jameson, G. N. L., Davydov, R., Eidsness, M. K., Hoffman, B. M., Huynh, B. H. and Johnson, M. K. (2002) The $[4Fe\text{-}4S]^{2+}$ cluster in reconstituted biotin synthase binds *S*-adenosyl-L-methionine. *J. Am. Chem. Soc.* **124**, 14006-14007.

Coomber, S. A., Jones, R. M., Jordan, P. M. and Hunter, C. N. (1992) A putative anaerobic coproporphyrinogen III oxidase in *Rhodobacter sphaeroides*. I. Molecular cloning, transposon mutagenesis and sequence analysis of the gene. *Mol. Microbiol.* **6**, 3159-3169.

Dailey, H. A. (ed.) (1990a) *Biosynthesis of heme and chlorophylls.* McGraw-Hill Publishing, New York.

Dailey, H. A. (1990b) Conversion of coproporphyrinogen to protoheme in higher eukaryotes and bacteria: terminal three enzymes. In *Biosynthesis of heme and chlorophylls.* (Dailey, H. A., ed.) McGraw-Hill Publishing, New York, 123-162.

Dailey, H. A. (2002) Terminal steps of haem biosynthesis. *Biochem. Soc. Trans.* **30**, 590-595.

Dailey, T. A., Meissner P. and Dailey, H. A. (1993) Expression of a cloned protopor-

phyrinogen oxidase. *J. Biol. Chem.* **269**, 813-815.

Datsenko, K. A. and Wanner, B. L. (2000) One-step inactivation of chromosomal genes in *Escherichia coli* K-12 using PCR products. *Proc. Natl. Acad. Sci. USA* **97**, 6640-6645.

Demple, B., Ding, H. and Jorgensen, M. (2002) *Escherichia coli* SoxR protein: sensor/transducer of oxidative stress and nitric oxide. *Methods Enzymol.* **348**, 355-364.

Ding, H. and Demple, B. (1997) *In vivo* kinetics of a redox-regulated transcriptional switch. *Proc. Natl. Acad. Sci. USA* **94**, 8445-8449.

Duboc-Toia, C., Hassan, A. K., Mulliez, E., Ollagnier-de Choudens, S., Fontecave, M., Leutwein, C. and Heider, J. (2003) Very high-field EPR study of glycyl radical enzymes. *J. Am. Chem. Soc.* **125**, 38-39.

Erskine, P. T., Senior, N., Awan, S., Lambert, R., Lewis, G., Tickle, I. J., Sarwar, M., Spencer, P., Thomas, P., Warren, M. J., Shoolingin-Jordan, P. M., Wood, S. P. and Cooper, J. B. (1997) X-ray structure of 5-aminolaevulinate dehydratase, a hybrid aldolase. *Nat. Struct. Biol.* **4**, 1025-1031.

Escalettes, F., Florentin, D., Tse Sum Bui, B., Lesage, D. and Marquet, A. (1999) Biotin synthase mechanism: evidence for hydrogen transfer from the substrate into deoxyadenosine. *J. Am. Chem. Soc.* **121**, 3571-3578.

Ferreira, G. C., Andrew, T. L., Karr, S. W. and Dailey, H. A. (1988) Organization of the terminal two enzymes of the heme biosynthetic pathway. Orientation of protoporphyrinogen oxidase and evidence for a membrane complex. *J. Biol. Chem.* **263**, 3835-3839.

Fischer, H.-M., Velasco, L., Delgado, M. J., Bedmar, E. J., Schären, S., Zingg, D., Göttfert, M. and Hennecke, H. (2001) One of two *hemN* genes in *Bradyrhizobium japonicum* is functional during anaerobic growth and in symbiosis. *J. Bacteriol.* **183**, 1300-1311.

Foran, S. E. and György, A. (2003) Guide to porphyrias. A historical and clinical perspective. *Am. J. Clin. Pathol.* **119**, 86-93.

Frankenberg, N., Erskine, P. T., Cooper, J. B., Shoolingin-Jordan, P. M., Jahn, D. and Heinz, D. W. (1999) High resolution crystal structure of a Mg^{2+} dependent porphobilinogen synthase. *J. Mol. Biol.* **289**, 591-602.

Frankenberg, N., Moser, J. and Jahn, D. (2003) Bacterial heme biosynthesis and its biotechnological application. *Appl. Microbiol. Biotechnol.* **63**, 115-127.

Frazzon, J. and Dean, D. R. (2003) Formation of iron-sulfur clusters in bacteria: an emerging field in bioinorganic chemistry. *Curr. Opin. Chem. Biol.* **7**, 166-173.

Frère, F., Reents, H., Schubert, W.-D., Heinz, D. W. and Jahn, D. (2005) Tracking the evolution of porphobilinogen synthase metal dependence *in vitro*. *J. Mol. Biol.* **345**, 1059-1070.

Frey, P. A. (1990) Importance of organic radicals in enzymatic cleavage of unactivated C-H bonds. *Chem. Rev.* **90**, 1343-1357.

Frey, P. A. and Reed, G. H. (2000) Radical mechanisms in adenosylmethionine- and adenosylcobalamin-dependent enzymatic reactions. *Arch. Biochem. Biophys.* **382**, 6-14.

Frey, P. A. (2001) Radical mechanisms of enzymatic catalysis. *Annu. Rev. Biochem.* **70**, 121-148.

Frey, P. A. and Magnusson, O. T. (2003) *S*-adenosylmethionine: a wolf in sheep's clothing, or a rich man's adenosylcobalamin? *Chem. Rev.* **103**, 2129-2148.

Friedmann, H. C., Klein, A. and Thauer, R. K. (1991) Biochemistry of coenzyme F_{430}, a nickel porphinoid involved in methanogenesis. In *Biosynthesis of tetrapyrroles*. (Jordan, P. M., ed.) Elsevier Science Ltd., Amsterdam, pp. 139-154.

Fuchs, J., Weber, S., Kaufmann, R. (2000) Genotoxic potential of porphyrin type photosensitizers with particular emphasis on 5-aminolevulinic acid: implications for clinical photodynamic therapy. *Free Radic. Biol. Med.* **28**, 537-548.

Gibson, K. D., Laver, W. G. and Neuberger, A. (1958) Initial stages in the biosynthesis of porphyrins. 2. The formation of δ-aminolaevulic acid from glycine and succinyl-coenzymeA by particles from chicken erythrocytes. *Biochem. J.* **70**, 71-81.

Grandchamp, B. and Nordmann, Y. (1982) Coproporphyrinogen III oxidase assay. *Enzyme* **28**, 196-205.

Guianvarc'h, D., Florentin, D., Tse Sum Bui, B., Nunzi, F. and Marquet, A. (1997) Biotin synthase, a new member of the family of enzymes which uses *S*-adenosylmethionine as a source of deoxyadenosyl radical. *Biochem. Biophys. Res. Commun.* **236**, 402-406.

Hänzelmann, P. and Schindelin, H. (2004) Crystal structure of the *S*-adenosylmethionine-dependent enzyme MoaA and its implications for molybdenum cofactor deficiency in humans. *Proc. Natl. Acad. Sci. USA* **101**, 12870-12875.

Hansson, M., Rutberg, L., Schröder, I. and Hederstedt, L. (1991) The *Bacillus subtilis hemAXCDBL* gene cluster, which encodes enzymes of the biosynthetic pathway from glutamate to uroporphyrinogen III. *J. Bacteriol.* **173**, 2590-2599.

Hansson, M. and Hederstedt, L. (1992) Cloning and characterization of the *Bacillus subtilis hem EHY* gene cluster, which encodes protoheme IX biosynthetic enzymes. *J. Bacteriol.* **174**, 8081-8093.

Hansson, M. and Hederstedt, L. (1994) *Bacillus subtilis* HemY is a peripheral membrane protein essential for protoheme IX synthesis which can oxidize coproporphyrinogen III and protoporphyrinogen IX. *J. Bacteriol.* **176**, 5962-5970.

Hansson, M., Gustafsson, M. C. U., Kannangara, C. G. and Hederstedt, L. (1997) Isolated *B. subtilis* HemY has coproporphyrinogen III to coproporphyrin III oxidase activity. *Biochim. Biophys. Acta* **1340**, 97-104.

Hippler, B., Homuth, G., Hoffmann, T., Hungerer, C., Schumann, W. and Jahn, D. (1997) Characterization of *B. subtilis hemN*. *J. Bacteriol.* **179**, 7181-7185.

Homuth, G., Heinemann, M., Zuber, U. and Schumann, W. (1996) The genes *lepA* and *hemN* form a bicistronic operon in *Bacillus subtilis*. *Microbiology* **142**, 1641-1649.

Homuth, G., Rompf, A., Schumann, W. and Jahn, D. (1999) Transcriptional control of *Bacillus subtilis hemN* and *hemZ*. *J. Bacteriol*. **181**, 5922-5929.

Jackson, A. H., Sancovich, H. A., Ferrmola, A. M., Evans, N., Games, D. E., Matlin, S. A., Elder, G. H. and Smith S. G. (1976) Macrocyclic intermediates in the biosynthesis of porphyrins. *Phil. Trans. R. Soc. Lond. B. Biol. Sci.* **273**, 191-206.

Jackson, A. H., Jones, D. M., Philip, G., Lash, T. D., del C. Batlle, A. M. and Smith, S. G. (1980) Synthetic and biosynthetic studies of porphyrins, part IV. Further studies of the conversion of coproporphyrinogen-III to protoporphyrinogen-IX: mass spectrometric investigations of the incubation of specifically deuteriated coproporphyrinogen-III with chicken red cell haemolysates. *Int. J. Biochem.* **12**, 681-688.

Jahn, D., Verkamp, E. and Söll, D. (1992) Glutamyl-transfer RNA: a precursor of heme and chlorophyll biosynthesis. *Trends Biochem. Sci.* **17**, 215-218.

Jahn, D. (1996) Enzymatik und Regulation der Bildung bakterieller Tetrapyrrole. In *Colloquia Academica. Akademievorträge junger Wissenschaftler.* Franz Steiner Verlag, Stuttgart.

Jahn, D., Hungerer, C. and Troup, B. (1996) Ungewöhnliche Wege und umweltregulierte Gene der bakteriellen Hämbiosynthese. *Naturwissenschaften* **83**, 389-400.

Jarrett, J. T. (2003) The generation of 5'-deoxyadenosyl radicals by adenosylmethionine-dependent radical enzymes. *Curr. Opin. Chem. Biol.* **7**, 174-182.

Jordan, P. M. and Warren, M. J. (1987) Evidence for a dipyrromethane cofactor at the catalytic site of *E. coli* porphobilinogen deaminase. *FEBS Lett.* **225**, 87-92.

Jordan, P. M. (ed.) (1991a) *Biosynthesis of tetrapyrroles.* Elsevier Science Ltd., Amsterdam.

Jordan, P. M. (1991b) The biosynthesis of 5'-aminolaevulinic acid and its transformation into uroporphyrinogen III. In *Biosynthesis of tetrapyrroles*. (Jordan, P. M., ed.) Elsevier Science Ltd., Amsterdam, pp. 1-66.

Jordan, P. M. (1994) Porphobilinogen deaminase: mechanism of action and role in the biosynthesis of uroporphyrinogen III. In *The biosynthesis of tetrapyrrole pigments; Ciba Foundation Symposium 180*. (Chadwick, D. J. and Ackrill, K., eds.) Wiley, Chichester, pp. 70-96.

Keithly, J. H. and Nadler, K. D. (1983) Protoporphyrinogen formation in *Rhizobium japonicum*. *J. Bacteriol.* **154**, 838-845.

Kennedy, G. Y., Jackson, A. H., Kenner, G. W. and Suckling, C. J. (1970) Isolation, structure and synthesis of a tricarboxylic porphyrin from the harderian glands of the rat. *FEBS Lett.* **6**, 9-12.

Khoroshilova, N., Popescu, C., Münck, E., Beinert, H. and Kiley, P. (1997) Iron-sulfur cluster

disassembly in the FNR protein of *Escherichia coli* by O_2: [4Fe-4S] to [2Fe-2S] conversion with loss of biological activity. *Proc. Natl. Acad. Sci. USA* **94**, 6087-6092.

Kikuchi, G., Kumar, A. M., Tamalge, P. and Shemin, D. (1958) The enzymatic synthesis of δ-aminolevulinic acid. *J. Biol. Chem.* **233**, 1214-1219.

Kiley, P. J. and Beinert, H. (2003) The role of Fe-S proteins in sensing and regulation in bacteria. *Curr. Opin. Microbiol.* **6**, 181-185.

Koch, M., Breithaupt, C., Kiefersauer, R., Freigang, J., Huber, R. and Messerschmidt, A. (2004) Crystal structure of protoporphyrinogen IX oxidase: a key enzyme in haem and chlorophyll biosynthesis. *EMBO J.* **23**, 1720-1728.

Kohno, H., Furukawa, T., Tokunaga, R., Taketani, S. and Yoshinaga, T. (1996) Mouse coproporphyrinogen oxidase is a copper-containing enzyme: expression in *Escherichia coli* and site-directed mutagenesis. *Biochim. Biophys. Acta* **1292**, 156-162.

Krebs, C., Henshaw, T. F., Cheek, J., Huynh, B. H. and Broderick, J. B. (2000) Conversion of 3Fe-4S to 4Fe-4S clusters in native pyruvate formate-lyase activating enzyme: Mössbauer characterization and implications for mechanism. *J. Am. Chem. Soc.* **122**, 12497-12506.

Krebs, C., Broderick, W. E., Henshaw, T. F., Broderick, J. B. and Huynh, B. H. (2002) Coordination of adenosylmethionine to a unique iron site of the [4Fe-4S] of pyruvate formate-lyase activating enzyme: A Mössbauer spectroscopic study. *J. Am. Chem. Soc.* **124**, 912-913.

Laemmli, U. K. (1970) Cleavage of structural proteins during the assembly of the head of bacteriophage T4. *Nature* **227,** 680-685.

Lascelles, J. (1964) Tetrapyrrole biosynthesis and its regulation. *Microbial and molecular biology series.* (Davis, B. D., ed.) W. A. Benjamin, New York.

Layer, G. (2001) Untersuchung der sauerstoffunabhängigen Coproporphyrinogen III Oxidase (HemN) aus *Escherichia coli*. *Diplomarbeit*. Albert Ludwigs-Universität, Freiburg.

Layer, G., Verfürth, K., Mahlitz, E. and Jahn, D. (2002) Oxygen-independent coproporphyrinogen III oxidase HemN from *Escherichia coli*. *J. Biol. Chem.* **277**, 34136-34142.

Layer, G., Moser, J., Heinz, D. W., Jahn, D. and Schubert, W.-D. (2003) Crystal structure of coproporphyrinogen III oxidase reveals cofactor geometry of Radical SAM enzymes. *EMBO J.* **22**, 6214-6224.

Layer, G. (2004) Structure and function of the oxygen-independent coproporphyrinogen III oxidase HemN from *Escherichia coli*. *Dissertation*. Technische Universität Carolo-Wilhelmina, Braunschweig.

Layer, G., Grage, K., Teschner, T., Schünemann, V., Breckau, D., Masoumi, A., Jahn, M., Heathcote, P., Trautwein, A. X. and Jahn, D. (2005) Radical SAM enzyme coproporphyrinogen III oxidase HemN: functional features of the [4Fe-4S] cluster and the two bound *S*-adenosyl-L-methionines. *J. Biol. Chem.* **280**, 29038-29046.

Lecerof, D., Fodje, M., Hansson, A., Hansson, M. and Al-Karadaghi, S. (2000) Structural and

mechanistic basis of porphyrin metallation by ferrochelatase. *J. Mol. Biol.* **297**, 221-232.

Lieb, C., Siddiqui, A., Hippler, B., Jahn, D. and Friedrich, B. (1998) The *Alcaligenes eutrophus hemN* gene encoding the oxygen-independent coproporphyrinogen III oxidase, is required for heme biosynthesis during anaerobic growth. *Arch. Microbiol.* **169**, 52-60.

Lovenberg, W., Buchanan, B. B. and Rabinowitz, J. L. (1963) Studies on the chemical nature of clostridial ferredoxin. *J. Biol. Chem.* **238**, 3899-3913.

Lüer, C., Schauer, S., Möbius, K., Schulze, J., Schubert, W.-D., Heinz, D. W., Jahn, D. and Moser, J. (2005) Complex formation between glutamyl-tRNA reductase and glutamate-1-semialdehyde 2,1-aminomutase in *Escherichia coli* during the initial reactions of porphyrin biosynthesis. *J. Biol. Chem.* **280**, 18568-18572.

Magnusson, O. T., Reed, G. H. and Frey, P. A. (1999) Spectroscopic evidence for the participation of an allylic analogue of the 5'-deoxyadenosyl radical in the reaction of lysine 2,3-aminomutase. *J. Am. Chem. Soc.* **121**, 9764-9765.

Magnusson, O. T., Reed, G. H. and Frey, P. A. (2001) Characterization of an allylic analogue of the 5'-deoxyadenosyl radical: an intermediate in the reaction of lysine 2,3-aminomutase. *Biochemistry* **40**, 7773-7782.

Martens, J.-H., Barg, H., Warren, M. J. and Jahn, D. (2002) Microbial production of vitamin B_{12}. *Appl. Microbiol. Biotechnol.* **58**, 275-285.

Martins, B. M., Grimm, B., Mock, H.-P., Huber, R. and Messerschmidt, A. (2001) Crystal structure and stubstrate binding modeling of the uroporphyrinogen III decarboxylase from *Nicotiana tabacum*. *J. Biol. Chem.* **276**, 44108-44116.

McConville, M. L. and Charles, H. P. (1979) Isolation of haemin-requiring mutants of *Escherichia coli* K12. *J. Gen. Microbiol.* **113**, 155-164.

Medlock, A. E. and Dailey, H. A. (1996) Human coproporphyrinogen oxidase is not a metalloprotein. *J. Biol. Chem.* **271**, 32507-32510.

Mills, M. and Payne, S. M. (1995) Genetics and regulation of heme iron transport in *Shigella dysenteriae* and detection of an analogous system in *Escherichia coli* O157:H7. *J. Bacteriol.* **177**, 3004-3009.

Moser, J., Lorenz, S., Hubschwerlen, C., Rompf, A. and Jahn, D. (1999) *Methanopyrus kandleri* glutamyl-tRNA reductase. *J. Biol. Chem.* **274**, 30679-30685.

Moser, J., Schubert, W.-D., Heinz, D. W. and Jahn, D. (2002) Structure and function of glutamyl-tRNA reductase involved in 5-aminolaevulinic acid formation. *Biochem. Soc. Trans.* **30**, 579-584.

Moss, M. L. and Frey, P. A. (1987) The role of *S*-adenosylmethionine in the lysine 2,3-aminomutase reaction. *J. Biol. Chem.* **262**, 14859-14862.

Moss, M. L. and Frey, P. A. (1990) Activation of lysine 2,3-aminomutase by *S*-adenosyl-methionine. *J. Biol. Chem.* **265**, 18112-18115.

Mulliez, E., Padovani, D., Atta, M., Alcouffe, C. and Fontecave, M. (2001) Activation of class III ribonucleotide reductase by flavodoxin: a protein radical-driven electron transfer to the iron-sulfur center. *Biochemistry* **40**, 3730-3736.

Narita, S., Taketani, S. and Inokuchi, H. (1999) Oxidation of protoporphyrinogen IX in *Escherichia coli* is mediated by the aerobic coproporphyrinogen oxidase. *Mol. Gen. Genet.* **261**, 1012-1020.

Nicolet, Y. and Drennan, C. L. (2004) AdoMet radical proteins-from structure to evolution-alignment of divergent protein sequences reveals strong secondary structure element conservation. *Nucleic Acids Res.* **32**, 4015-4025.

O'Brian, M. R. and Thöny-Meyer, L. (2002) Biochemistry, regulation and genomics of haem biosynthesis in prokaryotes. *Adv. Microb. Physiol.* **46**, 257-318.

Ollagnier, S., Mulliez, E., Schmidt, P. P., Eliasson, R., Gaillard, J., Deronzier, C., Bergman, T., Gräslund, A., Reichhard, P. and Fontecave, M. (1997) Activation of the anaerobic ribonucleotide reductase from *Escherichia coli*. The essential role of the iron-sulfur center for *S*-adenosylmethionine reduction. *J. Biol. Chem.* **272**, 24216-24223.

Ollagnier-de Choudens, S., Sanakis, Y., Hewitson, K. S., Roach, P., Münck, E. and Fontecave, M. (2002) Reductive cleavage of *S*-adenosylmethionine by biotin synthase from *Escherichia coli*. *J. Biol. Chem.* **277**, 13449-13454.

Padovani, D., Thomas, F., Trautwein, A. X., Mulliez, E. and Fontecave, M. (2001) Activation of class III ribonucleotide reductase from *E. coli*. The electron transfer from the iron-sulfur center to *S*-adenosylmethionine. *Biochemistry* **40**, 6713-6719.

Panek, H. and O'Brian, M. R. (2002) A whole genome view of prokaryotic haem biosynthesis. *Microbiology* **148**, 2273-2282.

Phillips, J. D. and Kushner, J. P. (1999) Measurement of uroporphyrinogen decarboxylase activity. In *Current Protocols in Toxicology*. John Wiley and Sons, Inc., New York, pp. 8.4.1-8.4.13.

Phillips, J. D., Whitby, F. G., Kushner, J. P. and Hill, C. P. (2003) Structural basis for tetrapyrrole coordination by uroporphyrinogen decarboxylase. *EMBO J.* **22**, 6225-6233.

Phillips, J. D., Whitby, F. G., Warby, C. A., Labbe, P., Yang, C., Pflugrath, J. W., Ferrera, J. D., Robinson, H., Kushner, J. P. and Hill, C. P. (2004) Crystal structure of the oxygen-dependant coproporphyrinogen oxidase (Hem13p) of *Saccharomyces cerevisiae*. *J. Biol. Chem.* **279**, 38960-38968.

Pierrel, F., Douki, T., Fontecave, M. and Atta, M. (2004) MiaB protein is a bifunctional Radical-*S*-adenosylmethionine enzyme involved in thiolation and methylation of tRNA. *J. Biol. Chem.* **279**, 47555-47563.

Proulx, K. L., Woodard, S. I. and Dailey, H. A. (1993) *In situ* conversion of copro-porphyrinogen to heme by murine mitochondria: terminal steps of the heme biosynthetic pathway. *Protein Sci.* **2**, 1092-1098.

Righetti, P. G., Gianazza, E., Gelfi, C. and Chairi, M. (1990) In *Gel electrophoresis of proteins: a practical approach.* (Hames, B. D. and Rickwood, D., eds.) 2nd ed., Oxford University Press, Oxford, pp. 149-214.

Rogers, M. S. and Dooley, D. M. (2003) Copper-tyrosyl radical enzymes. *Curr. Opin. Chem. Biol.* **7**, 189-196.

Rompf, A., Hungerer, C., Hoffmann, T., Lindenmeyer, M., Römling, U., Groß, U., Doss, M. O., Arai, H., Igarashi, Y. and Jahn, D. (1998) Regulation of *Pseudomonas aeruginosa hemF* and *hemN* by the dual action of the redox response regulators Anr and Dnr. *Mol. Microbiol.* **29**, 985-997.

Sambrook, J., Fritsch, E. F. and Maniatis, T. (1989) Liquid media for *E. coli*. In *Molecular cloning: a laboratory manual.* 2nd ed., vol. **3**, Cold Spring Harbor Laboratory Press, New York.

Sano, S. and Granick, S. (1961) Mitochondrial coproporphyrinogen oxidase and proto-porphyrinogen formation. *J. Biol. Chem.* **236**, 1173-1180.

Sasarman, A., Chartrand, P., Lavoie, M., Tardif, D., Proschek, R. and Lapointe, C. (1979) Mapping of a new *hem* gene in *Escherichia coli* K12. *J. Gen. Microbiol.* **113**, 297-303.

Sasarman, A., Letowski, J., Czaika, G., Ramirez, V., Nead, M. A., Jacobs, J. M. and Morais, R. (1993) Nucleotide sequence of the *hemG* gene involved in the protoporphyrinogen oxidase activity of *Escherichia coli* K12. *Can. J. Microbiol.* **39**, 1155-1161.

Schobert, M. and Jahn, D. (2003) Regulation of heme biosynthesis in non-phototrophic bacteria. *J. Mol. Microbiol. Biotechnol.* **4**, 287-294.

Schuller, D. J., Wilks, A., Ortiz de Montellano, P. R. and Poulos, T. L. (1999) Crystal structure of human heme oxygenase-1. *Nat. Struct. Biol.* **6**, 860-867.

Scott, A. I. and Santander, P. J. (1991) The biosynthesis of vitamin B_{12}. In *Biosynthesis of tetrapyrroles*. (Jordan, P. M., ed.) Elsevier Science Ltd., Amsterdam, pp. 101-138.

Seehra, J. S., Jordan, P. M. and Akhtar, M. (1983) Anaerobic and aerobic coproporphyrinogen III oxidases of *Rhodopseudomonas spheroides*. Mechanism and stereochemistry of vinyl group formation. *Biochem. J.* **209**, 709-718.

Shemin, D. and Russell, C. S. (1953) δ-aminolevulinic acid, its role in the biosynthesis of porphyrins and purines. *J. Am. Chem. Soc.* **75**, 4873-4874.

Shoolingin-Jordan, P. M. and Cheung, K.-M. (1999) Biosynthesis of heme. In *Comprehensive natural products chemistry.* vol. **4**, (Barton, D. H. R. and Nakanishi, K., eds.), Elsevier Science Ltd., Amsterdam, pp. 61-107.

Shoolingin-Jordan, P. M., Spencer, P., Sarwar, M., Erskine, P. E., Cheung, K.-M., Cooper, J. B. and Norton, E. B. (2002) 5-Aminolaevulinic acid dehydratase: metals, mutants and mechanism. *Biochem. Soc. Trans.* **30**, 584-590.

Sofia, H. J., Chen, G., Hetzler, B. G., Reyes-Spindola, J. F. and Miller, N. E. (2001) Radical

SAM, a novel protein superfamily linking unresolved steps in familiar biosynthetic pathways with radical mechanisms: functional characterization using new analysis and information visualization methods. *Nucleic Acids Res.* **29**, 1097-1106.

Stubbe, J. and van der Donk, W. A. (1998) Protein radicals in enzyme catalysis. *Chem. Rev.* **98**, 705-762.

Stubbe, J. (2003) Di-iron-tyrosyl radical ribonucleotide reductases. *Curr. Opin. Chem. Biol.* **7**, 183-188.

Tabor, S. and Richardson, C. C. (1985) A bacteriophage T7 RNA polymerase/promoter system for controlled exclusive expression of specific genes. *Proc. Natl. Acad. Sci. USA* **82**, 1074-1078.

Tait, G. H. (1969) Coproporhyrinogenase activity in extracts from *Rhodopseudomonas spheroides*. *Biochem. Biophys. Res. Commun.* **37**, 116-122.

Tait, G. H. (1972) Coproporhyrinogenase activities in extracts of *Rhodopseudomonas spheroides* and *Chromatium* strain D. *Biochem. J.* **128**, 1159-1169.

Tamarit, J., Gerez, C., Meier, C., Mulliez, E., Trautwein, A. and Fontecave, M. (2000) The activating component of the anaerobic ribonucleotide reductase from *Escherichia coli*. An iron-sulfur center with only three cysteines. *J. Biol. Chem.* **275**, 15669-15675.

Thauer, R. K. and Bonacker, L. G. (1994) Biosynthesis of coenzyme F_{430}, a nickel porphinoid involved in methanogenesis. In *The biosynthesis of tetrapyrrole pigments; Ciba Foundation Symposium 180*. (Chadwick, D. J. and Ackrill, K., eds.) Wiley, Chichester, pp. 210-227.

Troup, B. (1995) Regulation der Hämbiosynthese in *Escherichia coli*: Die Bildung von Protoporphyrinogen IX in Abhängigkeit von verschiedenen Umweltbedingungen. *Dissertation*. Philipps-Universität, Marburg/Lahn.

Troup, B., Hungerer, C. and Jahn, D. (1995) Cloning and characterization of the *Escherichia coli hemN* gene encoding the oxygen-independent coproporphyrinogen III oxidase. *J. Bacteriol.* **177**, 3326-3331.

Tse Sum Bui, B., Lotierzo, M., Escalettes, F., Florentin, D. and Marquet, A. (2004) Further investigation on the turnover of *Escherichia coli* biotin synthase with dethiobiotin and 9-mercaptodethiobiotin as substrates. *Biochemistry* **43**, 16432-16441.

Ugulava, N. B., Frederick, K. K. and Jarrett, J. T. (2003) Control of adenosylmethionine-dependent radical generation in biotin synthase: a kinetic and thermodynamic analysis of substrate binding to active and inactive forms of BioB. *Biochemistry* **42**, 2708-2719.

Verfürth, K. (1999) Das *Escherichia coli hemN* Gen kodiert für einen Bestandteil der sauerstoffunabhängigen Coproporphyrinogen III Oxidase. *Diplomarbeit*. Albert Ludwigs-Universität, Freiburg.

Walsby, C. J., Hong, W., Broderick, W. E., Cheek, J., Ortillo, D., Broderick, J. B. and Hoffman, B. M. (2002a) Electron-nuclear double resonance spectroscopic evidence that *S*-adenosylmethionine binds in contact with the catalytically active $[4Fe\text{-}4S]^{+}$ cluster of

pyruvate formate-lyase activating enzyme. *J. Am. Chem. Soc.* **124**, 3143-3151.

Walsby, C. J., Ortillo, D., Broderick, W. E., Broderick, J. B. and Hoffman, B. M. (2002b) An anchoring role for FeS clusters: chelation of the amino acid moiety of *S*-adenosylmethionine to the unique iron site of the [4Fe-4S] cluster of pyruvate formate-lyase activating enzyme. *J. Am. Chem. Soc.* **124**, 11270-11271.

Warren, M. J., Bolt, E. and Woodcock, S. C. (1994) 5-Aminolaevulinic acid synthase and uroporphyrinogen methylase: two key control enzymes of tetrapyrrole biosynthesis and modification. In *The biosynthesis of tetrapyrrole pigments; Ciba Foundation Symposium 180.* (Chadwick, D. J. and Ackrill, K., eds.) Wiley, Chichester, pp. 26-49.

Werst, M. M., Kennedy, M. C., Houseman, A. L., Beinert, H. and Hoffman, B. M. (1990) Characterization of the $[4Fe\text{-}4S]^{+}$ cluster at the active site of aconitase by ^{57}Fe, ^{33}S and ^{14}N electron nuclear double resonance spectroscopy. *Biochemistry* **29**, 10533-10540.

Whitby, F. G., Phillips, J. D., Kushner, J. P. and Hill, C. P. (1998) Crystal structure of human uroporphyrinogen decarboxylase. *EMBO J.* **17**, 2463-2471.

Wirth, R., Friesenegger, A. and Fiedler, S. (1989) Transformation of various species of gram-negative bacteria belonging to 11 different genera by electroporation. *Mol. Gen. Genet.* **216**, 175-177.

Wu, C. K., Dailey, H. A., Rose, J. P., Burden, A., Sellers, V. M. and Wang, B. C. (2001) The 2.0 Å structure of human ferrochelatase, the terminal enzyme of heme biosynthesis. *Nat. Struct. Biol.* **8**: 156-160.

Xu, K., Delling, J. and Elliott, T. (1992) The genes required for heme synthesis in *Salmonella typhimurium* include those encoding alternative functions for aerobic and anaerobic coproporphyrinogen oxidation. *J. Bacteriol.* **174**, 3953-3963.

Xu, K. and Elliott, T. (1994) Cloning, DNA sequence, and complementation analysis of the *Salmonella typhimurium hemN* gene encoding a putative oxygen-independent coproporphyrinogen III oxidase. *J. Bacteriol.* **176**, 3196-3203.

Zeilstra-Ryalls, J. H. and Kaplan, S. (1995) Aerobic and anaerobic regulation in *Rhodobacter sphaeroides* 2.4.1: the role of the *fnrL* gene. *J. Bacteriol.* **177**, 6422-6431.

7. APPENDICES

Sequence Alignment of HemN, HemZ and HemZ2 Proteins

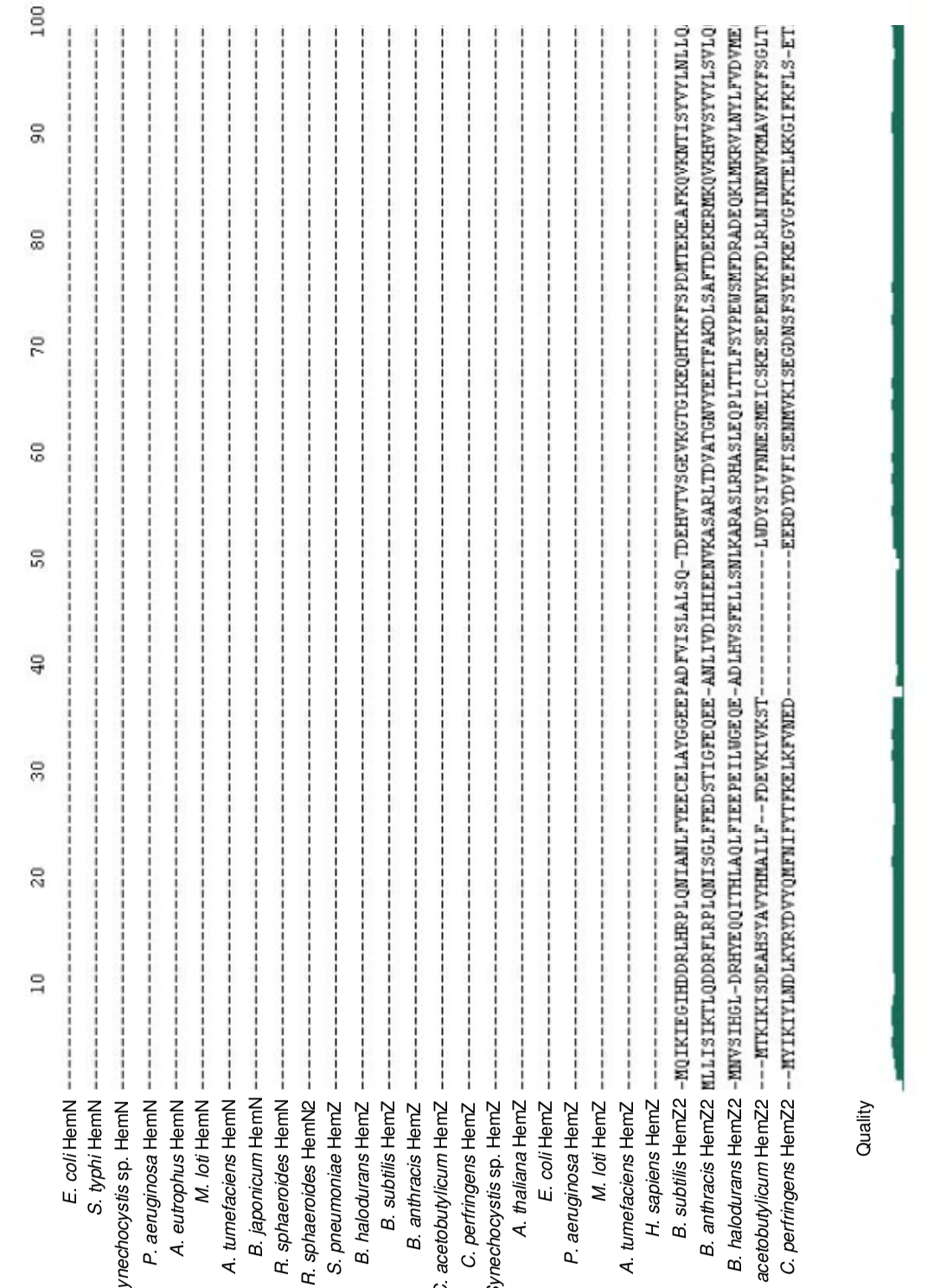

Sequence Alignment (cont.)

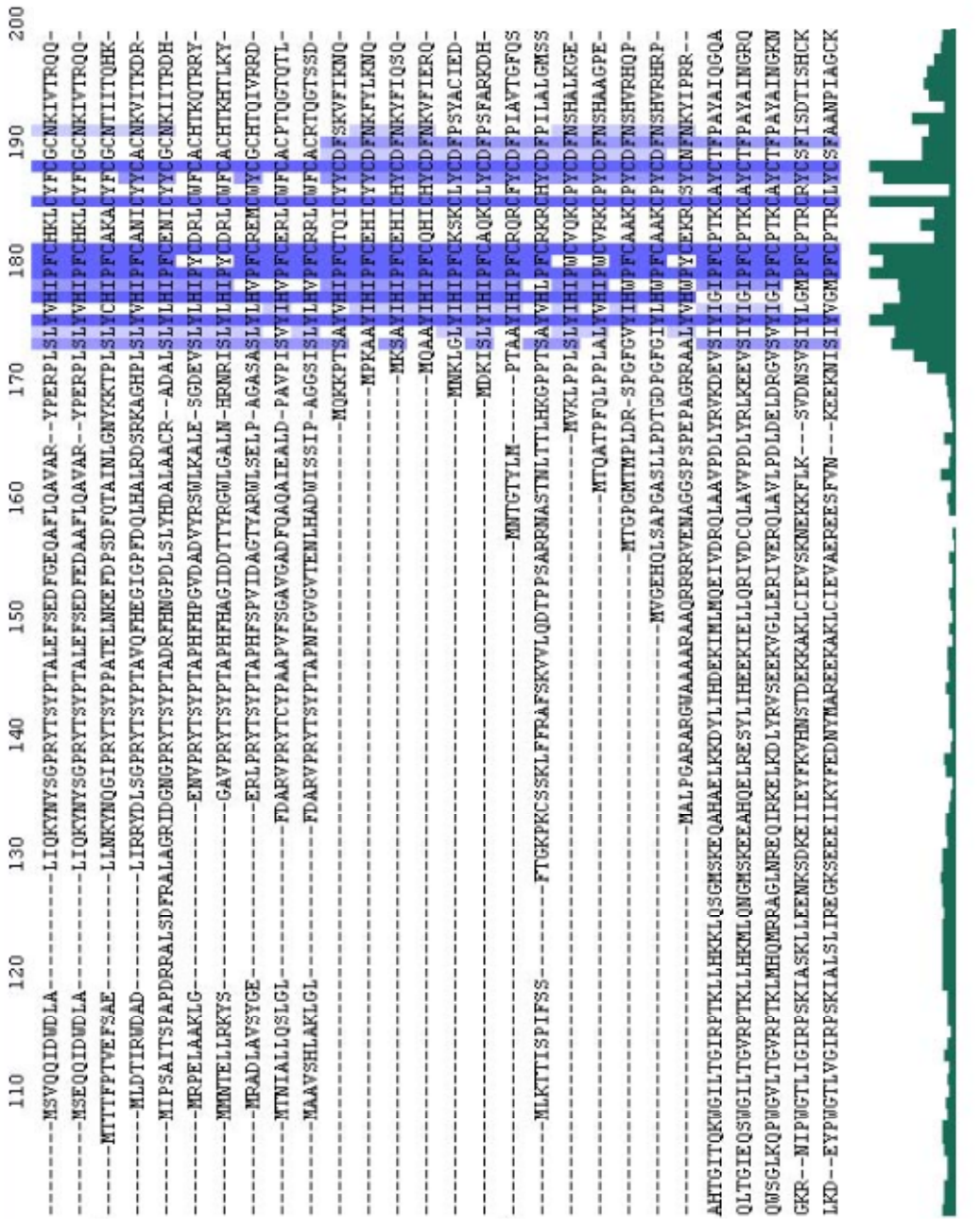

Sequence Alignment (cont.)

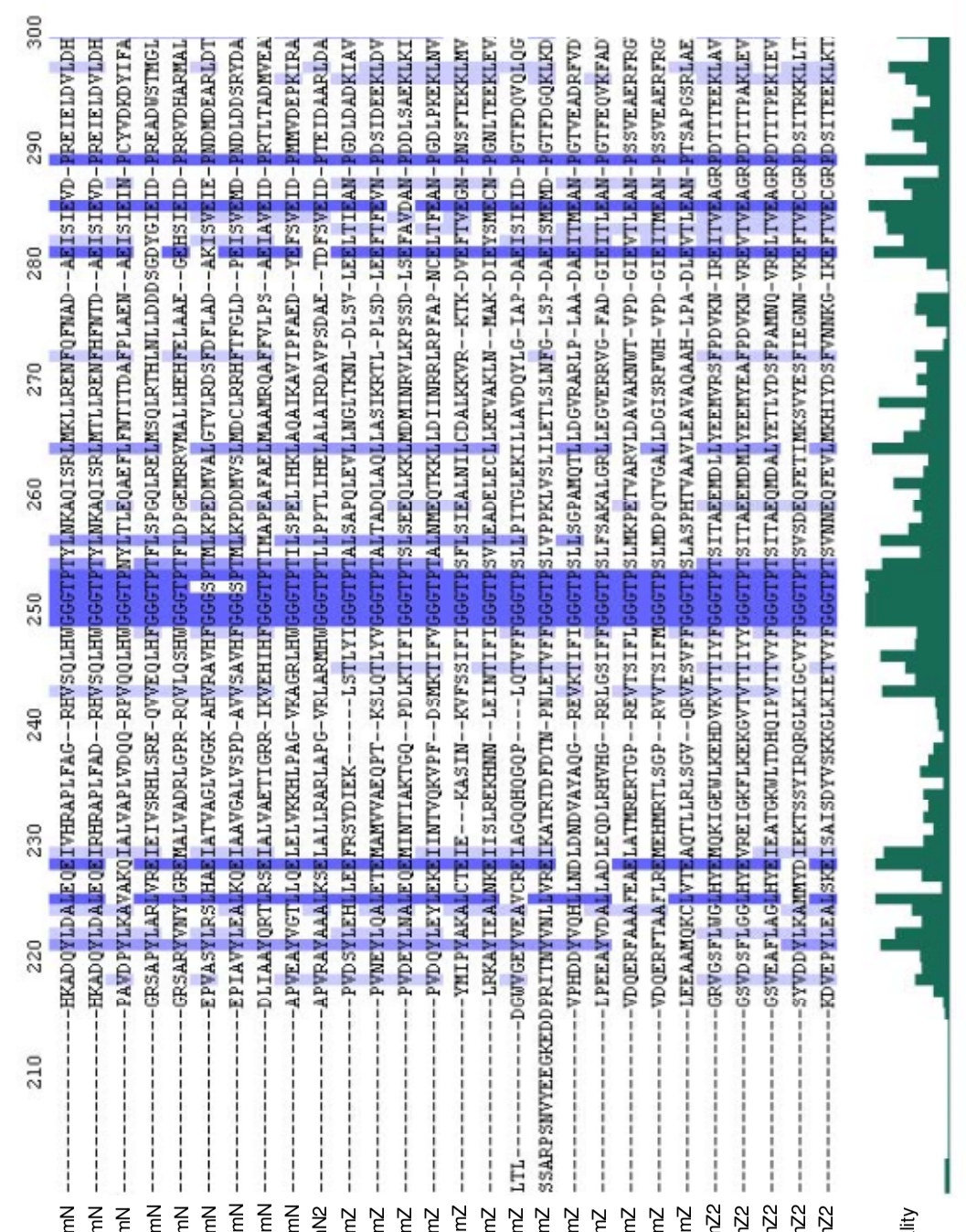

Sequence Alignment (cont.)

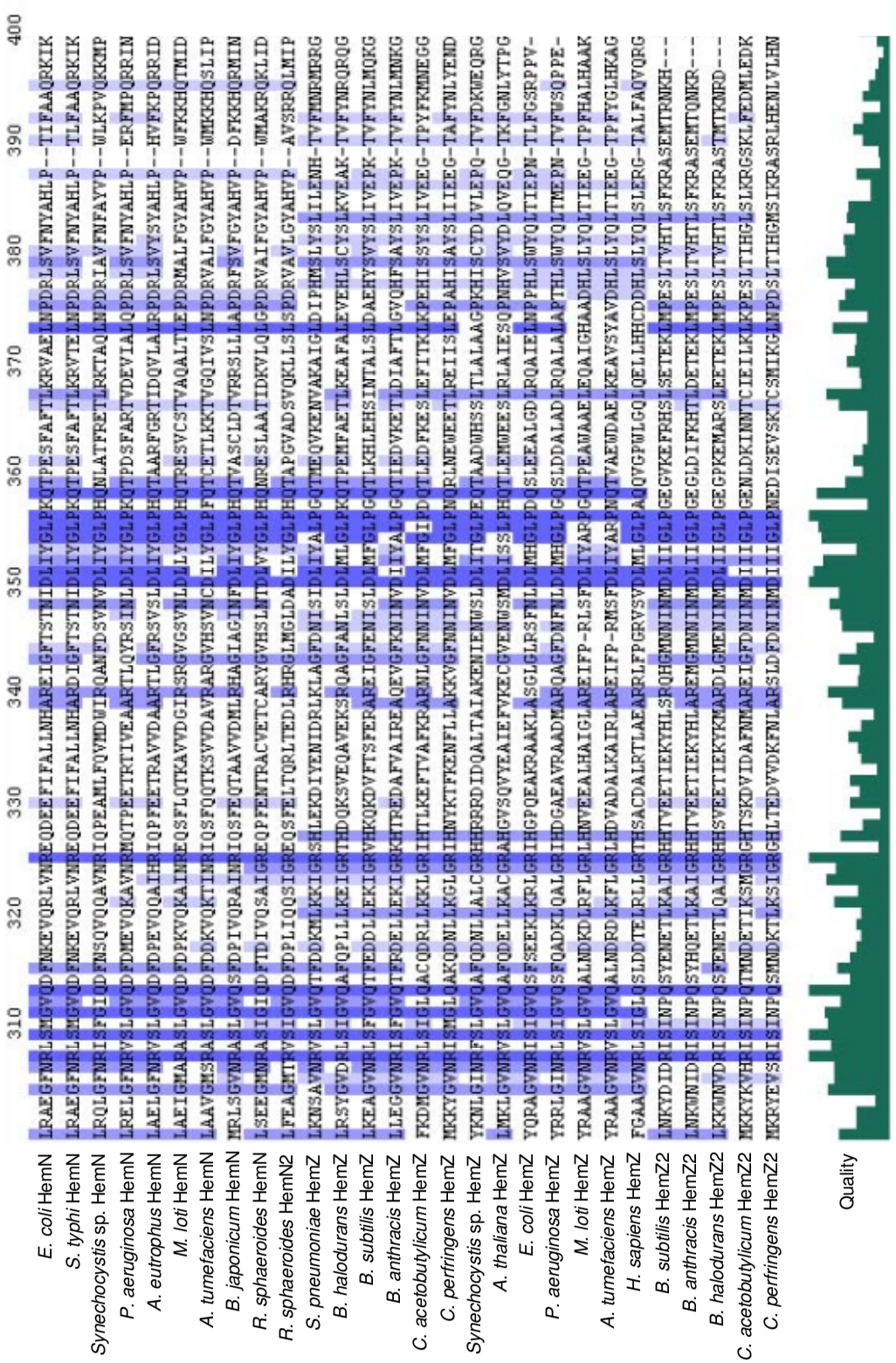

Sequence Alignment (cont.)

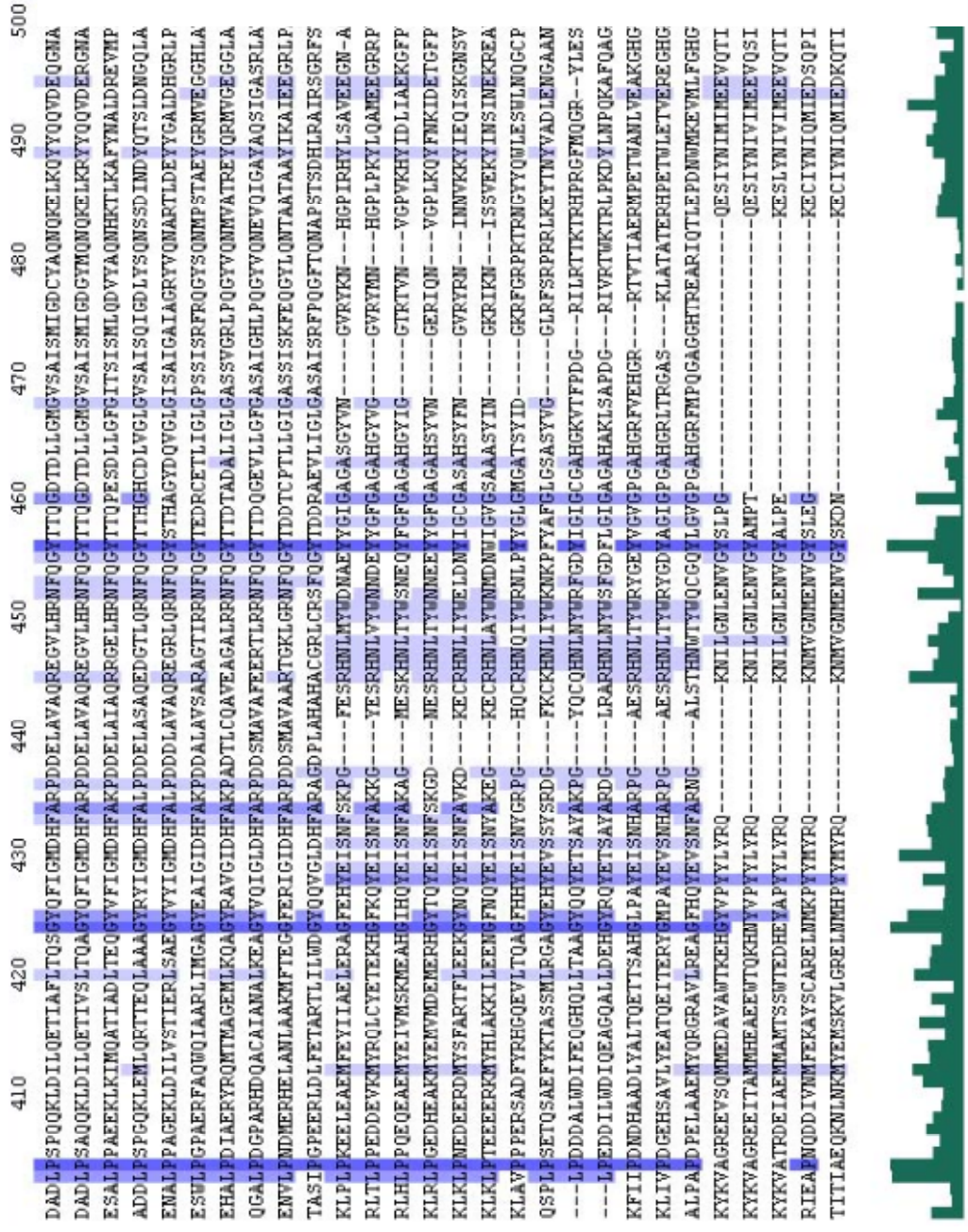

Sequence Alignment (cont.)

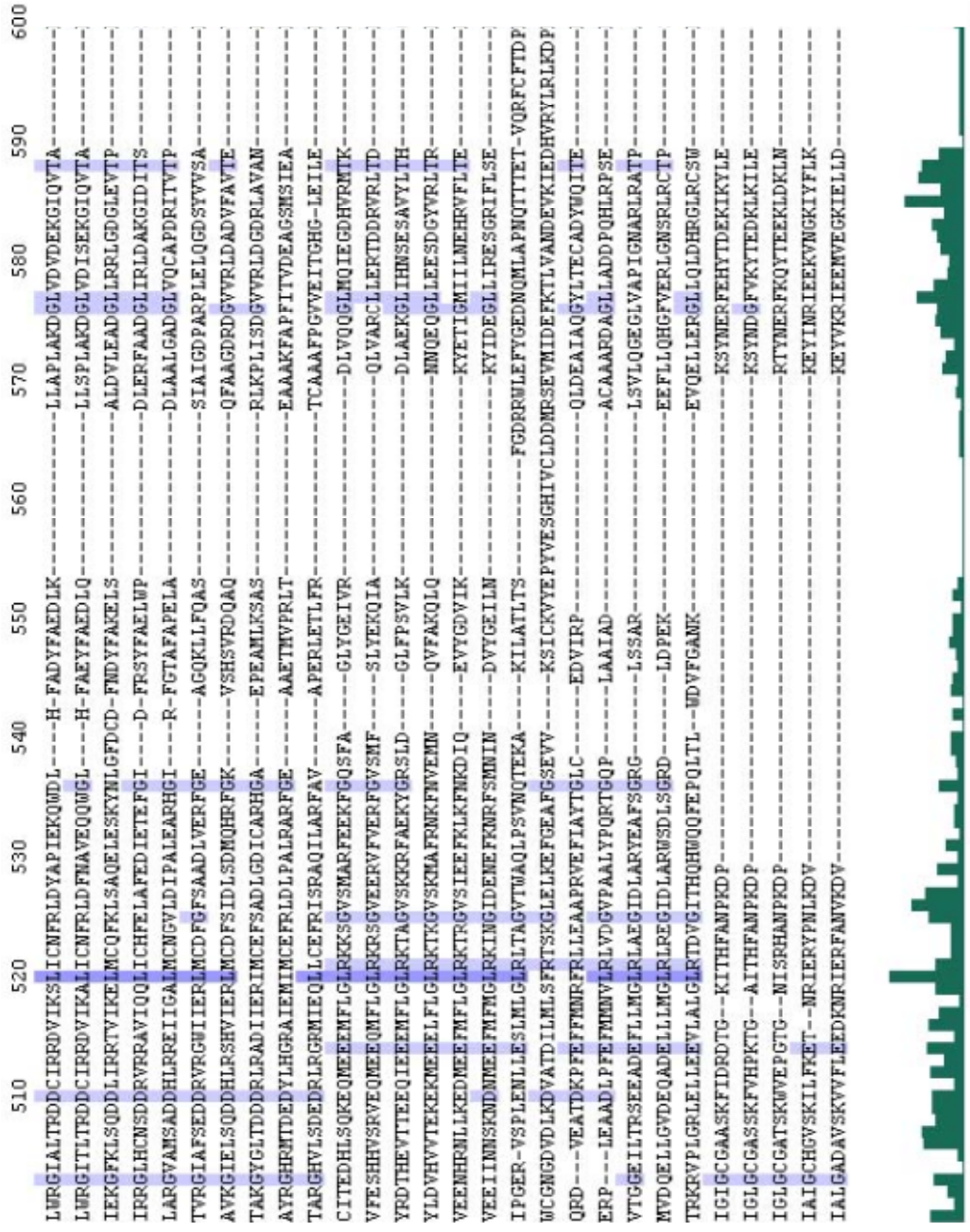

Sequence Alignment (cont.)

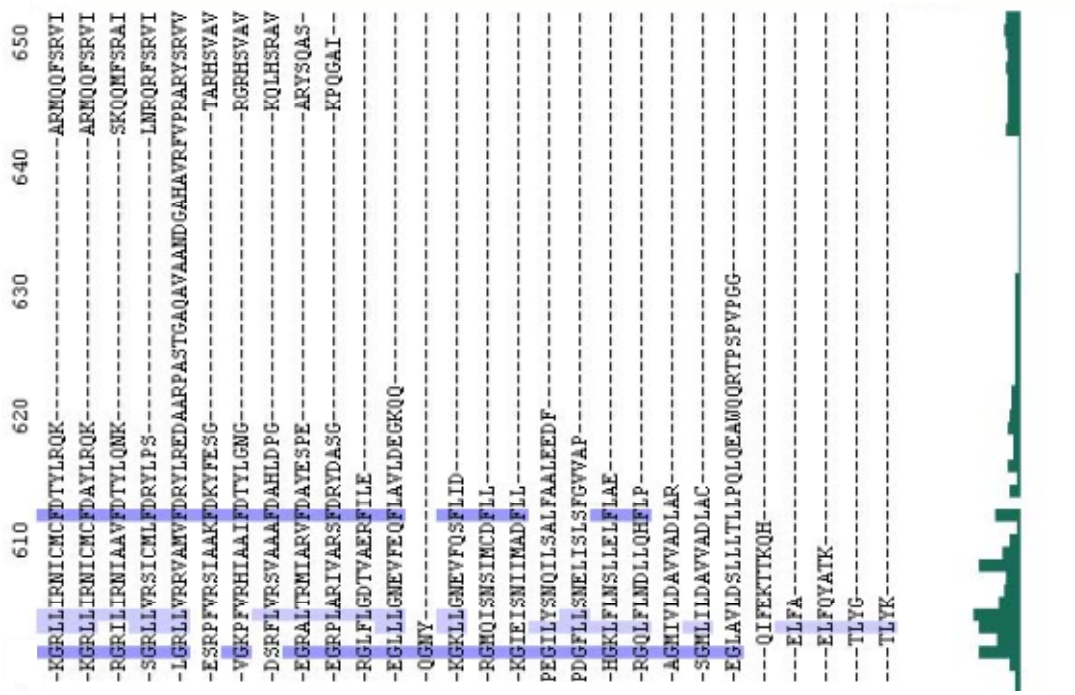

Appendix 1: Amino acid sequence alignment of different HemN, HemZ and HemZ2 proteins from a variety of organisms. The alignment was generated using ClustalW (http://www.ebi.ac.uk/clustalw/; Chenna *et al.*, 2003). Coloured shading indicates the percentage of agreement with the consensus sequence: blue, > 80 %, mid blue, > 60 %, light blue, > 40 %, white, ≤ 40 %.

Phylogenetic Tree of HemN, HemZ and HemZ2 Proteins

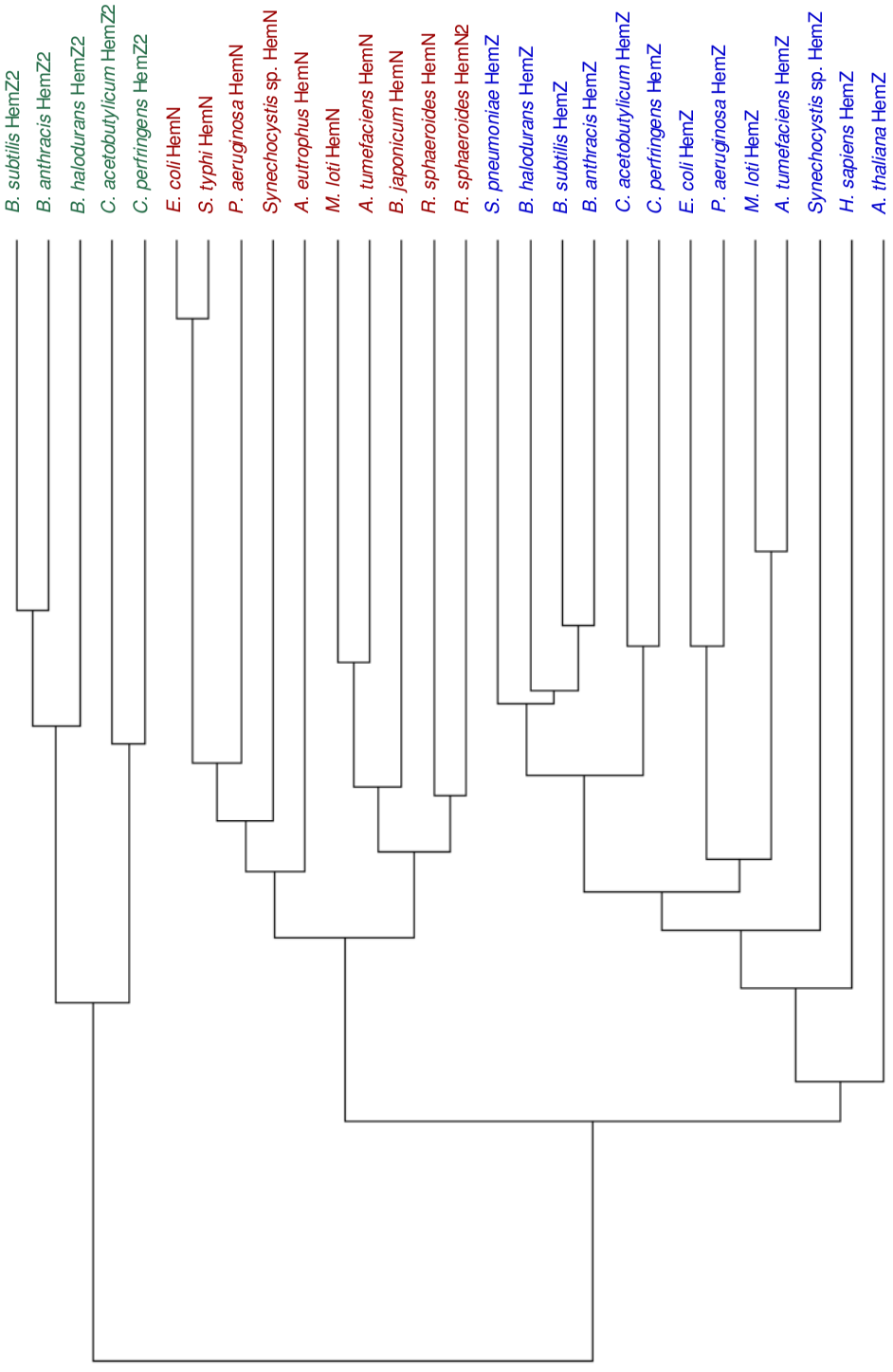

Appendix 2: Phylogenetic tree illustrating the distinction of three groups of (potential) O_2-independent coproporphyrinogen III oxidases. The tree was also created with ClustalW on the basis of the sequence alignment shown in appendix 1. For clearness the three groups HemN, HemZ and HemZ2 are depicted in different colours.

Possible Bacillus subtilis hemZ Sequence Error

A

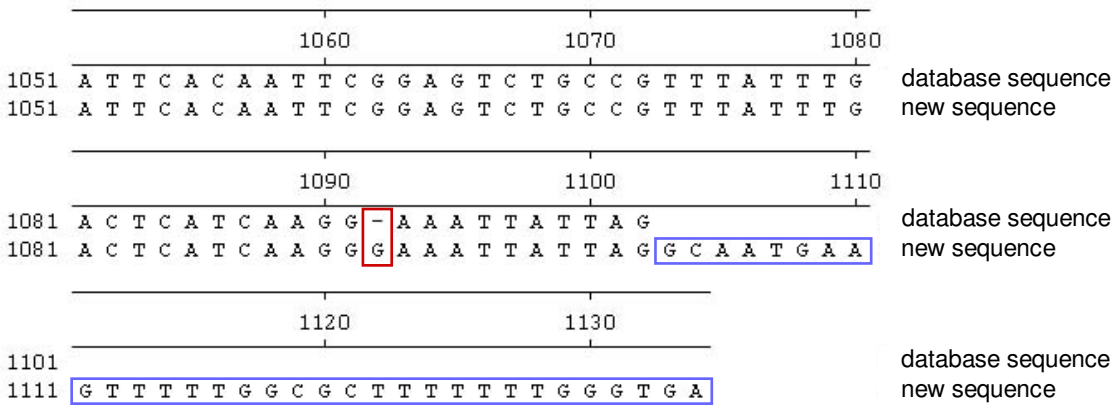

B

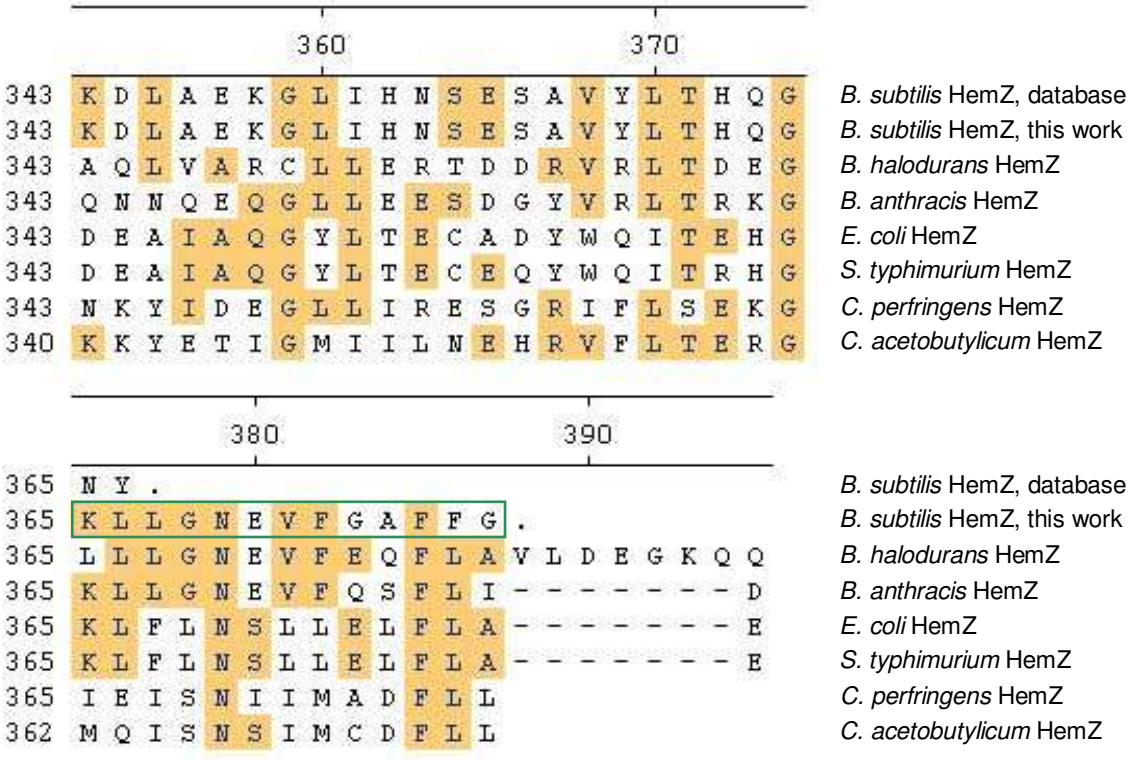

Appendix 3: Comparison of the *B. subtilis hemZ* database sequence with the sequence obtained in this work. A, 3'-end of the *B. subtilis hemZ* DNA sequence with the database sequence displayed above the newly obtained sequence. The position of the additional G in the new sequence is boxed in red, the segment of DNA between the original and the following stop codon is boxed in blue. **B**, Amino acid sequence alignment (C-terminal section) of the *B. subtilis* HemZ database sequence, the *B. subtilis* HemZ sequence deduced from the new, longer DNA sequence and the HemZ sequences of a few other organisms. Yellow boxes indicate sequence conservation. The potentially new C-terminal amino acid residues of *B. subtilis* HemZ are boxed in green.

Danksagung

Bei meinem Doktorvater Prof. Dr. Dieter Jahn möchte ich mich sehr herzlich bedanken für die Vergabe des Themas, seine stets motivierende Art sowie die Unterstützung und Diskussionsbereitschaft während der vergangenen drei Jahre.
Prof. Dr. Dirk Heinz danke ich für die Übernahme des Zweitgutachtens für diese Arbeit. Prof. Dr. Ralf Mendel sei gedankt für die Übernahme des Vorsitzes der Promotionskommission.
Dr. Gunhild Layer gilt besonderer Dank für das Einarbeiten in Thema und anaerobe Arbeitstechniken. Außerdem danke ich ihr, wie auch Daniela Breckau und Dr. Frederic Frère, für die nette Aufnahme in Labor 256/257, die stete Hilfs- und Diskussionsbereitschaft sowie die wirklich freundschaftliche Atmosphäre.
Natürlich geht auch ganz herzlicher Dank an die gesamte AG Jahn für das entspannte Arbeitsklima. Es hat Spaß gemacht, hier zu arbeiten - und auch die vielen „sonstigen Aktivitäten“ sollen nicht unerwähnt bleiben.
Dr. Jürgen Moser und Ronja Tasler sei zudem gedankt für das Korrekturlesen meiner Arbeit.
Bei Dr. Wolf-Dieter Schubert möchte ich mich für alle Hilfestellungen rund um die HemN Struktur bedanken.
Den Initiatoren des Internationalen Graduiertenkollegs „Molecular Complexes of Biomedical Relevance“ gilt mein Dank für die Finanzierung dieser Doktorarbeit sowie die Möglichkeit, im Rahmen des Programms zahlreiche Eindrücke und Erfahrungen zu sammeln. Den anderen „Fellows“ danke ich besonders für den guten Zusammenhalt in unserer kleinen Gruppe.
Außerdem möchte ich mich an dieser Stelle noch einmal bei meinen Eltern dafür bedanken, dass sie mir das Studium ermöglicht haben.
Herzlicher Dank natürlich auch an alle, die mir im Laufe der drei Jahre immer wieder Mut gemacht haben - allen voran Helge. Ebenso sei im voraus allen Freunden und Bekannten gedankt, die mir die längere „Funkstille“ hoffentlich verzeihen werden...